POLITECHNIKA GDAŃSKA

UNIVERSITÀ DEGLI STUDI
DELL'AQUILA

Erasmus Mundus Consortium "MathMods"

Double Master's Degree Programme in
Mathematical Modelling in Engineering: Theory, Numerics, Applications

Master of Science in Technical Physics Specialization Advanced Computational Methods in Materials Science	Laurea Magistrale in Ingegneria Matematica
POLITECHNIKA GDAŃSKA	UNIVERSITÀ DEGLI STUDI DELL'AQUILA

In the framework of the
Consortium Agreement and Award of a Joint/Multiple Degree 2013-2019

Master's thesis

Hessian of the AIREBO Potential

Supervisor

Candidate

Dr inz. Grzegorz Kwiatkowski

Cameron Wade
Matricola: 239000

2014/2015

Abstract

Computational studies of atomic and molecular systems help to give insight into the system's collective dynamics by modelling their inter-atomic and intra-molecular interactions. This allows the researcher to simultaneously investigate microscopic and macroscopic system properties, isolate single parameters, and to achieve control over the system that may otherwise be impossible in a laboratory setting.

For a number of applications, all that is required from computer simulation is the determination of the Hessian of the potential function for a system in equilibrium. This thesis concentrates on taking the Hessian of the adaptive intermolecular reactive empirical bond-order (AIREBO) potential for systems of Carbon atoms. The interaction radius of each term is then analyzed. The resulting Hessian is then implemented into a C++ computational program that receives an atomic list as input and outputs the corresponding Hessian matrix with respect to atomic position. In doing so, a number of discrepancies between the analytical form of the AIREBO potential and its C++ implementation were discovered.

The Hessian matrix can then be used directly to determine system quantities of interest in some cases (i.e. configurational temperature). For other system properties, such as vibrational and mechanical properties, a diagonalization of the Hessian is required in order to determine it's spectrum. This provides a number of interesting problems and opportunities for future work.

Contents

Chapter 1

Introduction

For centuries, science has been partitioned and shaped to impose more structure to what was once a very general concept. Certain areas of science could then be distinguished qualitatively from one another — theory versus experiment, classical versus quantum regimes, et cetera. The advent of computers marked a significant disruption by introducing both new fields of science, and investigation methods.

In their 1957 seminal paper, Alder and Wainwright introduced computer simulations to study the interactions of hard spheres [2] which led to what is now today the large, interdisciplinary field of molecular dynamics (MD). This introduction will first characterize and discuss both the aim and history of MD simulations. The importance of appropriate potential energy functions will be outlined and the development of the adaptive intermolecular reactive bond-order (AIREBO) potential will then be discussed. The concept of the Hessian of the potential function as well as insights derived from this Hessian matrix will be outlined.

1.1. Motivation for MD Computer Simulations

Molecular dynamics considers the building blocks of materials and their interactions in hopes of gaining valuable insight pertaining to the bulk properties. For this reason it can be thought of as a fundamental approach to modelling a system. As a direct consequence, MD is a rather unified study of the general physical properties of a material.

The collective dynamics reached by an ensemble of many particles allows the scientist to study many physical properties of the overall system. These include structural, mechanical, thermodynamic, and transport properties of a system of particles, valid for all states of matter (solid, liquid, gas). Expanding on this, simulations can be considered as a bridge between microscopic and macroscopic worlds. By assuming a suitable interaction potential, one can model these microscopic interactions and dynamics to then obtain exact[1] results for the macroscopic physical properties of

---

[1]exact in a deterministic sense. Here the output is limited by the quality / suitability of the potential function, spatial and temporal resolution, and computational strength.

the system in question. In doing so, the simulation delivers insights into the atomic and molecular level processes. This type of resolution is often not possible in an experimental setting where intrinsic limitations are inherent.

Another advantage of simulations rests in the fact that isolating single variables, such as temperature or pressure, or driving these variables to extremes values can often be impossible or extremely challenging to obtain in a laboratory setting. Simulations allow total control over these variables which then enables effective simulations in extreme conditions (vacuum, extremely low temperatures, etc...). Precise control over these variables can also be obtained via thermostating, barostating, or other control techniques and in this way one can isolate specific variables and parameters of interest.

Additionally, frequently in theoretical formulations of problems analytical solutions may be intractable or may not exist at all (consider non-linear phenomena or the three body problem). This leads to the necessity of numerical algorithms or simulations to gain approximate solutions and insight. Molecular dynamics and Monte Carlo simulations help to solve these issues within the context of material science, chemistry, and geology, among other fields.

1.2. Brief Overview of Molecular Dynamics

Together with Monte Carlo (MC) techniques, MD is a cornerstone for the theoretical studies of materials and chemical properties. In the most basic sense, the classical[2] MD method is the solving of Newton's classical equations of motion for a collection of atoms in a step-by-step fashion. Newton's second law captures the dynamics of a classical system and can be expressed as

$$m_i \ddot{\mathbf{r}}_i = \mathbf{f}_i. \tag{1.2.1}$$

The force, $\mathbf{f}_i$, acting on particle i with mass m_i at Euclidean coordinates $\mathbf{r}_i$ can be expressed as the negative of the derivative of the potential energy function, V, defined for the system

$$\mathbf{f}_i = -\frac{\partial}{\partial \mathbf{r}_i} V(\mathbf{r}_i) = -\nabla_i V(\mathbf{r}_i) \tag{1.2.2}$$

In combining equations 1.2.1 and 1.2.2 one obtains

$$m_i \ddot{\mathbf{r}}_i = -\nabla_i V(\mathbf{r}_i) \tag{1.2.3}$$

Equation 1.2.3 can be seen as the governing equation of MD. The integration of this governing equation then uncovers the position coordinates, $\mathbf{r}_i$, of the system. To accomplish this, the system must be well posed which requires three specific elements. An appropriate potential function must first be selected to describe the interaction between atoms. Potential functions can vary depending

---

[2]Quantum mechanical MD methods exist (so called *ab initio methods*) and these work with the Schödinger equation and associated Hamiltionian, however they are not the focus of this thesis.

on the types of atomic systems and the type of simulations and its objectives. This idea will be further explored in section 1.2.2. Secondly, appropriate initial conditions must be stated, and thirdly, an appropriate numerical integration algorithm must be employed. When these three elements are well defined and in place, a basic MD algorithm, as depicted in figure 1.1, is executed to obtain the desired output.

The calculation and subsequent conversion of the microscopic data to macroscopic observables (temperature, pressure, stress, strain, etc...) requires the application of statistical mechanics. This is outside the scope of this thesis, but it should be mentioned that the Ergodic hypothesis is the mechanism for accomplishing this. The hypothesis states that over long periods of time the ensemble average is equal to the time average, i.e.

$$\langle A \rangle_{ensemble} = \langle A \rangle_{time} \tag{1.2.4}$$

for some observable A.

The quality of a MD simulation largely relies on a suitably chosen potential function to model the atomic interactions / chemical bonding within the system. Bonding is essentially the movement and re-arrangement of the electronic structures in the system. Using this idea, atomic systems can then be subdivided into general groups based on their bonding type.

Metallic systems are envisioned as a sea of free electrons not associated with any one particular host atom, embedded in a matrix of positively charged cores (nuclei). In *ionic* bonding, one atom strongly attracts and effectively steals an electron from the other, and molecules with a structural charge are created in the process. In *covalent* bonding, such as in Carbon-Carbon bonds, substantial rearrangements of the electron cloud result in the amalgamation of electrons in between the two bonding atoms. This results in an overall electrically neutral system. Different classes of potential functions exist in an effort to properly describe the particular system and it's bonding properties.

This is a very brief and coarse overview of the MD method but captures its essence. A compact history of the MD method will be presented before returning to the MD method in more detail.

1.2.1. History of the MD Method

Computers became available to the general public in the 1950s, and with them, new scientific horizons. Computers allowed scientists to perform calculations much faster than what was possible beforehand. One particular scientific field to expose the strengths of computers was statistical mechanics. The beginnings of MD were marked by publications by Alder and Wainwright [2] using computers for the first time to simulate a system of particles. Since then, the field has expanded and is used in the disciplines of physics, chemistry, biology, and geology, amongst others.

In its early days, MD was used to discern information about generic families of systems rather than specific, realistic systems [22]. As most things do, MD grew in complexity with time. Specifically, different interaction potentials were defined for varying classes of systems. These systems are typically defined by the bonding types inherent to them, as earlier outlined.
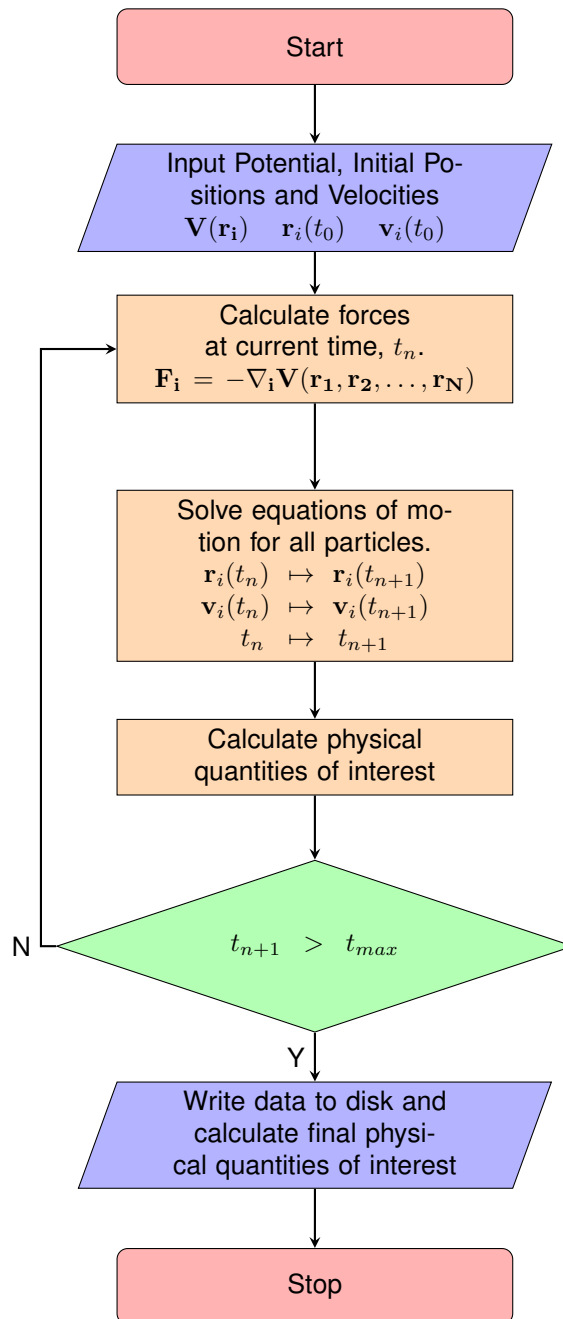
Figure 1.1: Simplified flow chart for a general MD simulation.

Certain potentials were defined for organic and biological systems, embedded atom potentials were defined for metallic systems, and bond-order potentials were created for covalent systems.

Since the MD method involves the integration of the equations of motion of the particles of the system, it was originally thought that the method could only be applied to systems characterized by a constant number of particles, constant volume and constant energy — a microcanonical system. While MD proved to be useful, its flexibility and robustness was a concern as most realistic systems are not completely isolated.

This problem was addressed by Andersen [8] and Nosé [32] in 1980 and 1984, respectively, and their development of the MD method for isoenthalpic-isobaric ensembles (constant enthalpy and pressure — NPH), canonical ensembles (conserved NVT) and isothermal-isobaric ensembles (NPT). This was made possible through the introduction of an Anderson thermostat and the Anderson barostat. Andersen and Nosé essentially introduced additional degrees of freedom to the system which was analogous to coupling the system to an external bath.

These advancements demonstrated that MD could achieve much more than the modelling of fictitious, overidealized isolated systems. Car and Parrinello extended this by the introduction of fictitious dynamical variables [16] which marked the commencement of ab-initio MD. Prior to this, MD consisted of either empirical potential functions or semi-empirical potential functions.

Ab-initio methods mark the highest precision models, but come at the price of high computational cost. These methods use first principles and quantum mechanics to calculate the electronic-structure of the system in question on the fly [28] and the system is then adapted accordingly. The computational cost of ab initio simulations limit the size of the physical systems that can be considered.

In an empirical potential function, one assumes a functional form for the potential and then the associated parameters are selected in an effort to reproduce sets of experimental data. Analytic, semi-empirical functional potentials are derived from quantum-mechanics to produce different approximations to electronic wave functions for systems of particles. In both empirical and semi-empirical methods, the potential is predefined and is static over the simulation.

All three of these methods have since been advanced and remain prevalent in a number of scientific fields today.

1.2.2. Molecular Interactions and Interatomic Potentials

The molecular interactions are captured in the potential energy function, $V(\mathbf{r}_i^N)$, where $\mathbf{r}_i^N = (\mathbf{r}_1, \mathbf{r}_2, \ldots, \mathbf{r}_N)$ is an N-dimensional vector of the atomic positions.

In empirical and semi-empircal models, the importance of the potential function cannot be overstated. Once this is prescribed, the dynamics of the system are totally deterministic and the accuracy is directly dependent on the selected function. In this section we will construct a potential function under an atomic description. A general potential function is composed of two terms, namely a non-bonded interaction term and a bonded interaction term.

$$V(\mathbf{r}_i^N) = V_{non-bonded}(\mathbf{r}_i^N) + V_{bonded}(\mathbf{r}_i^N) \tag{1.2.5}$$

Non-Bonded Interactions

The non-bonded interactions aim to model the interactions between non-bonded atoms. Generally, this is expressed as an infinite sum with the terms modelling 1-body, 2-body, 3-body interactions and so on.

$$V_{non-bonded}(\mathbf{r}^N) = \sum_i u(\mathbf{r}_i) + \sum_i \sum_{j>i} v(\mathbf{r}_i, \mathbf{r}_j) + \sum_i \sum_{j>i} \sum_{k \neq i,j} w(\mathbf{r}_i, \mathbf{r}_j, \mathbf{r}_k) + \cdots \tag{1.2.6}$$

The first term in equation 1.2.6 models external energies, either externally applied fields or interactions with the boundaries. In most cases this term is dropped for periodic simulations of bulk materials, i.e. $u(\mathbf{r}_i) = 0$. The three-body term and subsequent higher order terms are typically neglected as well, and the non-bonded potential typically reduces to pair potentials

$$V_{non-bonded}(\mathbf{r}^N) = \sum_i \sum_{j>i} v(\mathbf{r}_i, \mathbf{r}_j) = \sum_i \sum_{j>i} v(r_{ij}) \tag{1.2.7}$$

where r_{ij} is the Euclidean distance between atoms i and j.

These two body, non-bonded potentials can be modelled empirically or theoretically [26] [36]. The proper modelling of non-bonded (long-range) potentials and thus forces in the molecular or atomic system is of clear importance. An example where this type of bonding is sufficient to describe the system's dynamics is the modelling of nobel gases wherein bonding does not take place.

Bonded Interactions

The use of non-bonded potentials can successfully model physical processes, however it lacks in properly capturing chemical reactions [37]. It is well understood that chemical reactions are a product of bonding, and bonding is essentially the electronic interaction between atoms of interest. As such, quantum mechanics is the proper formulation to go about modelling bonding interactions. This leads to first principle methods that are computationally intensive and thus the applications are limited. However, covalent bonding can effectively[3] be modelled with classical potentials.

The most basic form of a potential describing intramolecular bonding interactions, V_{im}, has the form [3]

---

[3]of course, approximations are made. The art is in making smart approximations.

$$V_{IM} = \frac{1}{2}\sum_i \sum_j \lambda^r_{ij}(r_{ij} - r_{eqb})^2$$

$$+ \frac{1}{2}\sum_i \sum_j \sum_k \lambda^\theta_{ijk}(\theta_{ijk} - \theta_{eqb})^2 \tag{1.2.8}$$

$$+ \frac{1}{2}\sum_i \sum_j \sum_k \sum_l \sum_m \lambda^{\omega,m}_{ijkl}(1 + \cos(m\omega_{ijkl} - \gamma_m))^2$$

where $i, j, k,$ and l all represent atom indices, and r_{ij} is the Euclidean distance between atoms i and j. The bond angle, θ, and the torsion angle, ω, are explicitly represented in equations 1.2.9 and 1.2.10, respectively and are illustrated in figure 1.2 [4]. The set of λ's are scalars determining the relative magnitude of each term.

$$\cos(\theta_{ijk}) = \frac{\mathbf{r}_{ij} \cdot \mathbf{r}_{jk}}{|\mathbf{r}_{ij} \cdot \mathbf{r}_{jk}|} \tag{1.2.9}$$

$$\cos(\omega_{ijkl}) = \frac{\mathbf{r}_{ij} \cdot \mathbf{r}_{jk}}{|\mathbf{r}_{ij} \cdot \mathbf{r}_{jk}|} \cdot \frac{\mathbf{r}_{jk} \cdot \mathbf{r}_{kl}}{|\mathbf{r}_{jk} \cdot \mathbf{r}_{kl}|} \tag{1.2.10}$$

In the first term of equation 1.2.8 a harmonic form is assumed with given equilibrium distance r_{eqb}. Additionally, the bond angles are taken to be quadratic with respect to the angular displacement between the actual bond angle and the equilibrium bond angle, θ_{eqb}. In the general case, the potential due to the torsion angle terms is expressed as an mth-order expansion of periodic functions.
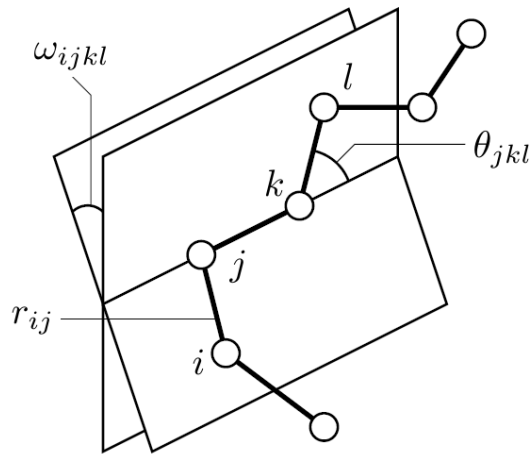
Figure 1.2: An arbitrary molecule showing the bond length r_{ij}, the bond angle θ_{jkl} and the torsion angle ω_{ijkl}.

Any given potential function will explicitly define the exact form of equation 1.2.8 and the rele-

[4]This figure was adapted from an image found in [3].

vant constants. More modern, complex potentials will additionally include cross terms and potentially weighting functions in an effort to capture the complete essence of the problem.

1.3. Popular Interaction Potentials

Over the years, many adjustments and improvements have been made to the general MD method as presented in figure 1.1. Noteworthy among these are the Verlet algorithm and Verlet list [43] to accelerate the process by only considering interactions with atoms on a specified list indicating nearest neighbours. Additionally, the introduction of periodic boundary conditions and the minimum-image convention to efficiently simulate infinite systems made large-scale simulations tractable.

Independent of the algorithm used, the success and accuracy of MD simulations is primarily dependent on the choice of the interaction potential. A large number of potentials exist, all with their respective strengths and weaknesses. As earlier outlined, many of these potentials can be partitioned into bonding (inter-atomic) or non-bonding (intra-molecular) interaction potentials. A general hierarchy of these potentials is shown in figure 1.3 [27]. A very brief overview of some popular interaction potentials will be given, and then a more detailed introduction to both the REBO and AIREBO potentials will be presented.
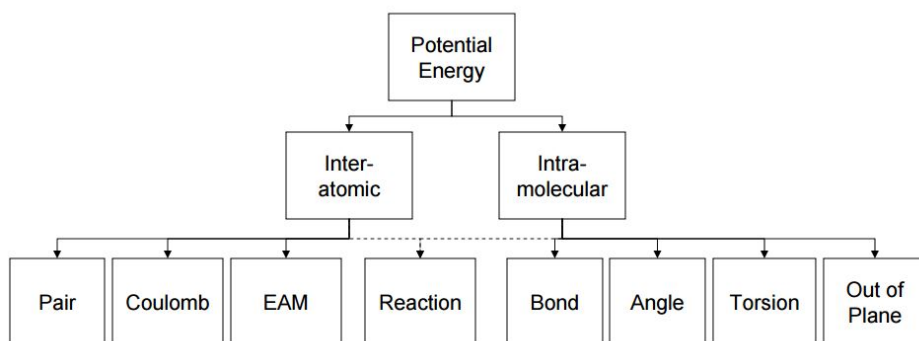
Figure 1.3: A general hierarchy and compartmentalization of potential energy functions used in MD.

1.3.1. Inter-atomic Potentials

Pair potentials model the van der Waals interactions between a pair of atoms. They contain a repulsive element as a direct result from the Pauli exclusion principle, and an attractive element that dominates at long distances due to London dispersion forces. An example of a pair potential is the Lennard-Jones (LJ) potential (sometimes referred to as the 12-6 potential) which models the interactions between a pair of neutral atoms or molecules. The LJ potential is controlled by two parameters controlling the depth of the potential well and the finite distance at which the potential is zero. The attractive term can be derived theoretically using physical arguments whereas the repulsive term has no such rigorous backbone, but is used to approximate the repulsion and is computationally conve-

nient due to it being the square of the attractive potential. For these three reasons, the LJ potential is commonly used in MD simulations.

If electrostatic charges are present, then the Coulomb potential is typically used to model the interactions. Finally, in the inter-atomic regime, embedded atom models (EAM) are used to model metallic systems [17].

1.3.2. Intra-molecular Potentials

As discussed in section 1.2.2 and shown in figure 1.3, intra-molecular interactions model the covalent bonding of systems and can be broken down into bond, angle, and torsion terms. Bond stretching models, such as the Morse bond potential [29] model the bonding interaction as an approximation to a harmonic well. Most intra-molecular potentials used in MD simulations include all of these terms (with the exception of the rarely used out-of-plane term) into one funcational form.

The MM3 and MM4 force-fields [6] [4] [5] [7] [30] [31] are used for modelling organic compounds . The Assisted Model Building with Energy Refinement (AMBER) [44] force field is commonly used for simulating the molecular dynamics of biomolecules. Additionally, the CHARMM [15] force fields are used in simulations of proteins, DNA, RNA, and lipids, and polymers.

1.3.3. Reactive Potentials

At the interface of intra-molecular and inter-atomic potentials are the reactive potentials. These potentials model chemical reactions via bond formation and disassociation. These potentials include the Tersoff potential [39], as well as the REBO and AIREBO potentials, and are discussed in the following subsections in more detail.

1.3.4. REBO Potential — A Qualitative Approach

Independent of the algorithm used, the success and accuracy of MD simulations is primarily dependent on the choice of the interaction potential that best suits the specific requirements and demands of the problem at hand. A large number of potentials exist, all with their strengths and weaknesses.

In 1990, Donald W. Brenner proposed an empirical potential for hydrocarbons [12] to effectively model chemical vapour deposition of diamond films – a short ranged potential allowing for quick numerical evaluations. The inspiration of this potential was to effectively model the essential features of the intra-molecular energies and bonding in essential hydrocarbon materials, and to allow bond breaking and forming (chemistry).

Brenner's work was based on a number of works before it. Abell first characterized and derived a general expression for the binding energy (E_b) of atoms i and j as

$$E_b = \sum_i \sum_{j<i} \left(V_R(r_{ij}) + b_{ij} V_A(r_{ij}) \right).$$
(1.3.1)

Qualitatively, the binding energy here is expressed simply as the sum of two-term repulsive potentials, V_R, and attractive potentials, V_A. The complexity of Abell's general expression is hidden in the bond-order term, b_{ij}, which dictates how likely a bond between the two atoms in question is to form. Abell showed that the bond was proportional to the inverse square root of the local coordination number, N_{ij} [1]. What Abell did was show that the binding energy could be effectively represented as a sum over nearest neighbours which allowed other terms to be neglected resulting in a drastic increase in computational speed.

Tersoff [38] [39] took this idea and developed an analytic, parametrized expression for the bond-order term. This form successfully modelled systems with the formation and dissociation of covalent chemical bonds, and in particular bonding of group IV elements in both ambient and high-pressure phases, as well as solid-state and surface defect energies [40]. The general Tersoff bond-order term[5], b_{ij}^T, is a many-body coupling between the bond from atom i to atom j and the local environment of atom i. It is a decreasing function of coordination, G_{ij}, assigned to that particular bond — that is $b_{ij}^T = b_{ij}^T(G_{ij})$ with Tersoff defining G to take the form

$$G_{ij} = \sum_k f_c(r_{ik}) g(\theta_{jik}) f(r_{ij} - r_{ik}) \tag{1.3.2}$$

where the functions f_c, g, and f are suitable functions to be fit to relevant data. The intuition is that the $i - j$ bond will be weakened in the presence of other bonds containing atom i. Notice that Tersoff's bond-order term is both a function of the local coordination number and the bond-angles. The bond-angles are introduced to stabilize open lattices from distortion due to shearing effects, and also helps to model elastic properties and defect energies [39]. Tersoff's approach allows individual atoms to not be constrained to be attached to particular neighbours or to stay in a specific hybridization state or coordination number. This approach, albeit classical in nature, is quite effective in modelling inherently quantum (binding) processes.

Although Tersoff's efforts effectively described single, double, and triple bond energies in Carbon structures, Brenner pointed out that this formulation introduces non-physical behaviour when certain radical effects are introduced as well as when conjugated and non-conjugated double bonds are examined [12] [13]. In an effort to account for these situations, Brenner expressed the bond-order term as

$$b_{ij}^B = \frac{1}{2} \left(b_{ij}^T + b_{ji}^T \right) + \frac{1}{2} F_{ij} \left(N_i, N_j, N_{ij}^{conj} \right). \tag{1.3.3}$$

The correcting function, F_{ij}, is a third order spline and adjusts the bond-order term to better model the overbinding of radicals for bonds between pairs of atoms that have different coordinations. Additionally, non-local effects can also be incorporated to a first approximation into this correcting function to account for conjugated versus non-conjugated bonding [12]. This reactive empirical bond-order (REBO) potential is then given a large set of experimental data from intelligently designed hydrocarbon reactions and is subsequently put through rigorous fitting procedures.

---

[5]Superscript T for Tersoff

Although the REBO potential was initially created to model covalent bonding interactions in hydrocarbon systems, and in particular to simulate the chemical vapour disposition of diamond, it has since been extended for use in other areas. This robust potential is now used to model the energetic, elastic, and vibrational properties of carbon and small hydrocarbon structures such as fullerenes [14] and carbon nanotubes [21].

Empirical potentials are typically designed for specific sets of chemical groups and experimental setups, and as a result fail to be general. The REBO potential is no exception, as it only has bonded-interaction terms and therefore lacks modelling non-bonded interactions. As such, the REBO potential fails to properly model dispersion and non-bonded repulsion in systems with non-negligible intermolecular interactions. This is a large class of materials, namely graphene, graphite, fullerenes, and interfacial systems [18] all of which benefit from terms modelling the non-bonded interactions.

Another factor limiting the application scope of the REBO potential is its lack of torsional term, which is considered a basic component of bonded interactions (see equation 1.2.8) and provides a penalty for rotation about single bonds.

1.3.5. AIREBO Potential — A Qualitative Approach

Stuart et al. proposed a new, adaptive intermolecular REBO potential (AIREBO) to overcome these shortcomings of Brenner's REBO potential [37]. The challenge is to allow this new potential to maintain the accuracy with regards to the reactive capabilities, while adding new functionality for non-bonded interactions and torsional events in hyrdrocarbons. As stated in [37], "*This new potential has been developed for use in simulating reactivity in condensed-phase systems where the REBO potential cannot be used, and can in principle be used for arbitrary hydrocarbon systems. But the primary goal is to make progress towards a fully reactive intermolecular potential, rather than to supplant the many existing potentials for modelling nonreactive hydrocarbons.*".

The overall approach is to effectively combine three separate potential functions, namely the REBO potential, the Lennard-Jones (LJ) potential, and a Torsional potential. The LJ potential acts to incorporate non-bonded interactions while the torsional potential acts to incorporate torsional effects in the system, both of which effects are not properly handled in the REBO formulation. Doing so is not as simply as simply adding three potentials together. Stuart et al. implement a strategy involving adaptively changing the relative weight of each term for each individual two-term interaction. A complete, concise mathematical description of the AIREBO potential is postponed until chapter 3.

1.4. Aim of Thesis Work

The aim of this thesis is straightforward and can be summarized in two, separate sections:

- to derive an analytic expression for the second derivative (Hessian) of the AIREBO potential with respect to its Euclidean coordinates, considering an atomic system composed entirely of Carbon atoms;

- to efficiently implement this analytic expression computationally using the C++ language.

1.5. Applications

A brief overview of intended applications of this work is now presented to give motivation of this proposed work.

1.5.1. Probing Graphene Defects

There exist numerous ways to probe a material to gain insight relating to its structure and properties. One general way to do this is to impinge a material with a monochromatic electromagnetic source and observe the resulting measured spectrum. Like any light-matter interaction, this impingement leads to scattering effects. Raman scattering occurs when the scattering is predominantly inelastic wherein energy is exchanged between the two systems and occurs when the impinging light couples with the vibrational, rotational, or other low-frequency modes in the material.

The direct interaction with the molecular vibrations, phonons, or other inherent material excitations, leads to an energy exchange and thus a red or blue-shift in the resulting spectrum. Subtracting the source spectrum from the resulting spectrum results in a series of peaks or troughs, corresponding to frequencies / modes where the two systems interacted. Further analysis produces a fingerprint of the molecule or material under consideration.

Graphene has recently been heralded for its novel properties and is currently an area of high impact research. While the physical properties of an ideal sheet of graphene can be analytically expressed, it is essentially impossible to produce such a pristine sheet in practice. Naturally, graphene structures produced in laboratories will be host to many defects and impurities. These imperfections can in theory alter the physical properties from those of an ideal sheet which can either make the specimen better or worse suited for a particular application domain. By understanding the effects of certain defects and impurities, graphene could be effectively probed to fully characterize its properties, or could be engineered with a specific combination of defects to tune it for certain applications.

Raman spectroscopy has been used to probe disorder in graphene via defect-activated peaks in its Raman Spectra [19]. In this same work, graphene samples are manipulated in a variety of ways to introduce specific defects. For instance, sp^3-defects were introduced by fluorination and mild oxidation, and vancancy-like defects were introduced by Ar^+ bombardment. The idea is to introduce specific, predictable defects in the graphene sheet and measure the resulting Raman spectra. By doing this, a catalogue of defects and their corresponding Raman spectral peaks can be created and used in the future to probe an arbitrary sheet of graphene.

An unavoidable weakness in this approach is that it relies on the creation of the desired defects. If the intended defect is defect A, and the result is defect B, a qualitatively and quantitatively different defect, then defect B's spectral properties will be catalogued as defect A's. This is inherently unavoidable in this style of experimental set-up wherein you experimentally introduce the phenomenon you are in turn measuring.

This thesis proposes an alternate methodology. By computationally constructing a graphene layer with specified and exact defects, one can then solve for the minimal energy configuration and subsequently set up the corresponding eigenvalue problem (see section 2.1.3, specifically equation 2.1.5 for details). The system's normal modes can then be computed and from this it is possible to directly calculate its spectral properties. This methodology ensures you probed the intended defect. The weakness, however, lies in the approximation of the underlying potential function. This results in a quicker, cheaper path to probing graphene defects which can be made arbitrarily accurate given a suitable potential. In addition, this can be done in theory for any types or combinations of defects so long as a minimal energy configuration exists. This allows scientists to uncover spectral properties of defects difficult to predictably produce in the laboratory.

1.5.2. Configurational Temperatures and Thermostats

As earlier discussed, the introduction of thermostating to MD simulations was a hallmark and turning point for the field. In a classical equilibrium ensemble of particles, temperature is typically defined as the particle's mean kinetic energy, and is thus formulated through particle momenta. In fact, kinetic thermostats are applied to center-of-mass momenta, but in dealing with molecules having many degrees of freedom, thermostating three of them may be insufficient [11].

Until the past decade, thermostating was implemented to control the kinetic temperature. However, alternatives to the kinetic temperature, and the ideal-gas thermometer controlling this kinetic temperature, exist. A thermodynamic temperature can also be defined through the relation

$$\frac{1}{T} = \left(\frac{\partial S}{\partial E}\right)\Bigg|_V \tag{1.5.1}$$

where S is the entropy, E is the internal energy and V is the system volume. Rugh [35] and Jepps et al. [23] have proved that at thermodynamic equilibrium several different versions of the thermodynamic temperature were equivalent to the kinetic temperature. Some of these versions express temperature as the configurational temperature — that is, the temperature depends exclusively on the position coordinates of the atoms. Configurational temperatures and thermodynamic temperatures are very useful in nonequilibrium statistical mechanics [11].

Several configurational temperature definitions exist and the derivations are quite involved. One such configurational temperature is given as

$$k_B T_{conf} = \frac{\left\langle \sum_{i=1}^N \left(\frac{\partial V}{\partial \mathbf{r}_i}\right)^2 \right\rangle}{\left\langle \sum_{i=1}^N \frac{\partial^2 V}{\partial \mathbf{r}_i^2} \right\rangle} \tag{1.5.2}$$

where K_B is the Boltzmann constant and T_{conf} is the configurational temperature. Notice this term only depends on the first and second derivatives of the potential function with respect to the position coordinates. Both terms can be pulled directly from the Hessian computation. In fact, if the configurational temperature is all that is desired, the computation time for the Hessian can be

drastically reduced owing to the fact that only the diagonal terms are required.

From this defintion of configurational temperature, Braga and Travis derive a Nosé-Hoover thermostat. The code developed in this thesis could then be quickly adapted to output the required variables and could then be supplemented with the thermostating to control the temperature of large Carbon systems, both at and away from thermodynamic equilibrium.

1.5.3. Measuring Mechanical Properties

There have been several models of bulk melting proposed in the past, namely those of Lindemann [42] and Born [10]. There have been no experimental results vallidating any one of these theories, however [24]. MD simulations are used to gain further insight on the phenomena of melting. Kanigel et al. showed that for NtT and NVT ensembles, the system's elastic constants can be calculated using fluctuation formulas derived by Ray and Rahman [34]. The computationally challenging aspect of this approach involves the evaluation of the Born term. This Born term contains first and second spatial derivatives of the potential energy function.

Thus the correct and efficient implementation of the first and second spatial derivatives of the potential energy function could lead to calculation of elastic constants, and later to the evaluation and simulation of phase transitions for Carbon structures.

1.5.4. Further Applications

Apart from the aforementioned applications, knowledge of the Hessian is of essential importance in other, broad fields. In optimization and searching algorithms, the evaluation of the Hessian matrix is essential for confirming the characteristics at or near a critical point. This is used two-fold,

1. For global search and energy minimization algorithms for geometrically optimized atomic networks. This, for example, is used within the context of finding new allotropes. Specific to Carbon, these hypothetical allotropes are graphyne [9], supergraphene [20], and squarographite [25], among others.

2. In determining the reaction paths and transition states of chemical reactions. Such a situation can be thought of as chemicals existing on a high dimensional energy hypersurface. If a reaction is to occur between molecules, it is energetically favourable for this to occur at the transition state, or in mathematical terms, the saddle point of this hypersurface. The difference in energy between the initial configuration and the saddle point configuration is the binding energy of the reaction. When simulating such events, one method is the steepest descent, or conjugate gradient method to locate the local energy minimum. Once the atomic system's geometry is in this specific configuration, the Hessian must be calculated and its eigenvalues investigated. If the calculated geometry is in fact an energy minimum, then there should be one negative eigenvalue representing the reaction coordinate. Thus again, the Hessian must be calculated for these purposes.

3. Second order optimization algorithms often require use of the Hessian matrix. This would allow such algorithms, i.e. Newton's algorithm, to be employed for systems modelled by the AIREBO potential.

Chapter 2

Preliminary Material and Methodology

2.1. Preliminary Material

This section briefly outlines required preliminary material and nomenclature. It also serves to give a more detailed description of normal modes and their importance in the domain of molecular dynamics.

2.1.1. The Hessian Matrix

Molecular systems are usually expressed in one of two coordinate systems. The first being the Euclidean system where in a system of N atoms there are then $3N$ degrees of freedom. Molecular systems are also often expressed in terms of internal coordinates (Z-Matrix is also used in the nomenclature) wherein coordinate descriptions are made relative to one another using interatomic distances, bond angles and torsion angles as intrinsic coordinates.

In the absence of an external field, the molecular system's energy does not depend on its particular orientation in space, thus you lose the 3 translational degrees of freedom. Similarly, the system does not depend on it's center of mass which drops the 3 rotational degrees of freedom (2 for linear molecules). This lack of an external field results in the total reduction of the degrees of freedom from $3N$ to $3N - 6$ ($3N - 5$ for linear molecules) which can be thought of as the system's vibrational degrees of freedom. This thesis exclusively uses Euclidean coordinates, although transformations to and from coordinate systems exist.

The Hessian of such a system is defined to be the matrix of second derivatives of the potential energy function with respect to the Euclidean coordinates. This is then the $3N \times 3N$ matrix with elements

$$\frac{\partial^2 V}{\partial u_{p_i} \partial u_{q_j}} \qquad (2.1.1)$$

where p and q are atom indices and $i, j \in \{x, y, z\}$ are specific directions. With atomic configurations such as graphene, the modelled systems may have on the order of 1000 atoms. In such a system the Hessian matrix would have on the order of 10 million elements. This introduces many problems, namely computational time and memory required to store such a system.

These problems, however, are mitigated for two main reasons. Firstly, if continuity of the partial derivatives is assumed, Hessian matrices are inherently symmetric — removing the need to compute and store nearly half the variables. Secondly, potential energy functions, and the AIREBO potential in particular, are characterized by cutoff radii. As such, the Hessian will be highly sparse. If proper methods and precautions are used in the numerical implementation one can forego calculating and storing many of the elements.

2.1.2. Notational Remarks

The degrees of freedom for our system are represented by the Euclidean coordinates of the N atoms, resulting in a set, $\mathcal{A}$, with $3N$ elements

$$\mathcal{A} = \{u_{1_x}, u_{1_y}, u_{1_z}, u_{2_x}, u_{2_y}, u_{2_z}, \ldots, u_{N_x}, u_{N_y}, u_{N_z}\}. \tag{2.1.2}$$

The above notation, albeit in some cases clear, is somewhat cumbersome. A more natural notation is introduced here as

$$\mathcal{A}' = \{u_1, u_2, u_3, \ldots, u_{3N}\}. \tag{2.1.3}$$

In following sections, $\mathcal{A}'$ will be indexed with the indices $\alpha = 3p + i \in \{1, 2, 3, \cdots, 3N\}$ and $\beta = 3q + j \in \{1, 2, 3, \cdots, 3N\}$. Note that $\mathcal{A}$ and $\mathcal{A}'$ are related via a trivial isomorphism and are thus equivalent — all we have done is a relabelling of elements.

2.1.3. Normal Modes

In the context of molecular and atomic systems, the potential energy function represents an energy hyper-surface directing the movement of atoms and thus charting possible chemical reaction paths.

Intuitively, this is done by Taylor expanding the potential energy function in terms of the mass-weighted coordinates, $\overline{u}_\alpha = \sqrt{m_\alpha} \Delta x_\alpha$. The systems handled in this thesis will strictly be composed of Carbon atoms and thus the mass can be considered to be unity, and as a result the position coordinates, u_α will only be of interest.

If the atomic configuration is in an energy minimum the first order term is identically zero and if the expansion is cut off at the quadratic term the Taylor expansion yields

$$V = \frac{1}{2} \sum_{p,q=1}^{N} \sum_{i,j=1}^{3} \left. \frac{\partial^2 V}{\partial u_{p_i} \partial u_{q_j}} \right|_{\mathcal{E}} u_{p_i} u_{q_j} \tag{2.1.4}$$

where the second derivative is evaluated at the equilibrium configuration, $\mathcal{E}$.

The result is that the energy hypersurface is represented by a high-dimensional parabola characterized by the second derivatives evaluated at the energy minimum. However, in a realistic system at non-zero temperatures, the energy hypersurface is characterized by many local energy minima with reaction paths traversing through saddle points of various heights from one minimum to a neighbouring one.

If the second derivatives of equation 2.1.4 are expressed in terms of their Hessian, H, then by casting it as an eigenvalue problem one can calculate the eigenvectors, $\mathbf{w}_\alpha$, and associated eigenvalues, ω_α^2.

$$\mathbf{H}\mathbf{w}_\alpha = \omega_\alpha^2 \mathbf{w}_\alpha \tag{2.1.5}$$

Solving this system of $3N$ equations equates to solving its secular determinant

$$\begin{vmatrix} H_{1,1} - \omega^2 & H_{1,2} & H_{1,3} & \dots & H_{1,3N} \\ H_{2,1} & H_{2,2} - \omega^2 & H_{2,3} & \dots & H_{2,3N} \\ \vdots & \vdots & \vdots & \ddots & \vdots \\ H_{3N,1} & H_{3N,2} & H_{3N,3} & \dots & H_{3N,3N} - \omega^2 \end{vmatrix} = 0 \tag{2.1.6}$$

Solving equation 2.1.6 for each eigenvalue is akin to matrix diagonalization. This is a highly non-trivial task, but the symmetric and sparse nature of the matrix $\mathbf{H}$ allows for certain numerical packages and techniques to be implemented making the diagonalization more tractable. Once the eigenvalues, ω_β^2, are calculated, the corresponding eigenvectors, $\mathbf{w}_\beta$, are easily calculated which then allows the motion of atom α for the given eigenvalue to be evaluated as

$$u_{\alpha\beta} = w_{\alpha\beta} \cos(\omega_\beta t + \phi_\beta) \tag{2.1.7}$$

due to the harmonic nature of the problem, where ϕ_β is a phase term. We can now define a new set of coordinates using these normal modes.

$$\xi_\beta = \sum_{\alpha=1}^{3N} w_{\alpha\beta} u_\alpha \tag{2.1.8}$$

This gives the "Normal Coordinates" of the system. By the finite-dimensional spectral theorem, a real and symmetric matrix $\mathbf{H}$ can be diagonalized by an orthogonal matrix. Furthermore, it is characterized by an orthonormal basis (set of eigenvectors).

Physically, the eigenvectors are the normal modes of vibration vibrating at the frequency

specified by its associated eigenvalue. Due to the orthonormality of the eigenvectors, the normal mode coordinates oscillate harmonically and independently (as one would expect by the naming convention) with angular frequency ω_β.

Equivalently, the entire movement of an atomic system can be expressed as a linear combination of normal mode vibrations. That is, atomic systems vibrate in certain ways specified by their eigenvectors at frequencies proportional to the corresponding eigenvalue. These normal mode coordinates are linear combinations of the atom-based Cartesian coordinates and thus the entire mechanical system can be thought of as complex vibrations of the Cartesian coordinates.

2.2. Thesis Methodology

2.2.1. Order of Operations

As briefly outlined in section 1.3.5, the AIREBO potential is a sum of the REBO potential, the LJ potential, and a torsional potential.

$$E = E^{REBO} + E^{LJ} + E^{tors}. \tag{2.2.1}$$

This thesis will present the analytical form of the 2nd derivative of the AIREBO potential for Carbon only systems. That is, symbolically:

$$\frac{\partial^2}{\partial u_p \partial u_q} E = \frac{\partial^2}{\partial u_p \partial u_q} E^{REBO} + \frac{\partial^2}{\partial u_p \partial u_q} E^{LJ} + \frac{\partial^2}{\partial u_p \partial u_q} E^{tors}. \tag{2.2.2}$$

This can and will alternatively be represented in more compact notation as

$$E'^\dagger = E^{REBO'^\dagger} + E^{LJ'^\dagger} + E^{tors'^\dagger}. \tag{2.2.3}$$

where both the $'$ and $\dagger$ superscripts denote derivatives and will be explained in the following subsection.

A detailed description of the all three involved potentials will be given, and their first and second derivatives will all thoroughly be analytically calculated. Since the three potential functions are independent, they will be handled completely separately. The order of such presentation is found in table 2.1.

2.2.2. Mathematical Formulation and Notation

The derivation in later chapters is lengthy and as a result many abbreviations and notations will be used. This subsection serves to provide these, as well as the mathematical framework.

Table 2.1: The order of presentation

	E^{REBO}	E^{LJ}	E^{tors}
Energy Term	1	4	7
1st Derivative	2	5	8
2nd Derivative	3	6	9

We begin by considering a system of N Carbon atoms all interacting through the AIREBO potential. Ths potential has two-term, three-term, and four-term interactions. As such, we must define the atoms used in the notation. The atoms, indexed by i, j, k, l, will always be considered in the order of

$$\text{atom } i \to \text{atom } j \to \text{atom } k \to \text{atom } l$$

That is, atom k is only considered in three and four term interactions, and atom l is only considered in four term interactions.

Since we are interested in the Hessian of the AIREBO potential, this will of course involve single and double derivatives. We must first get an intuitive understanding of what a derivative is within this Euclidean framework.

Consider the interaction between atoms i and j, separated by the distance r_{ij}. In theory, this interatomic distance can change if there is a small perturbation to the local position of any one of the N atoms. Consider a small perturbation of atom q. Then the associated derivative is $\frac{\partial}{\partial u_q} r_{ij}$.

This, however, must be refined even further. We will be working inside the Euclidean framework, so the position of atom q, u_q, actually has three components, namely u_{q_α} with $\alpha \in \{x, y, z\}$. It will be far too cumbersome and redundant to apply this notation throughout the entire text so for the remaining sections the α notation will be suppressed. That is everything will be a three dimensional vector with Euclidean components.

As mentioned, derivatives can be thought of the effect of perturbations of atomic positions. The second derivative is taken by applying a second perturbation to any of the N atoms. This is conceptually trivial.

The cornerstone of this paper will be taking the derivatives of the distance vector r_{ij}. As such, a thorough derivation is now presented, beginning with the definition of r_{ij}.

$$r_{ij} := \sqrt{(u_{j_x} - u_{i_x})^2 + (u_{j_y} - u_{i_y})^2 + (u_{j_z} - u_{i_z})^2} \tag{2.2.4}$$

All derivatives will be with respect to the position coordinate of an atom, $\mathbf{u}_q$. As such, regardless of the variable in question, there will always be a $\frac{\partial}{\partial u_q} r_{ij}$ term present in single derivatives and a $\frac{\partial^2}{\partial u_p \partial u_q} r_{ij}$ term present in double derivatives.

These derivatives will be presented here in their complete form. We begin by noting

$$\frac{\partial}{\partial u_q} r_{ij} = 0 \qquad\qquad \forall\, q \notin \{i, j\} \tag{2.2.5}$$

We will now calculate $\frac{\partial}{\partial u_{i_x}} r_{ij}$ by coordinate.

$$\frac{\partial}{\partial u_{i_x}} r_{ij} = \frac{1}{2\sqrt{(u_{j_x} - u_{i_x})^2 + (u_{j_y} - u_{i_y})^2 + (u_{j_z} - u_{i_z})^2}} \cdot 2(u_{j_x} - u_{i_x}) \cdot (-1) = \frac{-1}{r_{ij}}(u_{j_x} - u_{i_x}) \tag{2.2.6}$$

Likewise,

$$\frac{\partial}{\partial u_{i_y}} r_{ij} = \frac{-1}{r_{ij}}(u_{j_y} - u_{i_y}) \tag{2.2.7}$$

$$\frac{\partial}{\partial u_{i_z}} r_{ij} = \frac{-1}{r_{ij}}(u_{j_z} - u_{i_z}) \tag{2.2.8}$$

Note that by symmetry we have $\frac{\partial}{\partial u_j} r_{ij} = -\frac{\partial}{\partial u_i} r_{ij}$. Generalizing, then, we find

$$\frac{\partial}{\partial u_q} r_{ij} = \delta_{jq} \frac{u_j - u_i}{r_{ij}} - \delta_{iq} \frac{u_j - u_i}{r_{ij}} \tag{2.2.9}$$

where δ is the Kronecker delta function.

The double derivative is calculated as follows:

$$\frac{\partial^2}{\partial u_p \partial u_q} r_{ij} = \delta_{jq} \left[\frac{\partial}{\partial u_p} \frac{u_j - u_i}{r_{ij}} \right] - \delta_{iq} \left[\frac{\partial}{\partial u_p} \frac{u_j - u_i}{r_{ij}} \right] \tag{2.2.10}$$

where

$$
\begin{aligned}
\frac{\partial}{\partial u_p} \frac{u_j - u_i}{r_{ij}} &= \frac{\left(\delta_{jp} - \delta_{ip}\right) \cdot r_{ij} - \left(u_j - u_i\right) \cdot \frac{\partial}{\partial u_p}(r_{ip})}{r_{ij}^2} \\
&= \frac{\left(\delta_{jp} - \delta_{ip}\right) \cdot r_{ij} - \left(u_j - u_i\right) \left[\delta_{jp} \frac{u_j - u_i}{r_{ij}} - \delta_{ip} \frac{u_j - u_i}{r_{ij}} \right]}{r_{ij}^2}
\end{aligned}
\tag{2.2.11}
$$

So

26

$$\frac{\partial^2}{\partial u_p \partial u_q} r_{ij} = \left(\delta_{jq} - \delta_{iq}\right) \left[\frac{\left(\delta_{jp} - \delta_{ip}\right) \cdot r_{ij} - \left(u_j - u_i\right) \left[\left(\delta_{jp} - \delta_{ip}\right)\left(\frac{u_j - u_i}{r_{ij}}\right)\right]}{r_{ij}^2} \right] \tag{2.2.12}$$

$$\frac{\partial^2}{\partial u_p \partial u_q} r_{ij} = \left(\delta_{jq} - \delta_{iq}\right) \cdot \left(\delta_{jp} - \delta_{ip}\right) \cdot \left[\frac{r_{ij}^2 - \left(u_j - u_i\right)^2}{r_{ij}^3} \right] \tag{2.2.13}$$

Since $\frac{\partial}{\partial u_q} r_{ij}$, $\frac{\partial}{\partial u_p} r_{ij}$ and $\frac{\partial^2}{\partial u_p \partial u_q} r_{ij}$ will appear in many terms, we introduce the following notation that will be used throughout the entire document.

$$\frac{\partial}{\partial u_q} r_{ij} := r'_{ij}$$
$$\frac{\partial}{\partial u_p} r_{ij} := r^\dagger_{ij} \tag{2.2.14}$$
$$\frac{\partial^2}{\partial u_p \partial u_q} r_{ij} := r'^\dagger_{ij}$$

Of course, most functions do not depend explicitly on position variables. It is worthwhile to now look at the following examples in to taking derivatives of functions that depend only implicitly on position coordinates.

Consider taking the derivative of a general function f:

$$f'\left((g(r_{ij}), h(r_{ij})\right) \equiv \frac{\partial}{\partial u_q} f(g(r_{ij}), h(r_{ij})) = \frac{\partial}{\partial g(r_{ij})} f(g(r_{ij}), h(r_{ij})) \cdot \frac{\partial}{\partial u_q} g(r_{ij})$$
$$+ \frac{\partial}{\partial h(r_{ij})} f(g(r_{ij}), h(r_{ij})) \cdot \frac{\partial}{\partial u_q} h(r_{ij}) \tag{2.2.15}$$

One last thing that is very important to mention and easy to overlook is the following fact. Consider taking the second derivative of the function $f(g(r_{ij}))$. Immediately, one may think the result is

$$\frac{\partial^2}{\partial u_p \partial u_q} f(g(r_{ij})) = \frac{\partial^2 f(g(r_{ij}))}{\partial^2 g(r_{ij})} \cdot \frac{\partial^2 g(r_{ij})}{\partial u_p \partial u_q}$$

This is incorrect. Recall we do the first derivative in its entirety, and then take the second derivative to that result.

$$\frac{\partial^2}{\partial u_p \partial u_q} f(g(r_{ij})) = \frac{\partial}{\partial u_p} \left[\frac{\partial f(g(r_{ij}))}{\partial g(r_{ij})} \cdot \frac{\partial g(r_{ij})}{\partial u_q} \right]$$

$$= \frac{\partial^2 f(g(r_{ij}))}{\partial^2 g(r_{ij})} \cdot \frac{\partial g(r_{ij})}{\partial u_q} \cdot \frac{\partial g(r_{ij})}{\partial u_p} + \frac{\partial f(g(r_{ij}))}{\partial g(r_{ij})} \cdot \frac{\partial^2 g(r_{ij})}{\partial u_p \partial u_q} \qquad (2.2.16)$$

$$=: f^{'\dagger}(g(r_{ij}))$$

The derivatives taken in the remainder of the paper will be of this form. One may think it is misleading to hide all this information inside the notation of $f^{'\dagger}(g(r_{ij}))$. This would be understandable if other operators were to operate on this, but since no higher derivatives are taken, it is safe to keep the information in this compact form – mind you it is very important not to forget that this simple notation has more complex information behind it.

The primary focus of chapter 3 is to present the derivation of the Hessian in a symbolic and algebraic form. Due to the nature of the AIREBO potential having many terms, this will be presented in many smaller parts. Once the second derivatives of all individual parts are calculated, chapter 4 provides an overall summary as well as analysis on the individual terms' interaction radii.

Chapter 3

Calculations

3.1. REBO Potential for Carbon Only Systems

This will be a detailed mathematical treatment of the REBO potential. For further descriptions and motivation for the individual terms, consult [37]. We will present the REBO potential piece by piece. Recall the AIREBO potential is constructed for hydrocarbons, whereas the aim of this thesis is to present it's Hessian for Carbon systems. As such, the original AIREBO potential will be presented, but proper adjustments will immediately be made removing all Hydrogen dependencies.

In general, the REBO potential for interacting atoms i and j is given by

$$E_{ij}^{REBO} = V_{ij}^R + b_{ij}V_{ij}^A \tag{3.1.1}$$

We will investigate equation 3.1.1 in three separate parts, namely

- repulsive potential, V^R;

- bond order term, b_{ij};

- attractive potential, V^A.

3.1.1. Repulsive Term

The repulsive term is represented by

$$V_{ij}^R = w_{ij}(r_{ij})\left[1 + \frac{Q_{ij}}{r_{ij}}\right]A_{ij}e^{-\alpha_{ij}r_{ij}} \tag{3.1.2}$$

where the constants $Q, A,$ and α depend on the atom types of atoms i and j, and w is the bond weighting factor

$$w_{ij}(r_{ij}) = S_s\left(t_c(r_{ij})\right). \tag{3.1.3}$$

This shuts off (i.e. is 0) when distances exceed typical bonding distances. This switching function, S_s (with the subscript s representing sinusoidal), is described by

$$S_s(t) = \Theta(-t) + \Theta(t)\Theta(1-t)\frac{1}{2}\left[1 + \cos(\pi t)\right] \tag{3.1.4}$$

where $\Theta(t)$ is the Heaviside function. In our case the variable within the switch function is

$$t_c(r_{ij}) = \frac{r_{ij} - r_{ij}^{min}}{r_{ij}^{max} - r_{ij}^{min}} \tag{3.1.5}$$

where r_{ij}^{max} and r_{ij}^{min} are parameters defining the switching region. These parameters, along with all future ones, will not be explicitly given as they do not pertain to this thesis. The interested reader can consult [37] for numerical values.

The weight function presented in equation 3.1.3 are used ubiquitously in the AIREBO potential to adaptively set the weights for a number of functions and so a thorough understanding of them is essential. Equation 3.1.3 is plotted in figure 3.1 with parameters $r_{ij}^{max} = 1.0$ and $r_{ij}^{min} = 4.0$.
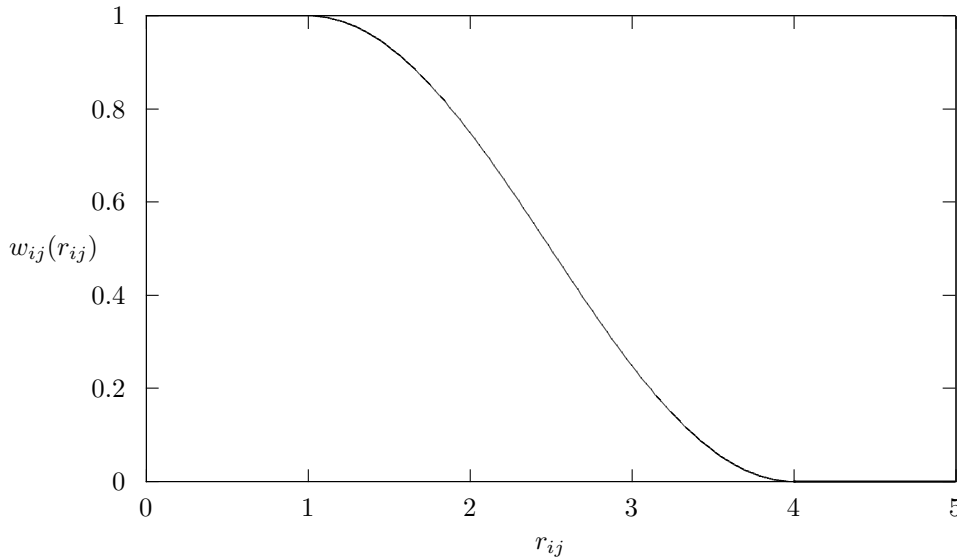
Figure 3.1: Weight function with $r_{ij}^{min} = 1.0$ and $r_{ij}^{max} = 4.0$.

From further analysis we see that $w_{ij}(r_{ij})$ is nonzero only on the interval of $r_{ij} \in [0, r^{max}]$. This concludes the repulsive term definition for general hydrocarbon systems.

With respect to the respulsive term, not much needs to change in removing the Hydrogen dependencies. The constants Q, A, and α from equation 3.1.2 no longer depend on bonding type and can thus lose their subscripts. Equation 3.1.2 now becomes

$$V_{ij}^R = w_{ij}(r_{ij}) \left[1 + \frac{Q}{r} \right] A e^{-\alpha r} \tag{3.1.6}$$

Similarly, the subscripts in equation 3.1.5 represent the bonding types. They can thus be removed and we will introduce the following notation

$$t_c(r_{ij}) = \frac{r_{ij} - r^{min}}{r^{max} - r^{min}} =: r_{ij}^c. \tag{3.1.7}$$

Summarizing, we find for the Hydrogen-less repulsive term

$$V_R(r_{ij}) = w_{ij}(r_{ij}) \left[1 + \frac{Q}{r_{ij}} \right] A e^{-\alpha r_{ij}} \tag{3.1.8}$$

with

$$w_{ij}(r_{ij}) = \Theta(-r_{ij}^c) + \Theta(r_{ij}^c)\Theta(1 - r_{ij}^c)\frac{1}{2}\left[1 + \cos(\pi r_{ij}^c) \right] \tag{3.1.9}$$

3.1.2. Bond-Order Term

The bond order models the likeliness and strength of bonding between between atoms i and j and is given by

$$b_{ij} = \frac{1}{2}\left[p_{ij}^{\pi\theta} + p_{ji}^{\pi\theta} \right] + \pi_{ij}^{rc} + \pi_{ij}^{dh} \tag{3.1.10}$$

Where the principal (p) terms are the covalent bond interaction terms outlined in the introduction, π_{ij}^{rc} models radical and conjugation effects, and π_{ij}^{dh} incorporates a penalty for rotation around multiple bonds.

Covalent Bond Interaction Terms

These terms, $p_{ij}^{\pi\theta}$ and $p_{ji}^{\pi\theta}$, are given by

$$p_{ij}^{\pi\theta} = \left[1 + \sum_{k \neq i,j} w_{ik}(r_{ik})g_i(\cos(\theta_{jik}))e^{\lambda_{jik}} + P_{ij} \right]^{-\frac{1}{2}} \tag{3.1.11}$$

Some things to note:

- $p_{ij}^{\pi\theta}$ does not necessarilly equal $p_{ji}^{\pi\theta}$;

- although their numerical value may not be equal, their analytical form is one and the same once

31

the indices are switched. Therefore, we will only present the analytical form for $p_{ij}^{\pi\theta}$.

We immediately notice that the covalent bond interaction terms depend on the neighbouring atoms. The relative strength of their interactions are again governed by a weighting function, $w_{ik}(r_{ik})$, as defined in equation 3.1.3.

Additionally, $g_i\big(\cos(\theta_{jik})\big)$ is a penalty function that imposes a cost on bonds that are too close to one another. Specifically, it is a fifth order spline in the variable $\cos(\theta_{jik})$ where θ_{jik} are the bond angles between the $\mathbf{r}_{ji}$ vector and the $\mathbf{r}_{ki}$ vectors to any other neighbouring atoms[1].

$$\cos(\theta_{jik}) = \frac{\mathbf{r}_{ji} \cdot \mathbf{r}_{ki}}{\sqrt{\mathbf{r}_{ji}^2 \mathbf{r}_{ki}^2}} \tag{3.1.12}$$

We will typically leave spline functions untouched, i.e. keep them in their concise, general form. This is because taking their derivatives later is simple and we know how to do this. But for completeness, when they are introduced we will provide their definitions[2]. We begin with $g_i\big(\cos(\theta_{jik})\big)$, where the subscript i on g refers to the atom type under consideration, which in the Carbon-only case reduce to $g_c\big(\cos(\theta_{jik})\big)$.

$$g_c\big(\cos(\theta_{jik})\big) = g_c^{(1)}(\cos(\theta_{jik})) + S_s(t_N(N_{ij}))\left[g_c^{(2)}(\cos(\theta_{jik})) - g_c^{(1)}(\cos(\theta_{jik}))\right] \tag{3.1.13}$$

where $g_c^{(1)}$ and $g_c^{(2)}$ are predefined functions fit to relevant experimental data. The switching function is as described before in equation 3.1.4, but this time the variable is defined as

$$t_N(N_{ij}) = \frac{N_{ij} - N_{ij}^{min}}{N_{ij}^{max} - N_{ij}^{min}} \tag{3.1.14}$$

In this context, the i, j subscript on the min and max terms refers to the atom types and can thus be ignored. Explicitly, and introducing the following notation, we have

$$t_N(N_{ij}) = \frac{N_{ij} - N^{min}}{N^{max} - N^{min}} =: N_{ij}^c \tag{3.1.15}$$

where N^{max} and N^{min} are given parameters and N_{ij} is the coordination number of atom i in the context of the $i - j$ bond (excludes the neighbour j from the count). It is defined by the sum of coordination numbers with respect to Hydrogen and Carbon.

---

[1]Note that $\mathbf{r}_{ij}$ is the vector connecting atoms i and j, and has length r_{ij}
[2]A total description of the spline functions and their derivatives is given in Appendix A

$$N_{ij} = N_{ij}^H + N_{ij}^C \qquad (3.1.16)$$

Clearly in the Carbon only context $N_{ij}^H = 0$. Further, we have

$$N_{ij} = N_{ij}^C = \left(\sum_{k \neq i} \delta_{kC} w_{ik}(r_{ik}) \right) - \delta_{jC} w_{ij}(r_{ij}) \qquad (3.1.17)$$

where δ is the Kronecker delta function. Clearly, in the absence of Hydrogen atoms, equation 3.1.17 reduces to

$$N_{ij} = \left(\sum_{k \neq i} w_{ik}(r_{ik}) \right) - w_{ij}(r_{ij}) \qquad (3.1.18)$$

which can then further be reduced to

$$N_{ij} = \sum_{k \neq i,j} w_{ik}(r_{ik}) \qquad (3.1.19)$$

The above simplifications can all concisely be represented as

$$S_s(t_N(N_{ij})) \equiv w_{ij}(N_{ij}) \qquad (3.1.20)$$

So in total, $g_c\big(\cos(\theta_{jik})\big)$ has the following functional form:

$$g_c\big(\cos(\theta_{jik})\big) = g_c^{(1)}(\cos(\theta_{jik})) + w_{ij}(N_{ij}) \left[g_c^{(2)}(\cos(\theta_{jik})) - g_c^{(1)}(\cos(\theta_{jik})) \right] \qquad (3.1.21)$$

As section 5.2 will outline, equation 3.1.21 was deemed an error by Stuart et al. in their paper, and the correct form is represented in equation 3.1.22. Again, section 5.2 will give a detailed explanation as to the reasoning and consequences of this. For a consistency between the C++ implementation of the Hessian and the analytical form presented herein, equation 3.1.22 is assumed to be correct for the remainder of the thesis.

$$g_c\big(\cos(\theta_{jik})\big) = g_c^{(2)}(\cos(\theta_{jik})) + w_{ij}(N_{ij}) \left[g_c^{(1)}(\cos(\theta_{jik})) - g_c^{(2)}(\cos(\theta_{jik})) \right] \qquad (3.1.22)$$

Continuing with the presentation of the AIREBO potential, the λ term in equation 3.1.11 is defined to be

$$\lambda_{jik} = 4\delta_{iH}J \tag{3.1.23}$$

where J represents a series of further functions. This notation is used because clearly $\lambda_{jik} \equiv 0$ in a Carbon only system and thus $e^{\lambda_{jik}} = 1$.

P_{ij} is definied to be a 2D cubic spline in the variables N_{ij}^C and N_{ij}^H, and thus for the Carbon-only setting reduces to a 1D cubic spline in N_{ij}^C. As such, it will be left as is and only mentioned in Appendix A.

We will now look at the π terms of equation 3.1.10.

π **terms**

The term π_{ij}^{rc} represents the radical and conjugation effects. This is a 3D cubic spline in the variables N_{ij}, N_{ji} and N_{ij}^{conj} . The 3D cubic spline will be left out here and presented in Appendix A. The coordination numbers N_{ij} and N_{ji} are as defined in equation 3.1.19 and N_{ij}^{conj} is a local measure of the conjugation of the $i - j$ bond.

$$N_{ij}^{conj} = 1 + \left[\sum_{k \neq i,j} \delta_{kC} w_{ik}(r_{ik}) S_s(t_{conj}(N_{ki}))\right]^2 + \left[\sum_{l \neq i,j} \delta_{lC} w_{jl}(r_{jl}) S_s(t_{conj}(N_{lj}))\right]^2 \tag{3.1.24}$$

For the Carbon only systems this becomes

$$N_{ij}^{conj} = 1 + \left[\sum_{k \neq i,j} w_{ik}(r_{ik}) S_s(t_{conj}(N_{ki}))\right]^2 + \left[\sum_{l \neq i,j} w_{jl}(r_{jl}) S_s(t_{conj}(N_{lj}))\right]^2 \tag{3.1.25}$$

where the switching function variable, due to the absence of Hydrogen, is the same as before.

$$t_{conj}(N_{ij}) = \frac{N_{ij} - N_{ij}^{min}}{N_{ij}^{max} - N_{ij}^{min}} =: N_{ij}^c \tag{3.1.26}$$

where $N_{ij}^{conj} \in [1, 9]$. Note that this can all be written more compactly as

$$N_{ij}^{conj} = 1 + \left[\sum_{k \neq i,j} w_{ik}(r_{ik}) w_{ki}(N_{ki})\right]^2 + \left[\sum_{l \neq i,j} w_{jl}(r_{jl}) w_{lj}(N_{lj})\right]^2 \tag{3.1.27}$$

The final contribution to the bond-order is π_{ij}^{dh}.

$$\pi_{ij}^{dh} = T_{ij}(N_{ij}, N_{ji}, N_{ij}^{conj}) \sum_{k \neq i,j} \sum_{l \neq i,j} (1 - \cos^2 \omega_{kijl}) \cdot$$
$$w_{ik}^T(r_{ik}) w_{jl}^T(r_{jl}) \Theta(\sin(\theta_{jik}) - s^{min}) \Theta(\sin(\theta_{ijl}) - s^{min}) \tag{3.1.28}$$

This term imposes a penalty for rotation around multiple bonds. Equation 3.1.28 is another instance of the analytical form not being equivalent to the form found in the C++ implementation. As section 5.2 will explain, it was deemed that the implementation version, as presented in equation 3.1.29, is the correct function. For now the explanation will not be given and the derivation will be continued.

$$\pi_{ij}^{dh} = T_{ij}(N_{ij}, N_{ji}, N_{ij}^{conj}) \sum_{k \neq i,j} \sum_{l \neq i,j} (1 - \cos^2 \omega_{kijl}) \cdot$$
$$w_{ik}^T(r_{ik}) w_{jl}^T(r_{jl}) \left(1 - S_s \left(t \left(\cos \left(\theta_{jik}\right)\right)\right)\right) \cdot \left(1 - S_s \left(t \left(\cos \left(\theta_{ijl}\right)\right)\right)\right) \tag{3.1.29}$$

where

$$t \left(\cos \left(\theta_{ijl}\right)\right) = \frac{\cos \left(\theta_{ijl}\right) - \cos \left(\theta_{ijl}\right)^{min}}{\cos \left(\theta_{ijl}\right)^{max} - \cos \left(\theta_{ijl}\right)^{min}} \tag{3.1.30}$$

Equation 3.1.29 is equivalently rewritten as

$$\pi_{ij}^{dh} = T_{ij}(N_{ij}, N_{ji}, N_{ij}^{conj}) \sum_{k \neq i,j} \sum_{l \neq i,j} (1 - \cos^2 \omega_{kijl}) \cdot$$
$$w_{ik}^T(r_{ik}) w_{jl}^T(r_{jl}) \left(1 - w \left(\cos \left(\theta_{jik}\right)\right)\right) \cdot \left(1 - w \left(\cos \left(\theta_{ijl}\right)\right)\right) \tag{3.1.31}$$

The function T_{ij} is another 3D cubic spline in the same variables and ω_{kijl} is the typical torsion angle defined by

$$\cos(\omega_{kijl}) = \frac{\mathbf{r_{ji}} \times \mathbf{r_{ik}}}{\left|\mathbf{r_{ji}} \times \mathbf{r_{ik}}\right|} \cdot \frac{\mathbf{r_{ij}} \times \mathbf{r_{jl}}}{\left|\mathbf{r_{ij}} \times \mathbf{r_{jl}}\right|}. \tag{3.1.32}$$

The weight function is defined by

$$w_{ij}^T(r_{ij}) = S_s \left(t_c^T(r_{ij})\right) \tag{3.1.33}$$

where

$$t_c^T(r_{ij}) = \frac{r_{ij} - r_{ij}^{min}}{r_{ij}^{maxT} - r_{ij}^{min}}. \tag{3.1.34}$$

For Carbon only systems, $r_{ij}^{maxT} = r_{ij}^{max}$ and thus $w_{ij}^T(r_{ij}) = w_{ij}(r_{ij})$. Therefore this entire term can be rewritten as

$$
\begin{aligned}
\pi_{ij}^{dh} = & T_{ij}(N_{ij}, N_{ji}, N_{ij}^{conj}) \sum_{k \neq i,j} \sum_{l \neq i,j} (1 - \cos^2 \omega_{kijl}) \cdot \\
& w_{ik}(r_{ik}) w_{jl}(r_{jl}) \left(1 - w \left(\cos \left(\theta_{jik} \right) \right) \right) \cdot \left(1 - w \left(\cos \left(\theta_{ijl} \right) \right) \right)
\end{aligned}
\tag{3.1.35}
$$

That concludes the bond-order term.

3.1.3. Attractive Potential

The final part of the REBO potential is the attractive potential, V_{ij}^A.

$$
V_{ij}^A = -w_{ij}(r_{ij}) \sum_{n=1}^{3} B_{ij}^{(n)} e^{-\beta_{ij}^{(n)} r_{ij}}
\tag{3.1.36}
$$

The n *does not* represent the bonding type (i.e. C-C, C-H, H-H) but the $i - j$ subscripts on B and β do. As such we remove this dependency on the relevant terms to find

$$
V_{ij}^A = -w_{ij}(r_{ij}) \sum_{n=1}^{3} B^{(n)} e^{-\beta^{(n)} r_{ij}}
\tag{3.1.37}
$$

3.1.4. Summary of REBO Potential for Carbon only Systems

The REBO potential for a system composed only of Carbon atoms can then concisely be represented as

$$
E_{ij}^{REBO} = \left[w_{ij}(r_{ij}) \left[1 + \frac{Q}{r_{ij}} \right] A e^{-\alpha r_{ij}} \right] + \left[\frac{1}{2} \left[p_{ij}^{\pi\theta} + p_{ji}^{\pi\theta} \right] + \pi_{ij}^{rc} + \pi_{ij}^{dh} \right] \cdot \left[-w_{ij}(r_{ij}) \sum_{n=1}^{3} B^{(n)} e^{-\beta^{(n)} r_{ij}} \right]
\tag{3.1.38}
$$

3.2. Derivative of the REBO energy

Recall the expression for the REBO energy:

$$
E_{ij}^{REBO} = V_{ij}^R + b_{ij} V_{ij}^A.
\tag{3.2.1}
$$

In general, the derivative takes the form

$$E_{ij}^{REBO'} = V_{ij}^{R'} + b_{ij}' V_{ij}^A + b_{ij} V_{ij}^{A'}. \tag{3.2.2}$$

The individual terms in equation 3.2.2 will be presented separately in the subsequent subsections.

3.2.1. Derivative of REBO Repulsive Term

Recall

$$V_R = w(r_{ij}) \left[1 + \frac{Q}{r_{ij}} \right] Ae^{-\alpha r_{ij}} \tag{3.2.3}$$

with

$$w_{ij}(r_{ij}) = \Theta(-r_{ij}^c) + \Theta(r_{ij}^c)\Theta(1 - r_{ij}^c)\frac{1}{2}\left[1 + \cos(\pi r_{ij}^c)\right] \tag{3.2.4}$$

where

$$t_c(r) = \frac{r_{ij} - r^{min}}{r^{max} - r^{min}} =: r_{ij}^c \tag{3.2.5}$$

and Θ is the Heaviside function.

Taking the derivative we find

$$V_R'(r_{ij}) = w_{ij}'(r_{ij}) \left[1 + \frac{Q}{r_{ij}} \right] Ae^{-\alpha r_{ij}} - w_{ij}(r_{ij}) \left[\frac{Q}{r_{ij}^2} \right] r_{ij}' Ae^{-\alpha r_{ij}} - w_{ij}(r_{ij}) \left[1 + \frac{Q}{r_{ij}} \right] r_{ij}' A\alpha e^{-\alpha r_{ij}} \tag{3.2.6}$$

The only non-trivial derivative term present is $w_{ij}'(r_{ij})$, which will now be presented.

Begin by taking the derivative of r_c:

$$r_{ij}^{c'} = \frac{1}{r^{max} - r^{min}} \cdot r_{ij}' =: \xi_r \cdot r_{ij}' \tag{3.2.7}$$

Then

$$
\begin{aligned}
w_{ij}'(r_{ij}) = & -\delta_{r_{min}} \cdot \xi_r \cdot r_{ij}' + \delta_{r_{min}} \cdot \xi_{ij} \cdot \Theta(1 - r_{ij}^c) \cdot \frac{1}{2}(1 + \cos(\pi r_{ij}^c)) \\
& - \delta_{r_{max}} \cdot \xi_r \cdot r_{ij}' \cdot \Theta(r_{ij}^c) \cdot \frac{1}{2}(1 + \cos(\pi r_{ij}^c)) \\
& - \frac{1}{2}\Theta(r_{ij}^c)\Theta(1 - r_{ij}^c) \cdot (\sin(\pi r_{ij}^c)) \cdot \pi\xi_r \cdot r_{ij}'
\end{aligned}
\tag{3.2.8}
$$

where δ is the Dirac delta function. Notice we can further simplify equation 3.2.8 by using properties of the delta-functions. Equation 3.2.8 then reduces to

$$w'_{ij}(r_{ij}) = -\frac{1}{2}\Theta(r^c_{ij})\Theta(1 - r^c_{ij}) \cdot (\sin(\pi r^c_{ij})) \cdot \pi\xi_r \cdot r'_{ij} \tag{3.2.9}$$

So, exhaustively, the derivative of the repulsive term is

$$V'_R(r_{ij}) = \underbrace{\left\{-\frac{1}{2}\Theta(r^c_{ij})\Theta(1 - r^c_{ij}) \cdot (\sin(\pi r^c_{ij})) \cdot \pi\xi_r \cdot r'_{ij}\right\} \cdot \left[1 + \frac{Q}{r_{ij}}\right]Ae^{-\alpha r_{ij}}}_{A}$$
$$\underbrace{+ w_{ij}(r_{ij})\left[-\frac{Q}{r^2_{ij}}\right]r'_{ij}Ae^{-\alpha r_{ij}}}_{B} \underbrace{- w_{ij}(r_{ij})\left[1 + \frac{Q}{r_{ij}}\right]r'_{ij}A\alpha e^{-\alpha r_{ij}}}_{C} \tag{3.2.10}$$

The dimension of the systems in question are on the order of 10^6, thus the range of interactions for each term must be kept in mind in an effort to improve computational memory and time constraints. The interaction radius for equation 3.2.10 will be presented below. However, to perform this type of analysis after introducing each term in derivation of the Hessian would be extremely tedious and repetitive. As such, further analysis is left for chapter 4 — this example is solely meant to stress the importance and outline the procedure in determining interaction radii.

From inspection we see that in equation 3.2.10 the support[3] of each component is dictated by the support of the weighting function or its derivative. This is explicitly given by

$$\text{supp}(A) = [r_{min}, r_{max}]$$
$$\text{supp}(B) = [0, r_{max}] \tag{3.2.11}$$
$$\text{supp}(C) = [0, r_{max}]$$

where supp(i) is the support for component $i \in \{A, B, C\}$ in equation 3.2.10.

The function and $w'_{ij}(r_{ij})$ is plotted with the parameters of $r_{min} = 1.0$ and $r_{max} = 4.0$ in figure 3.2.

---

[3]Let $f : X \to \mathbf{R}$ be a real valued function. Then the support of f is defined as $\text{supp}(f) := \{x \in X | f(x) \neq 0\}$.
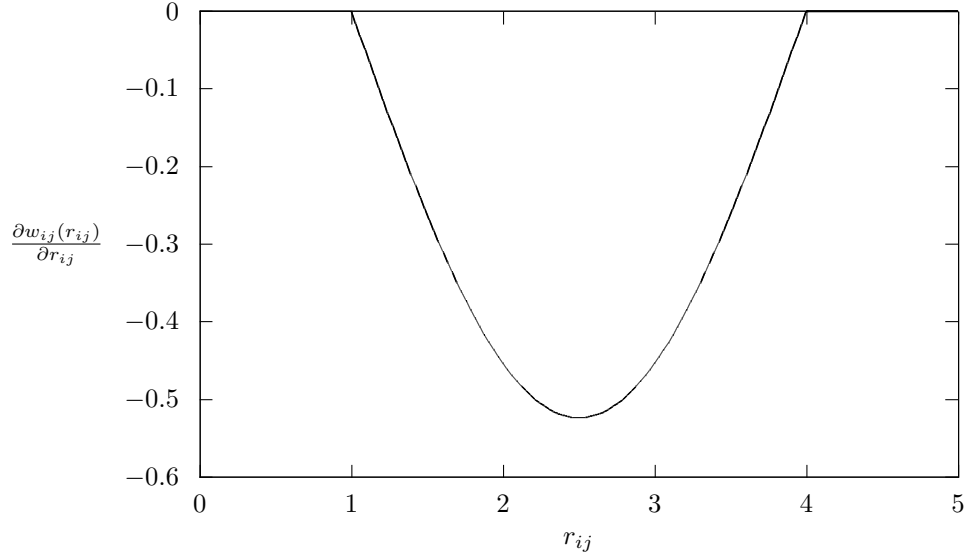
Figure 3.2: Weight function derivative with $r_{ij}^{min} = 1.0$ and $r_{ij}^{max} = 4.0$.

3.2.2. Derivative of the REBO Attractive term

The term $V_{ij}^{A'}$ is very similar to the repulsive term derivative. It is given by

$$V_{ij}^{A'} = -w_{ij}'(r_{ij}) \sum_{n=1}^{3} B^{(n)} e^{-\beta(n)r_{ij}} + w_{ij}(r_{ij}) r_{ij}' \sum_{n=1}^{3} B^{(n)} \beta^{(n)} e^{-\beta^{(n)} r_{ij}} \qquad (3.2.12)$$

3.2.3. Derivative of the REBO Bond-Order term

Recall the definition of the bond order term:

$$b_{ij} = \frac{1}{2} \left[p_{ij}^{\pi\theta} + p_{ji}^{\pi\theta} \right] + \pi_{ij}^{rc} + \pi_{ij}^{dh}. \qquad (3.2.13)$$

The derivative is given by

$$b_{ij}' = \frac{1}{2} \left[p_{ij}^{\pi\theta'} + p_{ji}^{\pi\theta'} \right] + \pi_{ij}^{rc'} + \pi_{ij}^{dh'} \qquad (3.2.14)$$

The four separate terms in equation 3.2.14 will now be expressed, starting with $p_{ij}^{\pi\theta'}$. Recall the definition of

$$p_{ij}^{\pi\theta} = \left[1 + \sum_{k \neq i,j} w_{ik}(r_{ik})g_c(\cos(\theta_{jik})) + P_{cc}\right]^{-\frac{1}{2}}. \tag{3.2.15}$$

Using this notation,

$$p_{ij}^{\pi\theta'} = -\frac{1}{2}\left[1 + \sum_{k \neq i,j} w_{ik}(r_{ik})g_c(\cos(\theta_{jik})) + P_{cc}\right]^{-\frac{3}{2}} \cdot$$
$$\left[\sum_{k \neq i,j} w'_{ik}(r_{ik})g_c\left(\cos(\theta_{jik})\right) + \sum_{k \neq i,j} w_{ik}(r_{ik})g'_c\left(\cos(\theta_{jik})\right) + P'_{cc}\right] \tag{3.2.16}$$

First notice that both the $w_{ik}(r_{ik})$ and $g_c\left(\cos(\theta_{jik})\right)$ terms are within a summation. This is a finite sum, and the derivative of a finite sum is just the sum of the derivatives. The derivative of $w_{ik}(r_{ik})$ is presented in equation 3.2.9 as

$$w'_{ik}(r_{ik}) = -\frac{1}{2}\Theta(r_{ik}^c)\Theta(1 - r_{ik}^c) \cdot (\sin(\pi r_{ik}^c)) \cdot \pi\xi_r \cdot r'_{ik} \tag{3.2.17}$$

Now consider $g'_c\left(\cos(\theta_{jik})\right)$. Recall the definition of $g_c\left(\cos(\theta_{jik})\right)$:

$$g_c\left(\cos(\theta_{jik})\right) = g_c^{(2)}(\cos(\theta_{jik})) + w_{ij}(N_{ij})\left[g_c^{(1)}(\cos(\theta_{jik})) - g_c^{(2)}(\cos(\theta_{jik}))\right] \tag{3.2.18}$$

It is important to realize here that $\cos(\theta_{jik})$ can be treated as the sole variable. That means when taking the derivative of a general function $f\left(\cos(\theta_{jik})\right)$ one obtains

$$\frac{\partial}{\partial u_q}f\left(\cos(\theta_{jik})\right) = \frac{\partial f\left(\cos(\theta_{jik})\right)}{\partial \cos(\theta_{jik})} \cdot \frac{\partial}{\partial u_q}\cos\left(\theta_{jik}\right) \tag{3.2.19}$$

The function f is generic, but the derivative of $\cos(\theta_{jik})$ is not and is thus presented in Appendix B due to its involved and lengthy calculation. Since $\cos\left(\theta_{jik}\right)$ is being treated as the sole variable, the derivative is straight forward.

$$\frac{\partial}{\partial u_q} g_c \left(\cos(\theta_{jik}) \right) = \left[\frac{\partial g_c^{(2)}(\cos(\theta_{jik}))}{\partial \cos(\theta_{jik})} + w_{ij}(N_{ij}) \left[\frac{\partial g_c^{(1)}(\cos(\theta_{jik}))}{\partial \cos(\theta_{jik})} - \frac{\partial g_c^{(2)}(\cos(\theta_{jik}))}{\partial \cos(\theta_{jik})} \right] \right] \frac{\partial}{\partial u_q} \cos(\theta_{jik})$$

$$+ \frac{\partial w_{ij}(N_{ij})}{\partial N_{ij}} \frac{\partial N_{ij}}{\partial u_q} \left[g_c^{(1)}(\cos(\theta_{jik})) - g_c^{(2)}(\cos(\theta_{jik})) \right]$$

$$=: g_c' \left(\cos(\theta_{jik}) \right)$$

$$(3.2.20)$$

The last derivative of interest in the $p_{ij}^{\pi\theta'}$ expression is the P_{cc}' term. We leave this in symbolic notation as it is a spline function which are generally not of particular interest and are dealt with in Appendix A.

This concludes the $p^{\pi\theta}$ term derivatives. The final terms of the bond-weighting term derivative must now be investigated.

The π_{ij}^{rc} term is a symmetric tricubic spline in the variables N_{ij}, N_{ji} and N_{ij}^{conj} and will thus be left symbolically. We must, however, differentiate the π_{ij}^{dh} term.

Recall

$$\pi_{ij}^{dh} = T_{ij}(N_{ij}, N_{ji}, N_{ij}^{conj}) \sum_{k \neq i,j} \sum_{l \neq i,j} \underbrace{(1 - \cos^2 \omega_{kijl})}_{d} \cdot$$

$$\underbrace{w_{ik}^T(r_{ik}) w_{jl}^T(r_{jl})}_{e} \underbrace{\left(1 - w \left(\cos \left(\theta_{jik} \right) \right) \right) \cdot \left(1 - w \left(\cos \left(\theta_{ijl} \right) \right) \right)}_{f}$$

$$(3.2.21)$$

T_{ij} is another tricubic spline[4] in the variables N_{ij}, N_{ji} and N_{ij}^{conj} and ω_{kijl} is the typical torsion angle defined by

$$\cos(\omega_{kijl}) = \frac{\vec{r_{ji}} \times \vec{r_{ik}}}{|\vec{r_{ji}} \times \vec{r_{ik}}|} \cdot \frac{\vec{r_{ij}} \times \vec{r_{jl}}}{|\vec{r_{ij}} \times \vec{r_{jl}}|} \qquad (3.2.22)$$

.

These angles are always provided via trigonometric function arguments. It is mathematically convenient to treat the entire trigonometric function as the variable when taking their derivatives. This is still mathematically sound and is presented in detail in Appendix B. For now, it must be understood that we are treating the entire trigonometric function as the variable, and not the (bonding / torsion) angle alone.

The derivative of π_{ij}^{dh} is then

---

[4]The tricubic cubic splines are characterized by their variables and their interpolation points.

$$\pi_{ij}^{dh'} = \left(T_{ij}' \cdot \sum_{k \neq i,j} \sum_{l \neq i,j} (d \cdot e \cdot f) \right) + \left(T_{ij} \cdot \sum_{k \neq i,j} \sum_{l \neq i,j} (d' \cdot e \cdot f) \right)$$
$$+ \left(T_{ij} \cdot \sum_{k \neq i,j} \sum_{l \neq i,j} (d \cdot e' \cdot f) \right) + \left(T_{ij} \cdot \sum_{k \neq i,j} \sum_{l \neq i,j} (d \cdot e \cdot f') \right) \tag{3.2.23}$$

Simplifying, we find

$$\pi_{ij}^{dh'} = \left(T_{ij}' \cdot \sum_{k \neq i,j} \sum_{l \neq i,j} (d \cdot e \cdot f) \right)$$
$$+ T_{ij} \cdot \sum_{k \neq i,j} \sum_{l \neq i,j} \left[(d' \cdot e \cdot f) + (d \cdot e' \cdot f) + (d \cdot e f') \right] \tag{3.2.24}$$

with

$$d' = -2 \cos(\omega_{kijl}) \cdot \frac{\partial}{\partial u_q} \cos(\omega_{kijl}) = -2 \cos(\omega_{kijl}) \cdot (\cos(\omega_{kijl}))' \tag{3.2.25}$$

$$e' = w_{ik}'(r_{ik}) w_{jl}(r_{jl}) \qquad + \\ w_{ik}(r_{ik}) w_{jl}'(r_{jl}) \tag{3.2.26}$$

$$f' = \left(-w' \left(\cos \left(\theta_{jik} \right) \right) \right) \cdot \left(1 - w \left(\cos \left(\theta_{ijl} \right) \right) \right) + \left(1 - w \left(\cos \left(\theta_{jik} \right) \right) \right) \cdot \left(-w' \left(\cos \left(\theta_{ijl} \right) \right) \right) \tag{3.2.27}$$

where

$$w' \left(\cos \left(\theta_{jik} \right) \right) = \frac{\partial \, w \left(\cos \left(\theta_{jik} \right) \right)}{\partial \cos \left(\theta_{jik} \right)} \cdot \frac{\partial \cos \left(\theta_{jik} \right)}{\partial u_q} \tag{3.2.28}$$

This concludes the derivative of π_{ij}^{dh} and thus the bond-order term. The entire first derivative of the REBO potential has now been presented.

3.3. Second Derivative of the REBO Potential

Recall $E_{ij}^{REBO'} = V_{ij}^{R'} + b_{ij}' V_{ij}^A + b_{ij} V_{ij}^{A'}$. Then

$$E_{ij}^{REBO'\dagger} = V_{ij}^{R'\dagger} + b_{ij}'^\dagger V_{ij}^A + b_{ij}' V_{ij}^{A\dagger} + b_{ij}^\dagger V_{ij}^{A'} + b_{ij} V_{ij}^{A'\dagger} \tag{3.3.1}$$

The only terms in equation 3.3.1 that have yet to be defined are the double derivative terms. These terms will again be provided in separate parts.

3.3.1. 2nd Derivative of REBO Repulsive term

$$
\begin{aligned}
V_R^{'\dagger}(r_{ij}) =& w_{ij}^{''\dagger}(r_{ij})\left[1+\frac{Q}{r_{ij}}\right]Ae^{-\alpha r_{ij}} \\
& -w_{ij}'(r_{ij})\left[\frac{Q}{r_{ij}^2}\right]r_{ij}^{\dagger}Ae^{-\alpha r_{ij}} \\
& -w_{ij}^{\dagger}(r_{ij})\left[\frac{Q}{r_{ij}^2}\right]r_{ij}'Ae^{-\alpha r_{ij}} \\
& -w_{ij}'(r_{ij})\left[1+\frac{Q}{r_{ij}}\right]r_{ij}^{\dagger}A\alpha e^{-\alpha r_{ij}} \\
& -w_{ij}^{\dagger}(r_{ij})\left[1+\frac{Q}{r_{ij}}\right]r_{ij}'A\alpha e^{-\alpha r_{ij}} \\
& +w_{ij}(r_{ij})\left[\frac{Q}{r_{ij}^3}\right]r_{ij}'r_{ij}^{\dagger}Ae^{-\alpha r_{ij}} \\
& +2w_{ij}(r_{ij})\left[\frac{Q}{r_{ij}^2}\right]r_{ij}'r_{ij}^{\dagger}A\alpha e^{-\alpha r_{ij}} \\
& -w_{ij}(r_{ij})\left[\frac{Q}{r_{ij}^2}\right]r_{ij}'^{\dagger}Ae^{-\alpha r_{ij}} \\
& -w_{ij}(r_{ij})\left[1+\frac{Q}{r_{ij}}\right]r_{ij}'^{\dagger}A\alpha e^{-\alpha r_{ij}} \\
& +w_{ij}(r_{ij})\left[1+\frac{Q}{r_{ij}}\right]r_{ij}'r_{ij}^{\dagger}A\alpha^2 e^{-\alpha r_{ij}}
\end{aligned}
\tag{3.3.2}
$$

And from this, the only term left to define is $w_{ij}'^{\dagger}(r_{ij})$.

$$
\begin{aligned}
w_{ij}'^{\dagger}(r_{ij}) =& -\frac{1}{2}\delta_{r_{min}}\xi_r r_{ij}^{\dagger}\Theta(1-r_{ij}^c)(\sin(\pi r_{ij}^c))\pi\xi_r \cdot r_{ij}' \\
& +\frac{1}{2}\delta_{r_{max}}\xi_r r_{ij}^{\dagger}\Theta(r_{ij}^c)(\sin(\pi r_{ij}^c))\pi\xi_r \cdot r_{ij}' \\
& -\frac{1}{2}\Theta(r_{ij}^c)\Theta(1-r_{ij}^c)\left[\cos(\pi r_{ij}^c)\pi^2\xi_r^2 \cdot r_{ij}' \cdot r_{ij}^{\dagger} + \sin(\pi r_{ij}^c)\pi\xi_r \cdot r_{ij}'^{\dagger}\right]
\end{aligned}
\tag{3.3.3}
$$

This can be simplified by implementing the properties of the Kronecker delta function to

$$
w_{ij}'^{\dagger}(r_{ij}) = -\frac{1}{2}\Theta(r_{ij}^c)\Theta(1-r_{ij}^c)\left[\cos(\pi r_{ij}^c)\pi^2\xi_r^2 \cdot r_{ij}' \cdot r_{ij}^{\dagger} + \sin(\pi r_{ij}^c)\pi\xi_r \cdot r_{ij}'^{\dagger}\right]
\tag{3.3.4}
$$

43

The second derivative of the weighting function with respect to r_{ij} is presented in figure 3.3 with parameters $r_{min} = 1.0$ and $r_{max} = 4.0$. It should be noted that this second derivative is not continuous[5].
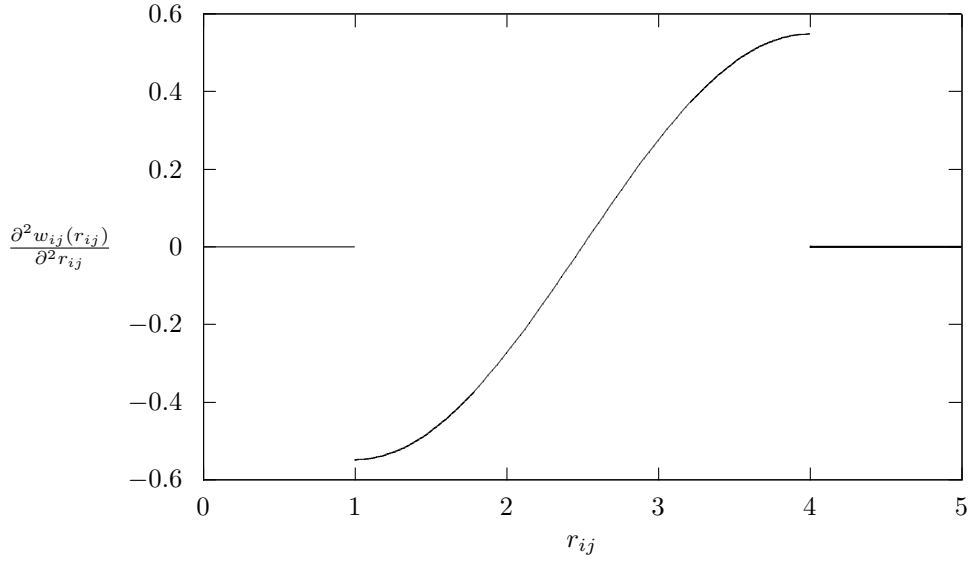
Figure 3.3: Weight function second derivative with $r_{ij}^{min} = 1.0$ and $r_{ij}^{max} = 4.0$.

3.3.2. 2nd Derivative of the REBO Attractive Term

The second derivative of the REBO attractive term is

$$
\begin{aligned}
V_{ij}^{A'\dagger} = &-w_{ij}^{'\dagger}(r_{ij}) \sum_{n=1}^{3} B^{(n)} e^{-\beta(n) r_{ij}} \\
&+ w_{ij}'(r_{ij}) \cdot r_{ij}^{\dagger} \sum_{n=1}^{3} B^{(n)} \beta^{(n)} e^{-\beta^{(n)} r_{ij}} \\
&+ w_{ij}^{\dagger}(r_{ij}) \cdot r_{ij}' \sum_{n=1}^{3} B^{(n)} \beta^{(n)} e^{-\beta^{(n)} r_{ij}} \\
&+ w_{ij}(r_{ij}) \cdot r_{ij}^{'\dagger} \sum_{n=1}^{3} B^{(n)} \beta^{(n)} e^{-\beta(n) r_{ij}} \\
&- w_{ij}(r_{ij}) \cdot r_{ij}' \cdot r_{ij}^{\dagger} \sum_{n=1}^{3} B^{(n)} \beta^{(n)^2} e^{-\beta^{(n)} r_{ij}}
\end{aligned}
\tag{3.3.5}
$$

where all relevant terms have been defined earlier.

---

[5]This will be discussed in chapter 6

3.3.3. 2nd Derivative of the REBO Bond-Order Term

The second derivative of the REBO bond-order term is represented as

$$b_{ij}^{'\dagger} = \frac{1}{2} \left[p_{ij}^{\pi\theta'\,\dagger} + p_{ji}^{\pi\theta'\,\dagger} \right] + \pi_{ij}^{rc'\,\dagger} + \pi_{ij}^{dh'\,\dagger}.$$

(3.3.6)

The expressions for the four terms will be tackled individually.

$$
\begin{aligned}
p_{ij}^{\pi\theta'\,\dagger} = & \frac{3}{4} \left[1 + \sum_{k\neq i,j} w_{ik}(r_{ik})g_c(\cos(\theta_{jik})) + P_{cc} \right]^{-\frac{5}{2}} \cdot \\
& \left[\sum_{k\neq i,j} \left[w_{ik}'(r_{ik})g_c\left(\cos(\theta_{jik})\right) + w_{ik}(r_{ik})g_c'\left(\cos(\theta_{jik})\right) \right] + P_{cc}' \right] \cdot \\
& \left[\sum_{k\neq i,j} \left[w_{ik}^{\dagger}(r_{ik})g_c\left(\cos(\theta_{jik})\right) + w_{ik}(r_{ik})g_c^{\dagger}\left(\cos(\theta_{jik})\right) \right] + P_{cc}^{\dagger} \right] - \\
& \frac{1}{2} \left[1 + \sum_{k\neq i,j} w_{ik}(r_{ik})g_c\left(\cos(\theta_{jik})\right) + P_{cc} \right]^{-\frac{3}{2}} \cdot \\
& \left[\sum_{k\neq i,j} \left[w_{ik}'^{\dagger}(r_{ik})g_c\left(\cos(\theta_{jik})\right) + w_{ik}'(r_{ik})g_c^{\dagger}\left(\cos(\theta_{jik})\right) + \right. \right. \\
& \left. \left. w_{ik}^{\dagger}(r_{ik})g_c'\left(\cos(\theta_{jik})\right) + w_{ik}(r_{ik})g_c'^{\dagger}\left(\cos(\theta_{jik})\right) \right] + P_{cc}'^{\dagger} \right]
\end{aligned}
$$

(3.3.7)

All that remains to do is to find the double derivative terms in equation 3.3.7.

The weight function second derivative, $w_{ik}'^{\dagger}(r_{ik})$, has already been defined in equation 3.2.9 keeping in mind the slight differences due to the different indices.

Recall

$$
\begin{aligned}
\frac{\partial}{\partial u_q} g_c\left(\cos(\theta_{jik})\right) = & \left[\frac{\partial g_c^{(2)}(\cos(\theta_{jik}))}{\partial \cos(\theta_{jik})} + w_{ij}(N_{ij}) \left[\frac{\partial g_c^{(1)}(\cos(\theta_{jik}))}{\partial \cos(\theta_{jik})} - \frac{\partial g_c^{(2)}(\cos(\theta_{jik}))}{\partial \cos(\theta_{jik})} \right] \right] \frac{\partial}{\partial u_q} \cos(\theta_{jik}) \\
& + \frac{\partial w_{ij}(N_{ij})}{\partial N_{ij}} \frac{\partial N_{ij}}{\partial u_q} \left[g_c^{(1)}(\cos(\theta_{jik})) - g_c^{(2)}(\cos(\theta_{jik})) \right] \\
=: & g_c'\left(\cos(\theta_{jik})\right)
\end{aligned}
$$

(3.3.8)

Taking the second derivative we find

$$\frac{\partial^2}{\partial u_p \partial u_q} g_c \left(\cos(\theta_{jik}) \right) = \left[\frac{\partial^2 g_c^{(2)}(\cos(\theta_{jik}))}{\partial^2 \cos(\theta_{jik})} + w_{ij}(N_{ij}) \left[\frac{\partial^2 g_c^{(1)}(\cos(\theta_{jik}))}{\partial^2 \cos(\theta_{jik})} - \frac{\partial^2 g_c^{(2)}(\cos(\theta_{jik}))}{\partial^2 \cos(\theta_{jik})} \right] \right] \cdot$$

$$\frac{\partial}{\partial u_q} \cos(\theta_{jik}) \frac{\partial}{\partial u_p} \cos(\theta_{jik})$$

$$+ \left[\frac{\partial g_c^{(2)}(\cos(\theta_{jik}))}{\partial \cos(\theta_{jik})} + w_{ij}(N_{ij}) \left[\frac{\partial g_c^{(1)}(\cos(\theta_{jik}))}{\partial \cos(\theta_{jik})} - \frac{\partial g_c^{(2)}(\cos(\theta_{jik}))}{\partial \cos(\theta_{jik})} \right] \right] \cdot \frac{\partial^2}{\partial u_p \partial u_q} \cos(\theta_{jik})$$

$$+ \frac{\partial^2 w_{ij}}{\partial^2 N_{ij}} \frac{\partial^2 N_{ij}}{\partial u_q \partial u_p} \left[g_c^{(1)}(\cos(\theta_{jik})) - g_c^{(2)}(\cos(\theta_{jik})) \right]$$

$$+ \frac{\partial w_{ij}}{\partial N_{ij}} \frac{\partial N_{ij}}{\partial u_q} \left[\frac{\partial g_c^{(1)}(\cos(\theta_{jik}))}{\partial \cos(\theta_{jik})} - \frac{\partial g_c^{(2)}(\cos(\theta_{jik}))}{\partial \cos(\theta_{jik})} \right] \cdot \frac{\partial}{\partial u_p} \cos(\theta_{jik})$$

$$=: g_c^{'\dagger} \left(\cos(\theta_{jik}) \right)$$

$$\tag{3.3.9}$$

Again, we leave $P_{cc}^{'\dagger}$ as is, symbolically. That concludes the $p^{\pi\theta}$ terms. We now investigate the π terms.

$$\pi_{ij}^{dh'^\dagger} = \left(T_{ij}^{'\dagger} \sum_{k \neq i,j} \sum_{l \neq i,j} (d \cdot e \cdot f) \right)$$

$$+ T_{ij}^{\dagger} \sum_{k \neq i,j} \sum_{l \neq i,j} \left((d' \cdot e \cdot f) + (d \cdot e' \cdot f) + (d \cdot e \cdot f') \right)$$

$$+ T_{ij}' \sum_{k \neq i,j} \sum_{l \neq i,j} \left(\left(d^\dagger \cdot e \cdot f\right) + \left(d \cdot e^\dagger \cdot f\right) + \left(d \cdot e \cdot f^\dagger\right) \right) \tag{3.3.10}$$

$$+ T_{ij} \sum_{k \neq i,j} \sum_{l \neq i,j} \left((d'^\dagger \cdot e \cdot f) + (d \cdot e'^\dagger \cdot f) + (d \cdot e \cdot f'^\dagger) \right.$$

$$+ (d' \cdot e^\dagger \cdot f) + (d' \cdot e \cdot f^\dagger) + (d \cdot e' \cdot f^\dagger)$$

$$\left. + (d^\dagger \cdot e' \cdot f) + (d^\dagger \cdot e \cdot f') + (d \cdot e^\dagger \cdot f') \right)$$

First recall that $T_{ij} = T_{ij}(N_{ij}, N_{ji}, N_{ij}^{conj})$ and so its derivatives will also involve the derivatives of its arguments. The derivatives of spline functions are presented in Appendix A. The $d'^\dagger, e'^\dagger$ and $f'^\dagger$ terms must now be evaluated.

$$d'^\dagger = -2 \left[\cos(\omega_{kijl})^\dagger \cdot (\cos(\omega_{kijl}))' + \cos(\omega_{kijl})'^\dagger \right] \tag{3.3.11}$$

$$e'^{\dagger} = w_{ik}'^{\dagger}(r_{ik})w_{jl}(r_{jl}) + w_{ik}'(r_{ik})w_{jl}^{\dagger}(r_{jl})$$
$$+ w_{ik}^{\dagger}(r_{ik})w_{jl}'(r_{jl}) + w_{ik}(r_{ik})w_{jl}'^{\dagger}(r_{jl}) \tag{3.3.12}$$

$$f'^{\dagger} = -w'^{\dagger}\Big(\cos\big(\theta_{jik}\big)\Big)\Big(1 - w\Big(\cos\big(\theta_{ijl}\big)\Big)\Big) + w'\Big(\cos\big(\theta_{jik}\big)\Big)w^{\dagger}\Big(\cos\big(\theta_{ijl}\big)\Big)$$
$$+ w^{\dagger}\Big(\cos\big(\theta_{jik}\big)\Big)w'\Big(\cos\big(\theta_{ijl}\big)\Big) + \Big(1 - w\Big(\cos\big(\theta_{jik}\big)\Big)\Big)\Big(-w'^{\dagger}\Big(\cos\big(\theta_{ijl}\big)\Big)\Big) \tag{3.3.13}$$

where

$$w'^{\dagger}\Big(\cos\big(\theta_{jik}\big)\Big) = \frac{\partial^2 w\Big(\cos\big(\theta_{jik}\big)\Big)}{\partial\cos\big(\theta_{jik}\big)^2} \cdot \frac{\partial\cos\big(\theta_{jik}\big)}{\partial u_q} \cdot \frac{\partial\cos\big(\theta_{jik}\big)}{\partial u_p}$$
$$+ \frac{\partial w\Big(\cos\big(\theta_{jik}\big)\Big)}{\partial\cos\big(\theta_{jik}\big)} \cdot \frac{\partial^2\cos\big(\theta_{jik}\big)}{\partial u_q \partial u_p} \tag{3.3.14}$$

In the scope of simulations, we should take into account the support of all functions. In this case, it is particularly important because the dirac-delta functions are defined on a set of measure zero, as are their derivatives. So in a numerics scope, terms 3, 6, 7, 8, 9, and 10 from equation 3.3.12 and $f'^{\dagger}$ would all be zero. This would then greatly reduce and simplify equation 3.3.10. Again, the entire Hessian of the AIREBO potential and the support of each term is presented in chapter 4.

This concludes the second derivative of π_{ij}^{dh} and thus the bond-order term. The entire seocond derivative of the REBO potential has now been presented.

3.4. Lennard-Jones Potential

The Lennard-Jones potential is a widely used potential and there are vast quantities of information available. This paper aims to provide a concise treatment of it within the context of the AIREBO potential.

The Lennard-Jones potential is given by

$$V_{ij}^{LJ}(r_{ij}) = 4\epsilon_{ij}\left[\left(\frac{\sigma_{ij}}{r_{ij}}\right)^{12} - \left(\frac{\sigma_{ij}}{r_{ij}}\right)^{6}\right] \tag{3.4.1}$$

In Carbon only systems we can represent this equivalently as

$$V_{ij}^{LJ}(r_{ij}) = 4\epsilon \left[\left(\frac{\sigma}{r_{ij}} \right)^{12} - \left(\frac{\sigma}{r_{ij}} \right)^{6} \right] \tag{3.4.2}$$

The total energy contribution from this Lennard Jones potential to the AIREBO potential is expressed as

$$
\begin{aligned}
E_{ij}^{LJ} = & S_p(t_r(r_{ij})) \cdot S_p(t_b(b_{ij}^*)) \cdot C_{ij} V_{ij}^{LJ}(r_{ij}) + \\
& \left[1 - S_p(t_r(r_{ij})) \right] \cdot C_{ij} V_{ij}^{LJ}(r_{ij})
\end{aligned}
\tag{3.4.3}
$$

with S_p representing the polynomial switching function (slightly different than S_s).

$$S_p(t) = \Theta(-t) + \Theta(t)\Theta(1-t) \left[1 - t^2(3 - 2t) \right] \tag{3.4.4}$$

where

$$t_r(r_{ij}) = \frac{r_{ij} - r^{LJmin}}{r^{LJmax} - r^{LJmin}} =: r_{ij}^{LJc} \tag{3.4.5}$$

is used to rescale the switching function domain. This switching function (Equation 3.4.4) is used to determine the overall strength of the LJ interactions at play. It will be zero when $r_{ij} > r_{ij}^{LJmax}$ and will be non-zero otherwise. Equation 3.4.4 is plotted in Figure 3.4[6] to give an idea to the shape of the switching functions. For notational simplicity, we make the the following declaration

$$w_{ij}^p(r_{ij}) = S_p(t_r(r_{ij}) \tag{3.4.6}$$

Within the context of the AIREBO potential, the parameters are chosen to be $r_{ij}^{LJmin} = \sigma$ and $r_{ij}^{LJmax} = 2^{\frac{1}{6}}\sigma$ so that the second derivative of the potential is continuous at is continuous at r^{LJmin}.

Equation 3.4.3 also has a switching function taking a bond-order term as an argument, $S_p(t_b(b_{ij}^*))$, and it shall be referred to as the bonding switch. It has the scaling variable

$$t_b(b_{ij}) = \frac{b_{ij} - b_{ij}^{min}}{b_{ij}^{max} - b_{ij}^{min}} = \frac{b_{ij} - b^{min}}{b^{max} - b^{min}} \tag{3.4.7}$$

where

$$b_{ij}^* = b_{ij}\big|_{r_{ij}=r^{min}} \tag{3.4.8}$$

---

[6]The first and second derivatives of the polynomial switch function will not be plotted due to their qualitative resemblance to the sinusoidal switch functions.
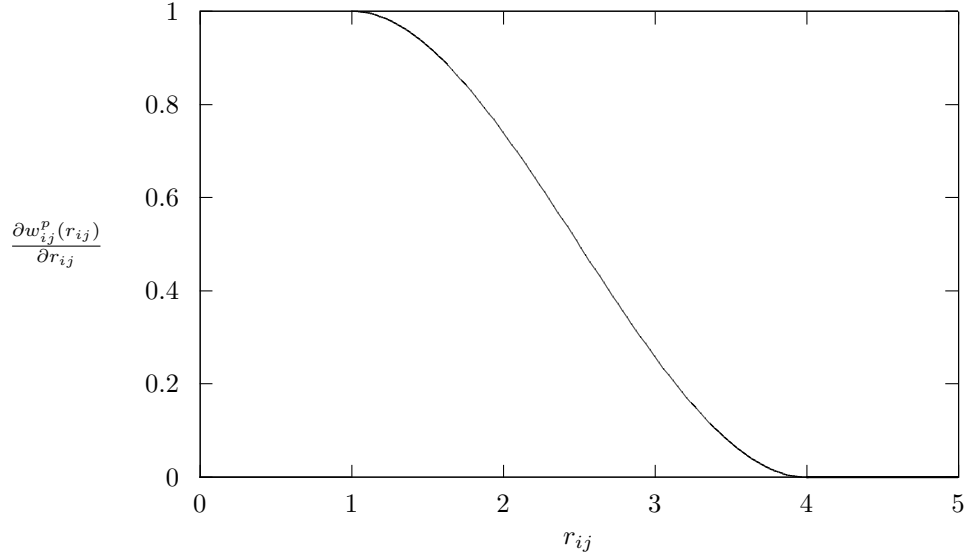
Figure 3.4: Polynomial weight function with $r_{ij}^{LJmin} = 1.0$ and $r_{ij}^{LJmax} = 4.0$.

converts the REBO bond-order term to a range suitable for the use in the switching function. It is clear that when the bond-order term is large, indicating covalent bonding is present, the repulsive LJ interactions become negligible, as they should. Likewise, for very low values of the bond-order term, indicating no covalent bonding is present, the LJ interaction will be unperturbed. so in total one has

$$t_b(b_{ij}^*) = \frac{b_{ij}^* - b^{min}}{b^{max} - b^{min}} =: b_{ij}^{*c} \tag{3.4.9}$$

Further, the connectivity switch, C_{ij}, is defined as

$$C_{ij} = 1 - \max \left\{ \underbrace{w_{ij}(r_{ij})}_{\Omega_1}, \ \underbrace{w_{ik}(r_{ik}) \cdot w_{kj}(r_{kj})}_{\Omega_2}, \ \underbrace{w_{ik}(r_{ik}) \cdot w_{kl}(r_{kl}) \cdot w_{lj}(r_{lj})}_{\Omega_3} \right\} \qquad \forall k, l \tag{3.4.10}$$

where, as before, $w_{ij}(r_{ij}) = S_s(t_c(r_{ij})) = S_s(r_{ij}^c)$.

3.5. Derivative of the LJ Energy

We now wish to take the derivative of expression 3.4.3.

$$\begin{aligned}
E_{ij}^{LJ'} =\; & w_{ij}^{p'}(r_{ij}^{LJ}) \cdot w_{ij}^{p}(b_{ij}^{*}) \cdot C_{ij}V_{ij}^{LJ}(r_{ij}) && + \\
& w_{ij}^{p}(r_{ij}^{LJ}) \cdot w_{ij}^{p'}(b_{ij}^{*}) \cdot C_{ij}V_{ij}^{LJ}(r_{ij}) && + \\
& w_{ij}^{p}(r_{ij}^{LJ}) \cdot w_{ij}^{p}(b_{ij}^{*}) \cdot C_{ij}'V_{ij}^{LJ}(r_{ij}) && + \\
& w_{ij}^{p}(r_{ij}^{LJ}) \cdot w_{ij}^{p}(b_{ij}^{*}) \cdot C_{ij}V_{ij}^{LJ'}(r_{ij}) && - \\
& \left[w_{ij}^{p'}(r_{ij}^{LJ}) \right] \cdot C_{ij}V_{ij}^{LJ}(r_{ij}) && + \\
& \left[1 - w_{ij}^{p}(r_{ij}^{LJ}) \right] \cdot C_{ij}'V_{ij}^{LJ}(r_{ij}) && + \\
& \left[1 - w_{ij}^{p}(r_{ij}^{LJ}) \right] \cdot C_{ij}V_{ij}^{LJ'}(r_{ij}) &&
\end{aligned} \tag{3.5.1}$$

where the single derivative terms are left to define. We must now take the derivative of the connectivity switch found in equation 3.4.10. The derivative of a max function is done in parts. One must first evaluate the piecewise definition of the function and then take the derivative of the respective parts. We can represent this as

$$C_{ij}' = \begin{cases}
w_{ij}'(r_{ij}) & \text{if } \Omega_1 \geq \max\{\Omega_2, \Omega_3\} \\[1em]
\begin{aligned}& w_{ik}'(r_{ik})w_{kj}(r_{kj})+ \\ & w_{ik}(r_{ik})w_{kj}'(r_{kj})\end{aligned} & \text{if } \Omega_2 \geq \max\{\Omega_1, \Omega_3\} \\[1em]
\begin{aligned}& w_{ik}'(r_{ik})w_{kl}(r_{kl})w_{lj}(r_{lj})+ \\ & w_{ik}(r_{ik})w_{kl}'(r_{kl})w_{lj}(r_{lj})+ \\ & w_{ik}(r_{ik})w_{kl}(r_{kl})w_{lj}'(r_{lj})\end{aligned} & \text{if } \Omega_3 \geq \max\{\Omega_1, \Omega_2\}
\end{cases} \tag{3.5.2}$$

Recall we already have an expression for $w_{ij}'(r_{ij})$ found in equation 3.2.9. We now define the variables within the switching functions.

Taking the derivatives of the polynomial switching functions, one gets

$$S_p'(t_r(r_{ij})) = S_p'(r_{LJ}^c) = w_{ij}^{p'}(r_{ij}^{LJ}) = \Theta(r_{ij}^{LJc})\Theta(1 - r_{ij}^{LJc}) \left[6r_{ij}^{LJc}(r_{ij}^{LJc} - 1) \right] \cdot \xi_{LJ} \cdot r_{ij}' \tag{3.5.3}$$

and

$$S_p'(t_b(b_{ij}^{*})) = S_p'(b_{ij}^{*c}) = w_{ij}^{p'}(b_{ij}^{*}) = \Theta(b_{ij}^{*c})\Theta(1 - b_{ij}^{*c}) \left[6b_{ij}^{*c}(b_{ij}^{*c} - 1) \right] \cdot \xi_b \cdot b_{ij}^{*'} \tag{3.5.4}$$

where

$$\xi_{LJ} = \frac{1}{r^{LJmax} - r^{LJmin}} \tag{3.5.5}$$

and

$$\xi_b = \frac{1}{b^{max} - b^{min}} \tag{3.5.6}$$

Please note that $b_{ij}^{*'}$ will be considered in subsection 3.6.

The only other derivative term we need is that of the Lennard Jones Potential.

$$V_{ij}^{LJ'}(r_{ij}) = 24\epsilon \left[\left(\frac{\sigma^6}{r_{ij}^7} \right) - 2 \left(\frac{\sigma^{12}}{r_{ij}^{13}} \right) \right] \cdot r_{ij}' \tag{3.5.7}$$

3.6.   Second Derivative of the LJ Energy

Taking the derivative of equation 3.5.1 we find

$$
\begin{aligned}
E_{ij}^{LJ'\dagger} =\ & w_{ij}^{p'\dagger}(r_{LJ}) \cdot w_{ij}^{p}(b_{ij}^{*}) \cdot C_{ij}V_{ij}^{LJ}(r_{ij}) && + \\
& w_{ij}^{p\dagger}(r_{ij}^{LJ}) \cdot w_{ij}^{p'}(b_{ij}^{*}) \cdot C_{ij}V_{ij}^{LJ}(r_{ij}) && + \\
& w_{ij}^{p'}(r_{ij}^{LJ}) \cdot w_{ij}^{p\dagger}(b_{ij}^{*}) \cdot C_{ij}V_{ij}^{LJ}(r_{ij}) && + \\
& w_{ij}^{p\dagger}(r_{ij}^{LJ}) \cdot w_{ij}^{p}(b_{ij}^{*}) \cdot C_{ij}'V_{ij}^{LJ}(r_{ij}) && + \\
& w_{ij}^{p'}(r_{ij}^{LJ}) \cdot w_{ij}^{p}(b_{ij}^{*}) \cdot C_{ij}^{\dagger}V_{ij}^{LJ}(r_{ij}) && + \\
& w_{ij}^{p\dagger}(r_{ij}^{LJ}) \cdot w_{ij}^{p}(b_{ij}^{*}) \cdot C_{ij}V_{ij}^{LJ'}(r_{ij}) && + \\
& w_{ij}^{p'}(r_{ij}^{LJ}) \cdot w_{ij}^{p}(b_{ij}^{*}) \cdot C_{ij}V_{ij}^{LJ\dagger}(r_{ij}) && + \\
& w_{ij}^{p}(r_{ij}^{LJ}) \cdot w_{ij}^{p'\dagger}(b_{ij}^{*}) \cdot C_{ij}V_{ij}^{LJ}(r_{ij}) && + \\
& w_{ij}^{p}(r_{ij}^{LJ}) \cdot w_{ij}^{p'}(b_{ij}^{*}) \cdot C_{ij}^{\dagger}V_{ij}^{LJ}(r_{ij}) && + \\
& w_{ij}^{p}(r_{ij}^{LJ}) \cdot w_{ij}^{p\dagger}(b_{ij}^{*}) \cdot C_{ij}'V_{ij}^{LJ}(r_{ij}) && + \\
& w_{ij}^{p}(r_{ij}^{LJ}) \cdot w_{ij}^{p'}(b_{ij}^{*}) \cdot C_{ij}V_{ij}^{LJ\dagger}(r_{ij}) && + \\
& w_{ij}^{p}(r_{ij}^{LJ}) \cdot w_{ij}^{p\dagger}(b_{ij}^{*}) \cdot C_{ij}V_{ij}^{LJ'}(r_{ij}) && + \\
& w_{ij}^{p}(r_{ij}^{LJ}) \cdot w_{ij}^{p}(b_{ij}^{*}) \cdot C_{ij}'^{\dagger}V_{ij}^{LJ}(r_{ij}) && + \\
& w_{ij}^{p}(r_{ij}^{LJ}) \cdot w_{ij}^{p}(b_{ij}^{*}) \cdot C_{ij}'V_{ij}^{LJ\dagger}(r_{ij}) && + \\
& w_{ij}^{p}(r_{ij}^{LJ}) \cdot w_{ij}^{p}(b_{ij}^{*}) \cdot C_{ij}^{\dagger}V_{ij}^{LJ'}(r_{ij}) && + \\
& w_{ij}^{p}(r_{ij}^{LJ}) \cdot w_{ij}^{p}(b_{ij}^{*}) \cdot C_{ij}V_{ij}^{LJ'\dagger}(r_{ij}) && - \\
& \left[w_{ij}^{p'\dagger}(r_{LJ})\right] \cdot C_{ij}V_{ij}^{LJ}(r_{ij}) && - \\
& \left[w_{ij}^{p'}(r_{ij}^{LJ})\right] \cdot C_{ij}^{\dagger}V_{ij}^{LJ}(r_{ij}) && - \\
& \left[w_{ij}^{p\dagger}(r_{ij}^{LJ})\right] \cdot C_{ij}'V_{ij}^{LJ}(r_{ij}) && - \\
& \left[w_{ij}^{p'}(r_{ij}^{LJ})\right] \cdot C_{ij}V_{ij}^{LJ\dagger}(r_{ij}) && + \\
& \left[w_{ij}^{p\dagger}(r_{ij}^{LJ})\right] \cdot C_{ij}V_{ij}^{LJ'}(r_{ij}) && + \\
& \left[1 - w_{ij}^{p}(r_{ij}^{LJ})\right] \cdot C_{ij}'^{\dagger}V_{ij}^{LJ}(r_{ij}) && + \\
& \left[1 - w_{ij}^{p}(r_{ij}^{LJ})\right] \cdot C_{ij}'V_{ij}^{LJ\dagger}(r_{ij}) && + \\
& \left[1 - w_{ij}^{p}(r_{ij}^{LJ})\right] \cdot C_{ij}^{\dagger}V_{ij}^{LJ'}(r_{ij}) && + \\
& \left[1 - w_{ij}^{p}(r_{ij}^{LJ})\right] \cdot C_{ij}V_{ij}^{LJ''}(r_{ij})
\end{aligned}
\tag{3.6.1}
$$

.

Of course we must now define all the individual second derivative terms within equation 3.6.1.Beginning with the polynomial weighting functions,

$$
\begin{aligned}
w_{ij}^{p'\dagger}(r_{ij}^{LJc}) =\ & \Theta(r_{ij}^{LJc})\Theta(1 - r_{ij}^{LJc}) \left[6(2r_{ij}^{LJc} - 1)\right] \cdot \xi_{LJ}^{2} \cdot r_{ij}' \cdot r_{ij}^{\dagger} + \\
& \Theta(r_{ij}^{LJc})\Theta(1 - r_{ij}^{LJc}) \left[6r_{ij}^{LJc}(r_{ij}^{LJc} - 1)\right] \cdot \xi_{LJ} \cdot r_{ij}'^{\dagger},
\end{aligned}
\tag{3.6.2}
$$

$$w_{ij}^{p'^\dagger}(b_{ij}^*) = \Theta(b_{ij}^*)\Theta(1 - b_{ij}^*)\left[6(2b_{ij}^* - 1)\right] \cdot \xi_b^2 \cdot b_{ij}^{*'} \cdot b_{ij}^{*\dagger} +$$
$$\Theta(b_{ij}^*)\Theta(1 - b_{ij}^*)\left[6b_{ij}^*(b_{ij}^* - 1)\right] \cdot \xi_b \cdot b_{ij}^{*'^\dagger} \tag{3.6.3}$$

where these have already been simplified by implementing properties of the Kronecker delta function. Please note that $b_{ij}^{*'^\dagger}$ will be considered in subsection 3.6. For the second derivative of the connectivity switch we have

$$
C_{ij}^{'\dagger} = \begin{cases}
w_{ij}^{'\dagger}(r_{ij}) & \text{if } \Omega_1 \geq \max\{\Omega_2, \Omega_3\} \\[2ex]
\begin{aligned}
&w_{ik}^{'\dagger}(r_{ik})w_{kj}(r_{kj}) + \\
&w_{ik}'(r_{ik})w_{kj}^\dagger(r_{kj}) + \\
&w_{ik}^\dagger(r_{ik})w_{kj}'(r_{kj}) + \\
&w_{ik}(r_{ik})w_{kj}^{'\dagger}(r_{kj})
\end{aligned} & \text{if } \Omega_2 \geq \max\{\Omega_1, \Omega_3\} \\[2ex]
\begin{aligned}
&w_{ik}^{'\dagger}(r_{ik})w_{kl}(r_{kl})w_{lj}(r_{lj}) + \\
&w_{ik}'(r_{ik})w_{kl}^\dagger(r_{kl})w_{lj}(r_{lj}) + \\
&w_{ik}^\dagger(r_{ik})w_{kl}'(r_{kl})w_{lj}(r_{lj}) + \\
&w_{ik}'(r_{ik})w_{kl}(r_{kl})w_{lj}^\dagger(r_{lj}) + \\
&w_{ik}^\dagger(r_{ik})w_{kl}(r_{kl})w_{lj}'(r_{lj}) + \\
&w_{ik}(r_{ik})w_{kl}^{'\dagger}(r_{kl})w_{lj}(r_{lj}) + \\
&w_{ik}(r_{ik})w_{kl}'(r_{kl})w_{lj}^\dagger(r_{lj}) + \\
&w_{ik}(r_{ik})w_{kl}^\dagger(r_{kl})w_{lj}'(r_{lj}) + \\
&w_{ik}(r_{ik})w_{kl}(r_{kl})w_{lj}^{'\dagger}(r_{lj})
\end{aligned} & \text{if } \Omega_3 \geq \max\{\Omega_1, \Omega_2\}
\end{cases} \tag{3.6.4}
$$

and lastly, the second derivative of the LJ potential,

$$V_{ij}^{LJ'^\dagger}(r_{ij}) = 24\epsilon\left[26\left(\frac{\sigma^{12}}{r_{ij}^{14}}\right) - 7\left(\frac{\sigma^6}{r_{ij}^8}\right)\right] \cdot r_{ij}' \cdot r_{ij}^\dagger + 24\epsilon\left[\left(\frac{\sigma^6}{r_{ij}^7}\right) - 2\left(\frac{\sigma^{12}}{r_{ij}^{13}}\right)\right] \cdot r_{ij}'^\dagger \tag{3.6.5}$$

Bond-Order Switch Function Derivatives

Equations 3.5.4 and 3.6.3 both included terms taking the derivative of b_{ij}^*. These first and second derivatives ($b_{ij}^{*'}$ and $b_{ij}^{*'^\dagger}$) were not explicitly given. However, these must be defined. Recall

$$b_{ij}^* = b_{ij}\big|_{r_{ij}=r^{min}}.$$ (3.6.6)

As a result, the first and second derivatives follow the exact outline as provided in taking the first and second derivatives of the normal bond-order term found in the REBO potential (b'_{ij} and $b'^\dagger_{ij}$). Since the process is nearly the exact same, it will not be presented herein.

The changes that must be made when calculating $b_{ij}^{*'}$ and $b_{ij}^{*'\dagger}$ is that r_{ij} must be treated as a constant. As a result, any term with a derivative of r_{ij} is identically zero. This simplifies things a considerable amount.

3.7.   Torsional Interaction Potential

The final contribution to the AIREBO potential is the torsional term, which takes dihedral angles as arguments. Recall that this term was added to impose penalties for rotations around bonds. This introduction to the torsional potential will be kept brief as we are interested in the mathematical treatment. Consult [37] for further information.

The contribution to the AIREBO energy from the torsional potential is given by

$$E^{tors} = \frac{1}{2} \sum_i \sum_{j \neq i} \sum_{k \neq i,j} \sum_{l \neq i,j,k} w_{ij}(r_{ij}) \cdot w_{jk}(r_{jk}) \cdot w_{kl}(r_{kl}) \times V^{tors}(\omega_{ijkl})$$ (3.7.1)

where

$$V^{tors}(\omega) = \epsilon \left[\frac{256}{405} \cos^{10}\left(\frac{\omega}{2}\right) - \frac{1}{10} \right]$$ (3.7.2)

and ω_{kijl} is the torsion angle defined by

$$\cos(\omega_{kijl}) = \frac{\vec{r}_{ji} \times \vec{r}_{ik}}{|\vec{r}_{ji} \times \vec{r}_{ik}|} \cdot \frac{\vec{r}_{ij} \times \vec{r}_{jl}}{|\vec{r}_{ij} \times \vec{r}_{jl}|}.$$ (3.7.3)

This angle will always be presented as an argument to a trigonometric function, so we treat the entire trigonometric function as the variable. Further definitions and the torsional derivatives are carefully presented in Appendix B.

3.8.   Derivative of Torsional Energy

The derivative of equation 3.7.1 is then

$$E^{tors'} = \frac{1}{2} \sum_i \sum_{j \neq i} \sum_{k \neq i,j} \sum_{l \neq i,j,k} \left[\left(w'_{ij}(r_{ij}) \cdot w_{jk}(r_{jk}) \cdot w_{kl}(r_{kl}) \times V^{tors}(\omega_{ijkl}) \right) + \right.$$

$$\left(w_{ij}(r_{ij}) \cdot w'_{jk}(r_{jk}) \cdot w_{kl}(r_{kl}) \times V^{tors}(\omega_{ijkl}) \right) +$$

$$\left(w_{ij}(r_{ij}) \cdot w_{jk}(r_{jk}) \cdot w'_{kl}(r_{kl}) \times V^{tors}(\omega_{ijkl}) \right) +$$

$$\left. \left(w_{ij}(r_{ij}) \cdot w_{jk}(r_{jk}) \cdot w_{kl}(r_{kl}) \times V^{tors'}(\omega_{ijkl}) \right) \right]$$

(3.8.1)

where w' has been defined in equation 3.2.9 and

$$V^{tors'}(\omega) = 10\epsilon \left[\frac{256}{405} \cos^9 \left(\frac{\omega}{2} \right) \left(\cos \left(\frac{\omega}{2} \right) \right)' \right]$$

(3.8.2)

Refer to Appendix B for the $\cos(\omega)$ derivatives.

3.9.   Second Derivative of the Torsional Energy

Evaluating the second derivative of 3.7.1 we find

$$E^{tors'^\dagger} = \frac{1}{2} \sum_i \sum_{j \neq i} \sum_{k \neq i,j} \sum_{l \neq i,j,k} \left[\left(w_{ij}'^\dagger(r_{ij}) \cdot w_{jk}(r_{jk}) \cdot w_{kl}(r_{kl}) \times V^{tors}(\omega_{ijkl}) \right) + \right.$$

$$\left(w_{ij}'(r_{ij}) \cdot w_{jk}^\dagger(r_{jk}) \cdot w_{kl}(r_{kl}) \times V^{tors}(\omega_{ijkl}) \right) +$$

$$\left(w_{ij}^\dagger(r_{ij}) \cdot w_{jk}'(r_{jk}) \cdot w_{kl}(r_{kl}) \times V^{tors}(\omega_{ijkl}) \right) +$$

$$\left(w_{ij}'(r_{ij}) \cdot w_{jk}(r_{jk}) \cdot w_{kl}^\dagger(r_{kl}) \times V^{tors}(\omega_{ijkl}) \right) +$$

$$\left(w_{ij}^\dagger(r_{ij}) \cdot w_{jk}(r_{jk}) \cdot w_{kl}'(r_{kl}) \times V^{tors}(\omega_{ijkl}) \right) +$$

$$\left(w_{ij}'(r_{ij}) \cdot w_{jk}(r_{jk}) \cdot w_{kl}(r_{kl}) \times V^{tors^\dagger}(\omega_{ijkl}) \right) +$$

$$\left(w_{ij}^\dagger(r_{ij}) \cdot w_{jk}(r_{jk}) \cdot w_{kl}(r_{kl}) \times V^{tors'}(\omega_{ijkl}) \right) +$$

$$\left(w_{ij}(r_{ij}) \cdot w_{jk}'^\dagger(r_{jk}) \cdot w_{kl}(r_{kl}) \times V^{tors}(\omega_{ijkl}) \right) +$$

$$\left(w_{ij}(r_{ij}) \cdot w_{jk}'(r_{jk}) \cdot w_{kl}^\dagger(r_{kl}) \times V^{tors}(\omega_{ijkl}) \right) +$$

$$\left(w_{ij}(r_{ij}) \cdot w_{jk}^\dagger(r_{jk}) \cdot w_{kl}'(r_{kl}) \times V^{tors}(\omega_{ijkl}) \right) +$$

$$\left(w_{ij}(r_{ij}) \cdot w_{jk}'(r_{jk}) \cdot w_{kl}(r_{kl}) \times V^{tors^\dagger}(\omega_{ijkl}) \right) +$$

$$\left(w_{ij}(r_{ij}) \cdot w_{jk}^\dagger(r_{jk}) \cdot w_{kl}(r_{kl}) \times V^{tors'}(\omega_{ijkl}) \right) +$$

$$\left(w_{ij}(r_{ij}) \cdot w_{jk}(r_{jk}) \cdot w_{kl}'^\dagger(r_{kl}) \times V^{tors}(\omega_{ijkl}) \right) +$$

$$\left(w_{ij}(r_{ij}) \cdot w_{jk}(r_{jk}) \cdot w_{kl}'(r_{kl}) \times V^{tors^\dagger}(\omega_{ijkl}) \right) +$$

$$\left(w_{ij}(r_{ij}) \cdot w_{jk}(r_{jk}) \cdot w_{kl}^\dagger(r_{kl}) \times V^{tors'}(\omega_{ijkl}) \right) +$$

$$\left. \left(w_{ij}(r_{ij}) \cdot w_{jk}(r_{jk}) \cdot w_{kl}(r_{kl}) \times V^{tors'^\dagger}(\omega_{ijkl}) \right) \right]$$

(3.9.1)

with

$$V^{tors'^\dagger}(\omega) = \frac{2560}{405} \epsilon \left[9 \cdot \cos^8\left(\frac{\omega}{2}\right) \left(\cos\left(\frac{\omega}{2}\right) \right)' \left(\cos\left(\frac{\omega}{2}\right) \right)^\dagger + \right.$$

$$\left. \cos^9\left(\frac{\omega}{2}\right) \left(\cos\left(\frac{\omega}{2}\right) \right)'^\dagger \right]$$

(3.9.2)

Where, again, the torsional derivatives are found in Appendix B.

Chapter 4

Summary of the Second Derivative of the AIREBO Potential Including Interaction Radii

4.1. Definition of Atomic Sets

Recall the definition of the AIREBO potential:

$$E'^{\dagger} = E^{REBO'^{\dagger}} + E^{LJ'^{\dagger}} + E^{tors'^{\dagger}} \tag{4.1.1}$$

We will first define different sets of atoms, and then we will break down 4.1.1 into its subsequent parts.

In general, we define

$$\mathcal{S}_q^n$$

as the set of atoms within the neighbourhood $n \in \{0, 1, \ldots, 7\}$ of atom q.

where the associated neighbourhoods are presented in 4.1.

As an example, $k \in \mathcal{S}_i^0$ would refer to all atoms k such that $0 \le r_{ik} \le r_{max}$.

4.2. Exhaustive Tables of the AIREBO Potential

Chapter 3 provided a mathematical derivation for the second derivatives of the three terms in equation 4.1.1. Due to the length of derivation, it was not a clear presentation of the total Hession. This section aims to summarize the entire Hessian of the AIREBO potential and provide interaction radii

57

Table 4.1: The mapping from the superscript n to its associated neighbourhood

n	range
0	$[0, r_{max}]$
1	$[r_{min}, r_{max}]$
2	$[0, N_{max}]$
3	$[N_{min}, N_{max}]$
4	$[0, r_{LJ}^{max}]$
5	$[r_{LJ}^{min}, r_{LJ}^{max}]$
6	$[0, b_{max}]$
7	$[b_{min}, b_{max}]$
8	$[\theta_{min}, \theta_{max}]$
9	$[\theta_{min}, \theta_{max}]$
∞	$\mathbb{R}$

for separate terms.

Again, owing to the sizeable nature of the AIREBO Hessian, this will be presented in table form. Three tables will be presented in total to define the entire AIREBO Hessian, one for each term in equation 4.1.1. Each table will have a different size, but will follow the same outline. In general, a table will have N columns and M rows, but only the columns are important in discussing the outline. A general table is presented in table 4.2.

Table 4.2: General table layout

0	1	2	...	N-2	N-1	N
...	...	...	...	...	...	...
...	...	...	...	...	...	...
...	...	...	...	...	...	...

Column 0 will simply be an enumeration of rows. This will help to later reference row numbers. In general, columns $1 - (N-2)$ will contain elements of the Hessian. The high-level terms appear in the left-most columns, and are expanded when needed towards the right. The idea is that the entire term the table is representing can be achieved by summing a given column. The second last column, column $(N-1)$ is always left blank, and the final column, column N contains the support (interaction radii) of the term in its row. This is best described through an example.

Imagine the function in question is

$$\Phi(x) = f(x) \cdot g(x) \cdot h(x) + k(x) \tag{4.2.1}$$

where $h(x)$ is a more complicated function and is represented as

$$h(x) = l(x) + t(x). \tag{4.2.2}$$

The equation 4.2.1 would be represented in table form as is shown in table 4.3.

Table 4.3: Table representation of equation 4.2.1

	A	B	C	D	E
1	$\Phi(x)$				
2		$f(x)$			supp($f(x)$)
3		$g(x)$			supp($g(x)$)
4		$h(x)+$			
5			$l(x)+$		supp($l(x)$)
6			$t(x)$		supp($t(x)$)
7		$k(x)$			supp($k(x)$)

4.2.1. Table for the Hessian of the REBO term

The second derivative for $E^{REBO'^\dagger}$ is presented in table 4.4.

Table 4.4: Table representation of $E^{REBO'^\dagger}$

	A	B	C	D	E	F	G
1	$E^{REBO'^\dagger}$						
2		$V^{R'^\dagger}+$					
3			$w_{ij}'^\dagger(r_{ij})\left[1+\frac{Q}{r_{ij}}\right]Ae^{-\alpha r_{ij}}-$				$j\in\mathcal{S}_i^1 \wedge p,q\in\{i,j\}$
4			$w_{ij}'(r_{ij})\left[\frac{Q}{r_{ij}^2}\right]r_{ij}^\dagger Ae^{-\alpha r_{ij}}-$				$j\in\mathcal{S}_i^1 \wedge p,q\in\{i,j\}$
5			$w_{ij}^\dagger(r_{ij})\left[\frac{Q}{r_{ij}^2}\right]r_{ij}'Ae^{-\alpha r_{ij}}-$				$j\in\mathcal{S}_i^1 \wedge p,q\in\{i,j\}$
6			$w_{ij}'(r_{ij})\left[1+\frac{Q}{r_{ij}}\right]r_{ij}^\dagger A\alpha e^{-\alpha r_{ij}}-$				$j\in\mathcal{S}_i^1 \wedge p,q\in\{i,j\}$
7			$w_{ij}^\dagger(r_{ij})\left[1+\frac{Q}{r_{ij}}\right]r_{ij}'A\alpha e^{-\alpha r_{ij}}+$				$j\in\mathcal{S}_i^1 \wedge p,q\in\{i,j\}$
8			$w_{ij}(r_{ij})\left[\frac{Q}{r_{ij}^3}\right]r_{ij}'r_{ij}^\dagger Ae^{-\alpha r_{ij}}+$				$j\in\mathcal{S}_i^0 \wedge p,q\in\{i,j\}$
9			$2w_{ij}(r_{ij})\left[\frac{Q}{r_{ij}^2}\right]r_{ij}'r_{ij}^\dagger A\alpha e^{-\alpha r_{ij}}-$				$j\in\mathcal{S}_i^0 \wedge p,q\in\{i,j\}$
10			$w_{ij}(r_{ij})\left[\frac{Q}{r_{ij}^2}\right]r_{ij}'^\dagger Ae^{-\alpha r_{ij}}-$				$j\in\mathcal{S}_i^0 \wedge p,q\in\{i,j\}$
11			$w_{ij}(r_{ij})\left[1+\frac{Q}{r_{ij}}\right]r_{ij}'^\dagger A\alpha e^{-\alpha r_{ij}}+$				$j\in\mathcal{S}_i^0 \wedge p,q\in\{i,j\}$
12			$w_{ij}(r_{ij})\left[1+\frac{Q}{r_{ij}}\right]r_{ij}'r_{ij}^\dagger A\alpha^2 e^{-\alpha r_{ij}}$				$j\in\mathcal{S}_i^0 \wedge p,q\in\{i,j\}$
13					w_{ij}		$j\in\mathcal{S}_i^0$
14					w_{ij}'		table 4.10
15					$w_{ij}'^\dagger$		table 4.11
16					r_{ij}'		table 4.7
17					$r_{ij}'^\dagger$		table 4.8

18		$b_{ij}^{'\dagger}\times$					
19			$\frac{1}{2}p_{ij}^{\pi\theta'^{\dagger}}+$				
20				$\frac{3}{4}\left[1+\sum_{k\neq i,j}w_{ik}(r_{ik})g_c(\cos(\theta_{jik}))+P_{cc}\right]^{-\frac{5}{2}}\cdot$			$k\in\mathcal{S}^{\infty}$
21				$\left[\sum_{k\neq i,j}\left[w'_{ik}(r_{ik})g_c\left(\cos(\theta_{jik})\right)+\right.\right.$			$k\in\mathcal{S}_i^1\setminus\{j\}\wedge q\in\{i,j\}$
22				$\left.w_{ik}(r_{ik})g'_c\left(\cos(\theta_{jik})\right)\right]+P'_{cc}\Big]\cdot$			$k\in\mathcal{S}_i^1\setminus\{j\}$
23				$\left[\sum_{k\neq i,j}\left[w^{\dagger}_{ik}(r_{ik})g_c\left(\cos(\theta_{jik})\right)+\right.\right.$			$k\in\mathcal{S}_i^1\setminus\{j\}\wedge p\in\{i,j\}$
24				$\left.w_{ik}(r_{ik})g^{\dagger}_c\left(\cos(\theta_{jik})\right)\right]+P^{\dagger}_{cc}\Big]-$			$k\in\mathcal{S}_i^1\setminus\{j\}$
25				$\frac{1}{2}\left[1+\sum_{k\neq i,j}w_{ik}(r_{ik})g_c\left(\cos(\theta_{jik})\right)+P_{cc}\right]^{-\frac{1}{2}}\cdot$			$k\in\mathcal{S}^{\infty}$
26				$\left[\sum_{k\neq i,j}\left[w^{'\dagger}_{ik}(r_{ik})g_c\left(\cos(\theta_{jik})\right)+\right.\right.$			$k\in\mathcal{S}_i^1\setminus\{j\}\wedge q,p\in\{i,j\}$
27				$w'_{ik}(r_{ik})g^{\dagger}_c\left(\cos(\theta_{jik})\right)+$			$k\in\mathcal{S}_i^1\setminus\{j\}\wedge p\in\{i,j\}$
28				$w^{\dagger}_{ik}(r_{ik})g'_c\left(\cos(\theta_{jik})\right)+$			$k\in\mathcal{S}_i^1\setminus\{j\}\wedge q\in\{i,j\}$
29				$\left.w_{ik}(r_{ik})g^{'\dagger}_c\left(\cos(\theta_{jik})\right)\right]+P^{'\dagger}_{cc}\Big]$			$k\in\mathcal{S}_i^1\setminus\{j\}$
30					$w_{ik}(r_{ik})$		$k\in\mathcal{S}_i^0\setminus\{j\}$
31					$w'_{ik}(r_{ik})$		$k\in\mathcal{S}_i^1\setminus\{j\}$
32					$w^{'\dagger}_{ik}(r_{ik})$		$k\in\mathcal{S}_i^1\setminus\{j\}$
33					g_c		$\mathcal{S}^{\infty}$
34					g'_c		$\mathcal{S}^{\infty}$
35					$g^{'\dagger}_c$		$\mathcal{S}^{\infty}$
36			$\frac{1}{2}p_{ji}^{\pi\theta'^{\dagger}}+$				switch indices ↑
37			$\pi_{ij}^{rc'^{\dagger}}+$				table A.3
38			$\pi_{ij}^{dh'^{\dagger}}$				
39				$T_{ij}^{'\dagger}(N_{ij},N_{ji},N_{ij}^{conj})\cdot$			
40					T		table A.1

41				T'		table A.2
42				$T'^{\dagger}$		table A.3
43			$\left(\sum_{k,l\neq i,j}(def)\right)+$			
44			$T'_{ij}\sum_{k,l\neq i,j}\left((d^{\dagger}ef)+(de^{\dagger}f)+(def^{\dagger})\right)+$			
45			$T^{\dagger}_{ij}\sum_{k,l\neq i,j}\left((d'ef)+(de'f)+(def')\right)+$			
46				d		table 4.12
47				d'		table 4.13
48				e		table 4.15
49				e'		table 4.16
50				f		table 4.18
51				f'		table 4.19
52			$T_{ij}\sum_{k,l\neq i,j}\left((d'^{\dagger}ef)+(de'^{\dagger}f)+(def'^{\dagger})+\right.$			
53			$(d'e^{\dagger}f)+(d'ef^{\dagger})+(de'f^{\dagger})+$			
54			$\left.(d^{\dagger}e'f)+(d^{\dagger}ef')+(de^{\dagger}f')\right)$			
55				$d'^{\dagger}$		table 4.14
56				$e'^{\dagger}$		table 4.17
57				$f'^{\dagger}$		table 4.20
58	$V^A_{ij}+$					
59		$-w_{ij}(r_{ij})\sum_{n=1}^{3}B^{(n)}_{ij}e^{-\beta^{(n)}_{ij}r_{ij}}$				$j\in\mathcal{S}^0_i$
60	$b'_{ij}\times$					
61		$\frac{1}{2}p^{\pi\theta'}_{ij}+$				$\mathcal{S}^{\infty}$
62			$-\frac{1}{2}\left[1+\sum_{k\neq i,j}w_{ik}(r_{ik})g_c\left(\cos(\theta_{jik})\right)+P_{cc}\right]^{-\frac{3}{2}}\cdot$			$k\in\mathcal{S}^1_i\setminus\{j\}\wedge q\in\{i,j\}$
63			$\left[\sum_{k\neq i,j}\left(w'_{ik}(r_{ik})g_c\left(\cos(\theta_{jik})\right)+\right.\right.$			$k\in\mathcal{S}^0_i\setminus\{j\}$
64			$\left.\left.w_{ik}(r_{ik})g'_c\left(\cos(\theta_{jik})\right)\right)+P'_{cc}\right]$			
65		$\frac{1}{2}p^{\pi\theta'}_{ji}+$				switch indices ↑

#					
66			$\pi_{ij}^{rc'}+$			spline
67			$\pi_{ij}^{dh'}+$			
68				$\left(T'_{ij}\sum_{k,l\neq i,j}(def)\right)+$		
69				$T_{ij}\sum_{k,l\neq i,j}\left[(d'ef)+(de'f)+(def')\right]$		
70		$V_{ij}^{A^\dagger}+$				
71			$-w'_{ij}(r_{ij})\sum_{n=1}^3 B^{(n)}e^{-\beta^{(n)}r_{ij}}+$			table 4.10
72			$w_{ij}(r_{ij})r'_{ij}\sum_{n=1}^3 B^{(n)}\beta^{(n)}e^{-\beta^{(n)}r_{ij}}$			$j\in\mathcal{S}_i^0$
73		$b_{ij}^\dagger\times$				
74		$V_{ij}^{A'}+$				
75		$b_{ij}\times$				
76			$\frac{1}{2}p_{ij}^{\pi\theta}+$			
77				$[1+P_{cc}+$		$\mathcal{S}^\infty$
78				$+\sum_{k\neq i,j}w_{ik}(r_{ik})\cdot g_c(\cos(\theta_{jik}))]^{-\frac{1}{2}}$		$k\in\mathcal{S}_i^0\setminus\{j\}$
79			$\frac{1}{2}p_{ji}^{\pi\theta}+$			↑ switch indices
80			$\pi_{ij}^{rc}+$			table A.1
81			$\pi_{ij}^{dh}+$			
82				$T_{ij}(N_{ij},N_{ji},N_{ij}^{conj})\cdot$		table A.1
83				$\sum_{k,l\neq i,j}(1-\cos^2\omega_{kijl})\cdot$		$\mathcal{S}^\infty$
84				$w_{jl}(r_{jl})w_{ik}(r_{ik})\cdot$		$l\in\mathcal{S}_j^0\setminus\{i\},k\in\mathcal{S}_i^0\setminus\{j\}$
85				$\left(1-w\left(\cos(\theta_{jik})\right)\right)\left(1-w\left(\cos(\theta_{ijl})\right)\right)$		j,i,k or i,j,l co-planar
86		$V_{ij}^{A'^\dagger}$				
87			$-w_{ij}'^{\dagger}(r_{ij})\sum_{n=1}^3 B^{(n)}e^{-\beta^{(n)}r_{ij}}+$			$j\in\mathcal{S}_i^0\wedge q\in\{i,j\}$
88			$w'_{ij}(r_{ij})r_{ij}^\dagger\sum_{n=1}^3 B^{(n)}\beta^{(n)}e^{-\beta^{(n)}r_{ij}}+$			$j\in\mathcal{S}_i^1\wedge q\in\{i,j\}$
89			$w_{ij}^\dagger(r_{ij})r'_{ij}\sum_{n=1}^3 B^{(n)}\beta^{(n)}e^{-\beta^{(n)}r_{ij}}+$			$j\in\mathcal{S}_i^1\wedge p\in\{i,j\}$
90			$w_{ij}(r_{ij})r_{ij}'^{\dagger}\sum_{n=1}^3 B^{(n)}\beta^{(n)}e^{-\beta^{(n)}r_{ij}}-$			$j\in\mathcal{S}_i^0\wedge q,p\in\{i,j\}$
91			$w_{ij}(r_{ij})r_{ij}^\dagger r'_{ij}\sum_{n=1}^3 B^{(n)}\beta^{(n)^2}e^{-\beta^{(n)}r_{ij}}$			$j\in\mathcal{S}_i^0\wedge q,p\in\{i,j\}$

4.2.2. Table for the Hessian of the Lennard-Jones term

The second derivative for $E^{LJ'^\dagger}$ is presented in table 4.5.

Table 4.5: Table representation of $E^{LJ'^\dagger}$

	A	B	C	D	E	F
1	$E^{LJ'^\dagger}$					
2		$w_{ij}^{p'^\dagger}(r_{LJ}) \cdot w_{ij}^{p}(b_{ij}^{*}) \cdot C_{ij} V_{ij}^{LJ}(r_{ij})+$				
3		$w_{ij}^{p'}(r_{ij}^{LJ}) \cdot w_{ij}^{p^\dagger}(b_{ij}^{*}) \cdot C_{ij} V_{ij}^{LJ}(r_{ij})+$				
4		$w_{ij}^{p^\dagger}(r_{ij}^{LJ}) \cdot w_{ij}^{p'}(b_{ij}^{*}) \cdot C_{ij} V_{ij}^{LJ}(r_{ij})+$				
5		$w_{ij}^{p'}(r_{ij}^{LJ}) \cdot w_{ij}^{p}(b_{ij}^{*}) \cdot C_{ij}^{\dagger} V_{ij}^{LJ}(r_{ij})+$				
6		$w_{ij}^{p^\dagger}(r_{ij}^{LJ}) \cdot w_{ij}^{p}(b_{ij}^{*}) \cdot C_{ij}' V_{ij}^{LJ}(r_{ij})+$				
7		$w_{ij}^{p'}(r_{ij}^{LJ}) \cdot w_{ij}^{p}(b_{ij}^{*}) \cdot C_{ij} V_{ij}^{LJ^\dagger}(r_{ij})+$				
8		$w_{ij}^{p^\dagger}(r_{ij}^{LJ}) \cdot w_{ij}^{p}(b_{ij}^{*}) \cdot C_{ij} V_{ij}^{LJ'}(r_{ij})+$				
9		$w_{ij}^{p}(r_{ij}^{LJ}) \cdot w_{ij}^{p'^\dagger}(b_{ij}^{*}) \cdot C_{ij} V_{ij}^{LJ}(r_{ij})+$				
10		$w_{ij}^{p}(r_{ij}^{LJ}) \cdot w_{ij}^{p'}(b_{ij}^{*}) \cdot C_{ij}^{\dagger} V_{ij}^{LJ}(r_{ij})+$				
11		$w_{ij}^{p}(r_{ij}^{LJ}) \cdot w_{ij}^{p^\dagger}(b_{ij}^{*}) \cdot C_{ij}' V_{ij}^{LJ}(r_{ij})+$				
12		$w_{ij}^{p}(r_{ij}^{LJ}) \cdot w_{ij}^{p'}(b_{ij}^{*}) \cdot C_{ij} V_{ij}^{LJ^\dagger}(r_{ij})+$				
13		$w_{ij}^{p}(r_{ij}^{LJ}) \cdot w_{ij}^{p^\dagger}(b_{ij}^{*}) \cdot C_{ij} V_{ij}^{LJ'}(r_{ij})+$				
14		$w_{ij}^{p}(r_{ij}^{LJ}) \cdot w_{ij}^{p}(b_{ij}^{*}) \cdot C_{ij}'^{\dagger} V_{ij}^{LJ}(r_{ij})+$				
15		$w_{ij}^{p}(r_{ij}^{LJ}) \cdot w_{ij}^{p}(b_{ij}^{*}) \cdot C_{ij}' V_{ij}^{LJ^\dagger}(r_{ij})+$				
16		$w_{ij}^{p}(r_{ij}^{LJ}) \cdot w_{ij}^{p}(b_{ij}^{*}) \cdot C_{ij}^{\dagger} V_{ij}^{LJ'}(r_{ij})+$				
17		$w_{ij}^{p}(r_{ij}^{LJ}) \cdot w_{ij}^{p}(b_{ij}^{*}) \cdot C_{ij} V_{ij}^{LJ'^\dagger}(r_{ij})-$				
18		$\left[w_{ij}^{p'^\dagger}(r_{LJ}) \right] \cdot C_{ij} V_{ij}^{LJ}(r_{ij})-$				
19		$\left[w_{ij}^{p'}(r_{ij}^{LJ}) \right] \cdot C_{ij}^{\dagger} V_{ij}^{LJ}(r_{ij})-$				

65

#						
20		$\left[w_{ij}^{p^\dagger}(r_{ij}^{LJ})\right] \cdot C'_{ij} V_{ij}^{LJ}(r_{ij})-$				
21		$\left[w_{ij}^{p'}(r_{ij}^{LJ})\right] \cdot C_{ij} V_{ij}^{LJ^\dagger}(r_{ij})+$				
22		$\left[w_{ij}^{p^\dagger}(r_{ij}^{LJ})\right] \cdot C_{ij} V_{ij}^{LJ'}(r_{ij})+$				
23		$\left[1-w_{ij}^{p}(r_{ij}^{LJ})\right] \cdot C_{ij}^{'\dagger} V_{ij}^{LJ}(r_{ij})+$				
24		$\left[1-w_{ij}^{p}(r_{ij}^{LJ})\right] \cdot C'_{ij} V_{ij}^{LJ^\dagger}(r_{ij})+$				
25		$\left[1-w_{ij}^{p}(r_{ij}^{LJ})\right] \cdot C_{ij}^{\dagger} V_{ij}^{LJ'}(r_{ij})+$				
26		$\left[1-w_{ij}^{p}(r_{ij}^{LJ})\right] \cdot C_{ij} V_{ij}^{LJ'^\dagger}(r_{ij})$				
27				$w_{ij}^{p}(r_{ij}^{LJ})$		$j \in \mathcal{S}_i^4$
28				$w_{ij}^{p'}(r_{ij}^{LJ})$		table 4.10
29				$w_{ij}^{p'^\dagger}(r_{LJ})$		table 4.11
30				$w_{ij}^{p}(b_{ij}^*)$		$j \in \mathcal{S}_i^6$
31				$w_{ij}^{p'}(b_{ij}^*)$		table 4.10
32				$w_{ij}^{p'^\dagger}(b_{ij}^*)$		table 4.11
33				C_{ij}		
34			$1 - \max$			
35			$\underbrace{w_{ij}(r_{ij})}_{\Omega_1},$			$j \in \mathcal{S}_i^0$
36			$\underbrace{w_{ik}(r_{ik}) \cdot w_{kj}(r_{kj})}_{\Omega_2},$			$(k \in \mathcal{S}_i^0) \wedge (j \in \mathcal{S}_k^0)$
37			$\underbrace{w_{ik}(r_{ik}) \cdot w_{kl}(r_{kl}) \cdot w_{lj}(r_{lj})}_{\Omega_3}$			$(k \in \mathcal{S}_i^0) \wedge (l \in \mathcal{S}_k^0) \wedge (j \in \mathcal{S}_l^0)$
38				C'_{ij}		

39					$\begin{cases} w'_{ij}(r_{ij}) & \text{if } \Omega_1 \geq \max\{\Omega_2,\Omega_3\} \\[4pt] \begin{aligned} &w'_{ik}(r_{ik})w_{kj}(r_{kj})+ \\ &w_{ik}(r_{ik})w'_{kj}(r_{kj}) \end{aligned} & \text{if } \Omega_2 \geq \max\{\Omega_1,\Omega_3\} \\[4pt] \begin{aligned} &w'_{ik}(r_{ik})w_{kl}(r_{kl})w_{lj}(r_{lj})+ \\ &w_{ik}(r_{ik})w'_{kl}(r_{kl})w_{lj}(r_{lj})+ \\ &w_{ik}(r_{ik})w_{kl}(r_{kl})w'_{lj}(r_{lj}) \end{aligned} & \text{if } \Omega_3 \geq \max\{\Omega_1,\Omega_2\} \end{cases}$		$\begin{cases} j \in \mathcal{S}_i^1 \wedge q \in \{i,j\} \\[6pt] \text{tables 4.9 and 4.10} \\[6pt] \text{tables 4.9 and 4.10} \end{cases}$
40			$C_{ij}^{'\dagger}$				
41					$\begin{cases} w_{ij}^{'\dagger}(r_{ij}) & \text{if } \Omega_1 \geq \max\{\Omega_2,\Omega_3\} \\[4pt] \begin{aligned} &w_{ik}^{'\dagger}(r_{ik})w_{kj}(r_{kj})+ \\ &w'_{ik}(r_{ik})w_{kj}^{\dagger}(r_{kj})+ \\ &w_{ik}^{\dagger}(r_{ik})w'_{kj}(r_{kj})+ \\ &w_{ik}(r_{ik})w_{kj}^{'\dagger}(r_{kj}) \end{aligned} & \text{if } \Omega_2 \geq \max\{\Omega_1,\Omega_3\} \\[4pt] \begin{aligned} &w'_{ik}(r_{ik})w_{kl}(r_{kl})w_{lj}(r_{lj})+ \\ &w'_{ik}(r_{ik})w_{kl}^{\dagger}(r_{kl})w_{lj}(r_{lj})+ \\ &w_{ik}^{\dagger}(r_{ik})w'_{kl}(r_{kl})w_{lj}(r_{lj})+ \\ &w'_{ik}(r_{ik})w_{kl}(r_{kl})w_{lj}^{\dagger}(r_{lj})+ \\ &w_{ik}^{\dagger}(r_{ik})w_{kl}(r_{kl})w'_{lj}(r_{lj})+ \\ &w_{ik}(r_{ik})w_{kl}^{'\dagger}(r_{kl})w_{lj}(r_{lj})+ \\ &w_{ik}(r_{ik})w'_{kl}(r_{kl})w_{lj}^{\dagger}(r_{lj})+ \\ &w_{ik}(r_{ik})w_{kl}^{\dagger}(r_{kl})w'_{lj}(r_{lj})+ \\ &w_{ik}(r_{ik})w_{kl}(r_{kl})w_{lj}^{'\dagger}(r_{lj}) \end{aligned} & \text{if } \Omega_3 \geq \max\{\Omega_1,\Omega_2\} \end{cases}$		$\begin{cases} j \in \mathcal{S}_i^1 \wedge p,q \in \{i,j\} \\[6pt] \text{tables 4.9, 4.10 and 4.11} \\[6pt] \text{tables 4.9, 4.10 and 4.11} \end{cases}$
42			$V_{ij}^{LJ}(r_{ij})$				

#						
43				$4\epsilon\left[\left(\frac{\sigma}{r_{ij}}\right)^{12}-\left(\frac{\sigma}{r_{ij}}\right)^{6}\right]$		$\mathcal{S}^{\infty}$
44			$V_{ij}^{LJ'}(r_{ij})$			
45				$24\epsilon\left[\left(\frac{\sigma^{6}}{r_{ij}^{7}}\right)-2\left(\frac{\sigma^{12}}{r_{ij}^{13}}\right)\right]\cdot\frac{\partial}{\partial u_{q}}r_{ij}$		$q\in\{i,j\}$
46			$V_{ij}^{LJ'^{\dagger}}(r_{ij})$			
47				$24\epsilon\left[26\left(\frac{\sigma^{12}}{r_{ij}^{14}}\right)-7\left(\frac{\sigma^{6}}{r_{ij}^{8}}\right)\right]\cdot\frac{\partial}{\partial u_{q}}r_{ij}\cdot\frac{\partial}{\partial u_{p}}r_{ij}+$		$p,q\in\{i,j\}$
48				$24\epsilon\left[\left(\frac{\sigma^{6}}{r_{ij}^{7}}\right)-2\left(\frac{\sigma^{12}}{r_{ij}^{13}}\right)\right]\cdot\frac{\partial^{2}}{\partial u_{p}\partial u_{q}}r_{ij}$		$p,q\in\{i,j\}$

4.2.3. Table for the Hessian of the torsional term

The second derivative for $E^{tors'^{\dagger}}$ is presented in table 4.6.

Table 4.6: Table representation of $E^{tors'^{\dagger}}$

	A	B	C	D	E	F
1	$E^{tors'^{\dagger}}$					
2		$\frac{1}{2}\sum_i \sum_{j\neq i} \sum_{k\neq i,j} \sum_{l\neq i,j,k} \big[$				
3		$\left(w_{ij}'^{\dagger}(r_{ij}) \cdot w_{jk}(r_{jk}) \cdot w_{kl}(r_{kl}) \times V^{tors}(\omega_{ijkl})\right) +$				tables 4.9-4.11
4		$\left(w_{ij}'(r_{ij}) \cdot w_{jk}^{\dagger}(r_{jk}) \cdot w_{kl}(r_{kl}) \times V^{tors}(\omega_{ijkl})\right) +$				tables 4.9-4.11
5		$\left(w_{ij}^{\dagger}(r_{ij}) \cdot w_{jk}'(r_{jk}) \cdot w_{kl}(r_{kl}) \times V^{tors}(\omega_{ijkl})\right) +$				tables 4.9-4.11
6		$\left(w_{ij}'(r_{ij}) \cdot w_{jk}(r_{jk}) \cdot w_{kl}^{\dagger}(r_{kl}) \times V^{tors}(\omega_{ijkl})\right) +$				tables 4.9-4.11
7		$\left(w_{ij}^{\dagger}(r_{ij}) \cdot w_{jk}(r_{jk}) \cdot w_{kl}'(r_{kl}) \times V^{tors}(\omega_{ijkl})\right) +$				tables 4.9-4.11
8		$\left(w_{ij}'(r_{ij}) \cdot w_{jk}(r_{jk}) \cdot w_{kl}(r_{kl}) \times V^{tors^{\dagger}}(\omega_{ijkl})\right) +$				tables 4.9-4.11
9		$\left(w_{ij}^{\dagger}(r_{ij}) \cdot w_{jk}(r_{jk}) \cdot w_{kl}(r_{kl}) \times V^{tors'}(\omega_{ijkl})\right) +$				tables 4.9-4.11
10		$\left(w_{ij}(r_{ij}) \cdot w_{jk}'^{\dagger}(r_{jk}) \cdot w_{kl}(r_{kl}) \times V^{tors}(\omega_{ijkl})\right) +$				tables 4.9-4.11
11		$\left(w_{ij}(r_{ij}) \cdot w_{jk}'(r_{jk}) \cdot w_{kl}^{\dagger}(r_{kl}) \times V^{tors}(\omega_{ijkl})\right) +$				tables 4.9-4.11
12		$\left(w_{ij}(r_{ij}) \cdot w_{jk}^{\dagger}(r_{jk}) \cdot w_{kl}'(r_{kl}) \times V^{tors}(\omega_{ijkl})\right) +$				tables 4.9-4.11
13		$\left(w_{ij}(r_{ij}) \cdot w_{jk}'(r_{jk}) \cdot w_{kl}(r_{kl}) \times V^{tors^{\dagger}}(\omega_{ijkl})\right) +$				tables 4.9-4.11
14		$\left(w_{ij}(r_{ij}) \cdot w_{jk}^{\dagger}(r_{jk}) \cdot w_{kl}(r_{kl}) \times V^{tors'}(\omega_{ijkl})\right) +$				tables 4.9-4.11
15		$\left(w_{ij}(r_{ij}) \cdot w_{jk}(r_{jk}) \cdot w_{kl}'^{\dagger}(r_{kl}) \times V^{tors}(\omega_{ijkl})\right) +$				tables 4.9-4.11
16		$\left(w_{ij}(r_{ij}) \cdot w_{jk}(r_{jk}) \cdot w_{kl}'(r_{kl}) \times V^{tors^{\dagger}}(\omega_{ijkl})\right) +$				tables 4.9-4.11
17		$\left(w_{ij}(r_{ij}) \cdot w_{jk}(r_{jk}) \cdot w_{kl}^{\dagger}(r_{kl}) \times V^{tors'}(\omega_{ijkl})\right) +$				tables 4.9-4.11

18		$\left(w_{ij}(r_{ij}) \cdot w_{jk}(r_{jk}) \cdot w_{kl}(r_{kl}) \times V^{tors'^{\dagger}}(\omega_{ijkl}) \right) \Big]$				tables 4.9-4.11
19			$V^{tors}(\omega_{ijkl})$			
20				$\epsilon \left[\frac{256}{405} \cos^{10}\left(\frac{\omega}{2}\right) - \frac{1}{10} \right]$		$\mathcal{S}^{\infty}$
21			$V^{tors'}(\omega_{ijkl})$			
22				$10\epsilon \left[\frac{256}{405} \cos^{9}\left(\frac{\omega}{2}\right) \left(\cos\left(\frac{\omega}{2}\right) \right)' \right]$		$\mathcal{S}^{\infty}$
23			$V^{tors'^{\dagger}}(\omega_{ijkl})$			
24				$\frac{2560}{405}\epsilon \left[9 \cdot \cos^{8}\left(\frac{\omega}{2}\right) \left(\cos\left(\frac{\omega}{2}\right) \right)' \left(\cos\left(\frac{\omega}{2}\right) \right)^{\dagger} + \right.$		$\mathcal{S}^{\infty}$
25				$\left. \cos^{9}\left(\frac{\omega}{2}\right) \left(\cos\left(\frac{\omega}{2}\right) \right)'^{\dagger} \right]$		$\mathcal{S}^{\infty}$

4.2.4. Additional Tables

Not all information could be fit in tables 4.4, 4.5, and 4.6. As such, these additional tables are presented within this subsection.

Table 4.7: Table representation of r'_{ij}

	A	B	C	D	E
1	r'_{ij}				$q \in \{i,j\}$
2		$\frac{\partial}{\partial u_q} r_{ij}$			
3			$\delta_{jq}\frac{u_j - u_i}{r_{ij}} -$		$q = j$
4			$\delta_{iq}\frac{u_j - u_i}{r_{ij}}$		$q = i$

Table 4.8: Table representation of $r'^{\dagger}_{ij}$

	A	B	C	D	E
1	$r'^{\dagger}_{ij}$				$p,q \in \{i,j\}$
2		$\frac{\partial^2}{\partial u_p \partial u_q} r_{ij}$			
3			$\left(\delta_{jq} - \delta_{iq}\right) \cdot \left(\delta_{jp} - \delta_{ip}\right) \cdot \left[\frac{r_{ij}^2 - \left(u_j - u_i\right)^2}{r_{ij}^3}\right]$		$p,q \in \{i,j\}$

Table 4.9: Table representation of w_{ij}

	A	B	C
1	$w_{ij}(\gamma)$		$\begin{cases} j \in \mathcal{S}_i^0 & \gamma = r_{ij}^c \\ k \in \mathcal{S}_i^2 \setminus \{j\} & \gamma = N_{ij}^c \\ j \in \mathcal{S}_i^4 & \gamma = r_{ij}^{LJ^c} \\ j \in \mathcal{S}_i^6 & \gamma = b_{ij}^{*c} \end{cases}$

Table 4.10: Table representation of w'_{ij}

	A	B	C	D	E
1	$w'_{ij}(\gamma)$				$\begin{cases} j \in \mathcal{S}_i^1 \wedge q \in \{i,j\} & \gamma = r_{ij}^c \\ k \in \mathcal{S}_i^1 \setminus \{j\} \wedge q \in \{i,k\} & \gamma = N_{ij}^c \\ j \in \mathcal{S}_i^5 \wedge q \in \{i,j\} & \gamma = r_{ij}^{LJ^c} \\ j \in \mathcal{S}_i^7 \wedge q \notin \{i,j\} & \gamma = b_{ij}^{*c} \end{cases}$
2		$\frac{\partial}{\partial u_q}\left(w_{ij}(\gamma)\right)$			
3			$\frac{\partial}{\partial \gamma} w_{ij}(\gamma)\cdot$		$\begin{cases} j \in \mathcal{S}_i^1 & \gamma = r_{ij}^c \\ k \in \mathcal{S}_i^1 \setminus \{j\} & \gamma = N_{ij}^c \\ j \in \mathcal{S}_i^5 & \gamma = r_{ij}^{LJ^c} \\ j \in \mathcal{S}_i^7 & \gamma = b_{ij}^{*c} \end{cases}$

4			$\frac{\partial}{\partial u_q}\gamma$		$\begin{cases} q \in \{i,j\} & \gamma \in \{r_{ij}^c, r_{ij}^{LJ^c}\} \\ q \in \{i,k\} & \gamma = N_{ij}^c \\ q \notin \{i,j\} & \gamma = b_{ij}^{*c} \end{cases}$

Table 4.11: Table representation of $w_{ij}^{'\dagger}$

	A	B	C	D	E
1	$w_{ij}^{'\dagger}(\gamma)$				$\begin{cases} j \in \mathcal{S}_i^1 \wedge p,q \in \{i,j\} & \gamma = r_{ij}^c \\ k \in \mathcal{S}_i^1 \setminus \{j\} \wedge p,q \in \{i,k\} & \gamma = N_{ij}^c \\ j \in \mathcal{S}_i^5 \wedge p,q \in \{i,j\} & \gamma = r_{ij}^{LJ^c} \\ j \in \mathcal{S}_i^7 \wedge p,q \notin \{i,j\} & \gamma = b_{ij}^{*c} \end{cases}$
2		$\frac{\partial^2}{\partial u_p \partial u_q}(w_{ij}(\gamma))$			
3			$\frac{\partial^2}{\partial \gamma^2}(w_{ij}(\gamma))\cdot$		$\begin{cases} j \in \mathcal{S}_i^1 & \gamma = r_{ij}^c \\ j \in \mathcal{S}_i^1 \setminus \{j\} & \gamma = N_{ij}^c \\ j \in \mathcal{S}_i^5 & \gamma = r_{ij}^{LJ^c} \\ j \in \mathcal{S}_i^7 & \gamma = b_{ij}^{*c} \end{cases}$
4			$\frac{\partial}{\partial u_p}\gamma \cdot \frac{\partial}{\partial u_q}\gamma +$		$\begin{cases} p,q \in \{i,j\} & \gamma \in \{r_{ij}^c, r_{ij}^{LJ^c}\} \\ p,q \in \{i,k\} & \gamma = N_{ij}^c \\ p,q \notin \{i,j\} & \gamma = b_{ij}^{*c} \end{cases}$
5			$\frac{\partial}{\partial \gamma}(w_{ij}(\gamma))\cdot$		$\begin{cases} j \in \mathcal{S}_i^1 & \gamma = r_{ij}^c \\ j \in \mathcal{S}_i^1 \setminus \{j\} & \gamma = N_{ij}^c \\ j \in \mathcal{S}_i^5 & \gamma = r_{ij}^{LJ^c} \\ j \in \mathcal{S}_i^7 & \gamma = b_{ij}^{*c} \end{cases}$
6			$\frac{\partial^2}{\partial u_p \partial u_q}\gamma$		$\begin{cases} p,q \in \{i,j\} & \gamma \in \{r_{ij}^c, r_{ij}^{LJ^c}\} \\ p,q \in \{i,k\} & \gamma = N_{ij}^c \\ p,q \notin \{i,j\} & \gamma = b_{ij}^{*c} \end{cases}$

Table 4.12: Table representation of d from equation 3.2.21

	A	B	C	D
1	d			
2		$(1 - \cos^2 \omega_{kijl})$		$\mathcal{S}^\infty$

Table 4.13: Table representation of d' from equation 3.2.25

	A	B	C	D
1	d'			

2		$-2\cos(\omega_{kijl})\cdot(\cos(\omega_{kijl}))'$		$\mathcal{S}^\infty$

Table 4.14: Table representation of $d'^\dagger$ from equation 3.3.11

	A	B	C	D
1	$d'^\dagger$			
2		$-2\left[\cos(\omega_{kijl})^\dagger\cdot(\cos(\omega_{kijl}))'+\right.$		$\mathcal{S}^\infty$
3		$\left.\cos(\omega_{kijl})'^\dagger\right]$		$\mathcal{S}^\infty$

Table 4.15: Table representation of e from equation 3.2.21

	A	B	C	D
1	e			
2		$w_{ik}(r_{ik})\cdot$		$k \in \mathcal{S}_i^0 \setminus \{j\}$
3		$w_{jl}(r_{jl})\cdot$		$l \in \mathcal{S}_i^0 \setminus \{j\}$

Table 4.16: Table representation of e' from equation 3.2.26

	A	B	C	D
1	e'			
2		$w'_{ik}(r_{ik})\cdot$		$k \in \mathcal{S}_i^1 \setminus \{j\} \wedge q \in \{i,k\}$
3		$w_{jl}(r_{jl})+$		$l \in \mathcal{S}_j^0 \setminus \{i\}$
4		$w_{ik}(r_{ik})\cdot$		$k \in \mathcal{S}_i^0 \setminus \{j\}$
5		$w'_{jl}(r_{jl})\cdot$		$l \in \mathcal{S}_j^1 \setminus \{i\} \wedge q \in \{j,l\}$

Table 4.17: Table representation of $e'^\dagger$ from equation 3.3.12

	A	B	C	D
1	$e'^\dagger$			
2		$w_{ik}'^\dagger(r_{ik})\cdot$		$k \in \mathcal{S}_i^1 \setminus \{j\} \wedge q,p \in \{i,k\}$
3		$w_{jl}(r_{jl})+$		$l \in \mathcal{S}_j^0 \setminus \{i\}$
4		$w'_{ik}(r_{ik})\cdot$		$k \in \mathcal{S}_i^0 \setminus \{j\} \wedge q \in \{i,k\}$
5		$w_{jl}^\dagger(r_{jl})+$		$l \in \mathcal{S}_j^1 \setminus \{i\} \wedge p \in \{j,l\}$
6		$w_{ik}^\dagger(r_{ik})\cdot$		$k \in \mathcal{S}_i^1 \setminus \{j\} \wedge p \in \{i,k\}$
7		$w'_{jl}(r_{jl})+$		$l \in \mathcal{S}_j^0 \setminus \{i\} \wedge q \in \{j,l\}$
8		$w_{ik}(r_{ik})\cdot$		$k \in \mathcal{S}_i^0 \setminus \{j\}$
9		$w_{jl}'^\dagger(r_{jl})\cdot$		$l \in \mathcal{S}_j^1 \setminus \{i\} \wedge q,p \in \{j,l\}$

Table 4.18: Table representation of f from equation 3.2.21

	A	B	C	D
1	f			
2		$\left(1 - w\left(\cos\left(\theta_{jik}\right)\right)\right)$		$\theta_{jik} \notin \mathcal{S}^8$
3		$\left(1 - w\left(\cos\left(\theta_{ijl}\right)\right)\right)$		$\theta_{ijl} \notin \mathcal{S}^8$

Table 4.19: Table representation of f' from equation 3.2.27

	A	B	C	D
1	f'			
2		$\left(-w'\left(\cos\left(\theta_{jik}\right)\right)\right) \cdot \left(1 - w\left(\cos\left(\theta_{ijl}\right)\right)\right) +$		$\theta_{jik} \in \mathcal{S}^9 \wedge \theta_{ijl} \notin \mathcal{S}^8, q \in \{j, i, k\}$
3		$\left(1 - w\left(\cos\left(\theta_{jik}\right)\right)\right) \cdot \left(-w'\left(\cos\left(\theta_{ijl}\right)\right)\right)$		$\theta_{jik} \notin \mathcal{S}^8 \wedge \theta_{ijl} \in \mathcal{S}^9, q \in \{j, i, l\}$

Table 4.20: Table representation of $f'^\dagger$ from equation 3.3.13

	A	B	C	D
1	$f'^\dagger$			
2		$-w'^\dagger\left(\cos\left(\theta_{jik}\right)\right)\left(1 - w\left(\cos\left(\theta_{ijl}\right)\right)\right) +$		$\theta_{jik} \in \mathcal{S}^9 \wedge \theta_{ijl} \notin \mathcal{S}^8 \wedge q, p \in \{j, i, k\}$
3		$w'\left(\cos\left(\theta_{jik}\right)\right) w^\dagger\left(\cos\left(\theta_{ijl}\right)\right) +$		$\theta_{jik} \in \mathcal{S}^9 \wedge \theta_{ijl} \in \mathcal{S}^9 \wedge q \in \{j, i, k\} \wedge p \in \{j, i, l\}$
3		$w^\dagger\left(\cos\left(\theta_{jik}\right)\right) w'\left(\cos\left(\theta_{ijl}\right)\right) +$		$\theta_{jik} \in \mathcal{S}^9 \wedge \theta_{ijl} \in \mathcal{S}^9 \wedge q \in \{j, i, k\} \wedge p \in \{j, i, l\}$
3		$\left(1 - w\left(\cos\left(\theta_{jik}\right)\right)\right)\left(-w'^\dagger\left(\cos\left(\theta_{ijl}\right)\right)\right)$		$\theta_{jik} \notin \mathcal{S}^8 \wedge \theta_{ijl} \in \mathcal{S}^9 \wedge q, p \in \{j, i, l\}$

Chapter 5

C++ Implementation

Stuart et al. made the C++ implementation of their AIREBO potential for the LAMMPS [33] software program publicly available for researchers to use. More recently, Szymon Winczewski reduced this to the Carbon only case, as presented in this work.

This code was adapted and built upon in this thesis to calculate the Hessian of the AIREBO potential for systems of Carbon atoms, derived in chapter 3.

5.1. C++ Program Architecture

The program architecture can be divided into four main parts, namely

1. structure and parameter initialization;

2. toolbox functions;

3. Hessian calculation;

4. clean up.

5.1.1. Structure and Parameter Initialization

Before any functions specific to the numerical calculation of the AIREBO Hessian are implemented, a number of preliminary classes and methods need to be clearly defined to give the overall program a coherent structure.

Two classes are designed to impose a high level structure on the overall program, these are the AIREBOForceField class and the Hessian class.

AIREBOForceField Class

The purpose of the AIREBOForceField class is to exhaustively contain all functions and parameters used in the calculation of the total AIREBO energy of a system of Carbon atoms. Naturally, this class contains much of the information needed for the entire calculation of the Hessian matrix. In total, the AIREBOForceField class has five main parts.

1. The class first reads in the CH.airebo file which contains all parameter information for the AIREBO force field numerical calculations. Specifically, this includes cutoff radii, spline knots, and other numerical parameters as presented in chapter 3. This class also defines other constants derived from these low-level parameters, and also defines data structures that will help to simplify later calculations. One important structure defined is the $vec3d$ structure. This structure is meant to completely characterize an atomic position by describing it as a vector, $\mathbf{v} \in \mathbb{R}^3$. The members of this class are the x,y, and z-components of the vector, as well as it's magnitude, r, and squared magnitude, r^2.

2. To read in a data file[1] describing the location and type of each atom in the system being modelled. For each atom, this class will create an instance of a $vec3d$ structure, storing relevant positional information.

3. To create data types able to effectively describe the neighbours of each atom, and ultimately read in neighbour information from an input file. The data types are as follows, assuming N is the number of atoms in the system.

   ```
   neighbours_num  = new int[N];
   neighbours_list = new int*[N];
   neighbours_bonds = new vec3d*[N];
   ```

   That is, a pointer to an array of integers is first created, where element $neighbours\_num[i]$ for $0 \leq i < N$ is the number of neighbours of atom i. Afterwards, a pointer to a pointer is created to describe the neighbour list of each atom. Illustrating again, $neighbours\_list[i]$ is an array of atom identifiers for each atom neighbouring atom i. For instance, $neighbours\_list[i][j]$ for $0 \leq j < neighbours\_num[i]$ is the atom identifier for the jth neighbour of atom i. Lastly, $neighbours\_bonds$ is a pointer to a pointer of $vec3d$'s describing the vector between the two bonding atoms in question. It should be noted that the word bonding here is used loosely because in the typical sense chemical bonding is not necessarily occurring — it is just that these two atoms are within the defined cut-off distance and thus interact within the AIREBO potential. Explicitly, $neighbours\_bonds[i][j]$ is a $vec3d$ instance describing the vector between atoms i and j, as outlined above.

4. To dynamically allocate memory for all of the required data structures. This can be seen in the C++ snippet above using the new command.

5. To declare all relevant functions involved with the calculation of the total energy of a system characterized by an AIREBO potential. These functions will be further explored in the following subsection.

---

[1] Typically in a .xyz file type format.

Hessian Class

The Hessian class characterizes the relevant information for the Hessian of the AIREBO potential. Since most of the relevant AIREBO information is contained within the AIREBOForceField class, the Hessian class is much simpler — containing two main parts.

1. The first part dynamically allocate memory. This involves creating elements for all values within the Hessian matrix. Symmetry is assumed and thus only

$$\sum_{\alpha}^{3N} \sum_{\beta \leq \alpha}^{3N} 1 = \frac{3N(3N+1)}{2} \tag{5.1.1}$$

   elements are required.

2. To define all relevant functions involved with the calculation of the Hessian elements for the AIREBO potential. This will be further explored in subsections 5.1.2 and 5.1.3.

The constructors of each of these classes are defined which act to initialize all of the parameters and variables needed for further computations. Furthermore, it should be noted that only one instance of each class needs to be created.

5.1.2. Toolbox Functions

A number of the functions implemented serve one specific purpose and are repeatedly called from other, higher-level functions. These functions are low-level functions, and due to their specific tasks, are referred to herein as toolbox functions. When implementing the AIREBO potential, the problem was well defined and an overall top-down abstraction was created by virtue of mathematically deriving the Hessian before its implementation. For the implementation itself, a bottom-up approach was used and thus the toolbox functions were the first to be defined.

These toolbox functions include functions like the weighting (switching) functions, spline functions, the cosine of the torsional and bond angles, coordination number functions, and others. Additionally, all the first and second derivatives of these functions are also considered toolbox functions. Most of these functions all intrinsically depend on the lowest level function, which is the first and second derivatives of the position vector, i.e. r', $r^{\dagger}$ and $r'^{\dagger}$ derived in section 2.2.2.

The explicit mathematical definitions for these toolbox functions have been given in chapter 3 and thus the C++ code will not be included herein. These toolbox functions allow higher level functions, which depend on toolbox functions, to then be implemented.

5.1.3. Hessian Calculation

This section of the implementation deals with the high-level functions that provide an overall structure and readability to the program. Generally, these C++ functions represent the functions appearing in

the left most columns of tables 4.4, 4.5 and 4.6, whereas the low level functions are represented of the right-most columns, and subsequent tables in chapter 4.

The highest level functions appear in the main function, shown below[2]

```
for (int p = 0; p < number_of_atoms; p++)
  for (int d1 = 0; d1 < 2; d1++)
    for (int q = p; q < number_of_atoms; q++ )
      for (int d2 = 0; d2 < 2; d2++)
        my_hessian->setElement(p, d1, q, d2, my_airebo->calculateHessianElement(p,d1,q,d2));
```

Here, p and q are atom numbers and $d1$ and $d2$ are Cartesian components where $x \mapsto 0, y \mapsto 1$ and $z \mapsto 2$. Clearly this is once the $my\_hessian$ instance of the Hessian class has been created. The $setElement$ method simply writes a double to a Hessian element, and the $calculateHessianElement$ method is expanded below.

```
double Hessian::calculateHessianElement(int p,int d1,int q,int d2)
{
    return Hessian::REBO_Hessian(p, d1 ,q, d2) +
           Hessian::LJ_Hessian(p, d1 ,q, d2) +
           Hessian::TORS_Hessian(p, d1 ,q, d2));
}
```

The three functions, $REBO\_Hessian$, $LJ\_Hessian$ and $TORS\_Hessian$, then all depend and subsequently make calls to the toolbox functions. Careful care and consideration was made in designing these functions to both ensure correct implementation, and to take into account the interaction radii of terms in order not to calculate needless terms, and to reduce redundancy.

5.1.4. Clean Up

Any time a variable is dynamically allocated to the computer's memory, it must be *freed* (equivalently called *deleted*). Once the Hessian is calculated and output into a file, the dynamically allocated memory is then deleted and the program is complete.

5.2. Discrepancies between analytical and computational forms

A number of discrepancies between the analytical form presented in Stuart's paper [37] and their C++ implementation were discovered. In all cases, the Hessian implementation assumed Stuart's C++ implementation was correct, and thus adjustments were made. These discrepancies will be outlined herein for completeness.

5.2.1. The g function

Recall that within the bond-order term, the following function appears

---

[2]The brackets have been omitted for readability purposes.

$$g_c\left(\cos(\theta_{jik})\right) = g_c^{(1)}(\cos(\theta_{jik})) + S_s(t_N(N_{ij})) \left[g_c^{(2)}(\cos(\theta_{jik})) - g_c^{(1)}(\cos(\theta_{jik}))\right]. \qquad (5.2.1)$$

However, in the implementation by Stuart et al., the following form is used

$$g_c\left(\cos(\theta_{jik})\right) = g_c^{(2)}(\cos(\theta_{jik})) + S_s(t_N(N_{ij})) \left[g_c^{(1)}(\cos(\theta_{jik})) - g_c^{(2)}(\cos(\theta_{jik}))\right]. \qquad (5.2.2)$$

This function imposes penalties for angle-bending and switches smoothly between two forms, $g_c^{(1)}$ and $g_c^{(2)}$. Stuart's paper states that $g_c^{(2)}$ is suitable for highly coordinated forms, i.e. when $N_{ij} \geq N_{ij}^{max}$. According to the following equation

$$t_N(N_{ij}) = \frac{N_{ij} - N^{min}}{N^{max} - N^{min}} =: N_{ij}^c \qquad (5.2.3)$$

when $N_{ij} = N_{ij}^{max}$, $t_N(N_{ij}) = 1$ and when $N_{ij} = N_{ij}^{min}$, $t_N(N_{ij}) = 0$. Then for $t = 0$, $S_s(t_N(N_{ij})) = 1$ and for $t = 1$, $S_s(t_N(N_{ij})) = 0$. So in the context of equation 5.2.2, we get the following implications

$$N_{ij} = N_{ij}^{max} \implies t = 1 \implies S_s(t_N(N_{ij})) = 0 \implies g_c = g_c^{(1)} \qquad (5.2.4)$$

and

$$N_{ij} = N_{ij}^{mmin} \implies t = 0 \implies S_s(t_N(N_{ij})) = 1 \implies g_c = g_c^{(2)} \qquad (5.2.5)$$

which is clearly wrong. Thus the correct form of the equation is that used in the implementation, and as a result that is what was built upon to construct the Hessian implementation.

5.2.2. The π^{dh} function

Within the bond-order term, the π^{dh} term imposed penalties for rotations around multiple bonds. Although it was originally defined in equation 3.1.35, it is repeated here for clarity.

$$\begin{aligned}
\pi_{ij}^{dh} = &T_{ij}(N_{ij}, N_{ji}, N_{ij}^{conj}) \sum_{k \neq i,j} \sum_{l \neq i,j} (1 - \cos^2 \omega_{kijl}) \cdot \\
&w_{ik}^T(r_{ik}) w_{jl}^T(r_{jl}) \Theta(\sin(\theta_{jik}) - s^{min}) \Theta(\sin(\theta_{ijl}) - s^{min})
\end{aligned} \qquad (5.2.6)$$

In Stuart et al.'s implementation, however, the term is represented as

$$\pi_{ij}^{dh} = T_{ij}(N_{ij}, N_{ji}, N_{ij}^{conj}) \sum_{k \neq i,j} \sum_{l \neq i,j} (1 - \cos^2 \omega_{kijl}) \cdot$$

$$w_{ik}^T(r_{ik}) w_{jl}^T(r_{jl}) \left(1 - S_s \left(t \left(\cos \left(\theta_{jik} \right) \right) \right) \right) \cdot \left(1 - S_s \left(t \left(\cos \left(\theta_{ijl} \right) \right) \right) \right) \tag{5.2.7}$$

where

$$t \left(\cos \left(\theta_{ijl} \right) \right) = \frac{\cos \left(\theta_{ijl} \right) - \cos \left(\theta_{ijl} \right)^{min}}{\cos \left(\theta_{ijl} \right)^{max} - \cos \left(\theta_{ijl} \right)^{min}} \tag{5.2.8}$$

That is, the following change was made

$$\Theta \left(\sin \left(\theta_{abc} \right) - s^{min} \right) \rightarrow \left(1 - S_s \left(t \left(\cos \left(\theta_{abc} \right) \right) \right) \right) \tag{5.2.9}$$

The function in this form guarantees that the interactions will be smoothly switched on between $1.0 < \cos(\theta_{jik}) < -0.995$, which corresponds to $180° < \theta_{jik} < 174°$. This means that the interactions are switched on if the vectors $\mathbf{r}_{ji}$ and $\mathbf{r}_{ik}$ are not parallel. This is as expected since the π^{dh} term imposes penalties for rotation around multiple bonds. As a result, this was the formulation used within the C++ implementation.

5.2.3. V^{tors} **function**

Recall that within the torsional energy term (equation 3.7.1), there was a torsional potential term, V^{tors} (Equation 3.7.2), and within that, the argument

$$\cos^{10} \left(\frac{\omega}{2} \right). \tag{5.2.10}$$

In Stuart et al.'s implementation, they calculate the torsional angle, $\cos(\omega)$, using the law of cosines. To get from there to the expression in equation 5.2.10 they use the half angle formulas:

$$\cos^2 \left(\frac{\omega}{2} \right) = \frac{1}{2} \left(1 + \cos(\omega) \right) \tag{5.2.11}$$

$$\sin^2 \left(\frac{\omega}{2} \right) = \frac{1}{2} \left(1 - \cos(\omega) \right) \tag{5.2.12}$$

However, in their implementation, they use equation 5.2.12 as opposed to equation 5.2.11. Meaning that they as a result calculate $\sin^{10} \left(\frac{\omega}{2} \right)$ as opposed to the stated equation in the analytical form of the potential (equation 5.2.10).

Although the past discrepancies could be reasoned by physical arguments, this particular

discrepancy may in fact be a bug in the AIREBO implementation. Stuart et al. claim this torsional potential, $V(\omega)$, has the nice property of having a single minimum when compared to a typical torsional potential form, $T(\omega)$ [37]. These two functions are plotted in figure 5.1 [37].
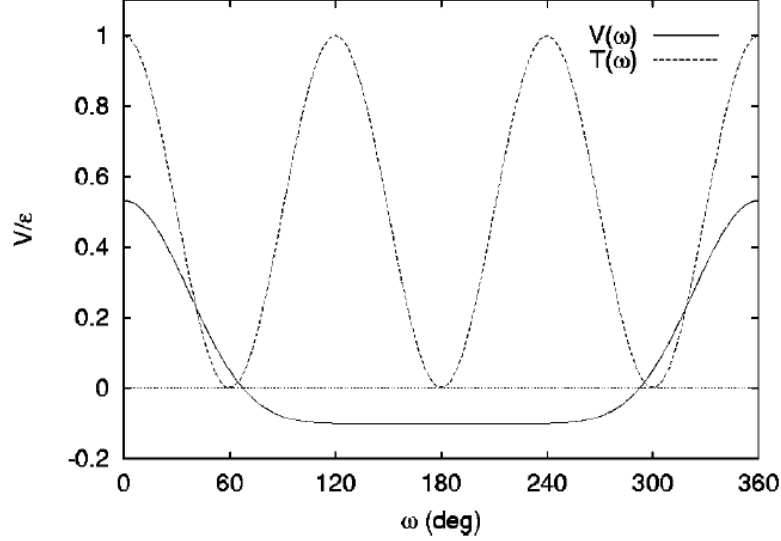

Figure 5.1: Plots of a typical torsional potential, $T(\omega)$, and the torsional potential used in the AIREBO potential, $V(\omega)$.

To rigorously test their implementation, both an analytical expression and computational expression were plotted to compare against figure 5.1. First, analytical expressions for

$$V^{tors}(\omega) = \epsilon \left[\frac{256}{405} \cos^{10}\left(\frac{\omega}{2}\right) - \frac{1}{10} \right]$$
(5.2.13)

and

$$V^{tors}(\omega) = \epsilon \left[\frac{256}{405} \sin^{10}\left(\frac{\omega}{2}\right) - \frac{1}{10} \right]$$
(5.2.14)

were plotted. After that, the implementation was plotted using both of the half angle formulas. This was done by first using the direct implementation of Stuart et al., which used equation 5.2.13, and then by secondly plotting the same thing only changing one line to use 5.2.14 instead.

Both the analytical results and implementation results yielded identical plots. These are shown in figure 5.2.

From inspections of figures 5.1 and 5.2 it is confirmed that the implementation does not agree with the analytical form, nor does it with the physical arguments made for such a functional form.

81
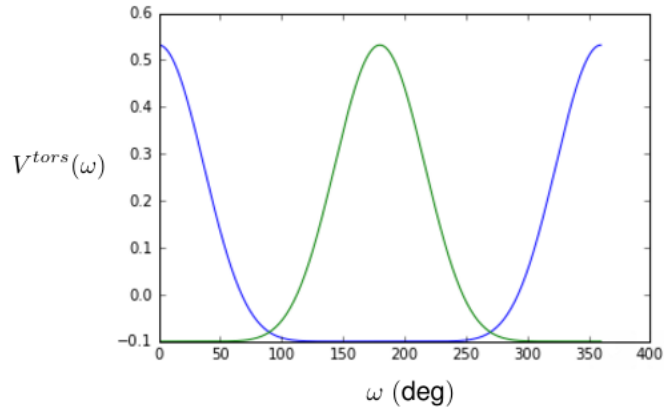
Figure 5.2: Plots representing the values yielded for both the analytical and implementation results of equation 5.2.13 (blue) and equation 5.2.14 (green).

5.2.4. Current Status

As of the submission of this thesis, the code is not currently outputting correct values for the Hessian. This is because the knot values for the derivative of the spline functions are not yet properly in place. This is actively being worked on and meaningful results are expected in the future.

Chapter 6

Summary

This thesis first reduced the AIREBO potential to the case for systems composed exclusively of Carbon atoms. Subsequently, the gradient of this reduced potential was calculated, and finally, the Hessian was calculated. It was noted that in such a large calculation, careful attention was required of the interaction radius of each term. Interaction radii, along with an exhaustive summary of the Hessian, were presented in table form in chapter 4. This was done in part so that needless calculations were not computed in the C++ implementation.

The bulk of the thesis work was in the C++ implementation of the results found in chapter 3 to a functioning program that would take an input file[1] of N atoms and output the $3N \times 3N$ Hessian. This process exposed a number of discrepancies between Stuart et al.'s analytical presentation of the AIREBO potential [37] and their corresponding C++ implementation. These discrepancies are outlined in chapter 5, and in all but one case it was shown that the C++ implementation was correct and was to override the errors in their analytical formulation. In the exceptional case, the authors were contacted.

Results from the C++ implementation can be directly applied to the applications that require only individual Hessian elements, such as configurational temperature. However, for many of the applications outlined in the introduction, the full spectrum[2] of the eigenvalue problem (equation 2.1.5) is required. This is a highly non-trivial task, but has been the focus of study in numerics for decades. Solving the spectrum of a large linear system often times reduces to the problem of diagonalizing the system (i.e. Hessian).

A result of Schwarz's theorem [41] is that if the function $f : \mathbb{R}^n \to \mathbb{R}$ has continuous second partial derivatives at a given point in the domain, then the partial derivatives are commutative at that point. This would then imply symmetry for the Hessian, which would in turn make diagonalizing the system much easier as specific algorithms could be employed.

It was noted, however, that within the current formulation for the AIREBO potential, there are specific regions of discontinuity for the second partial derivatives. Namely, these occurred within

---

[1]The input files follow the form required for the LAMMPS software, outlined here: `http://lammps.sandia.gov/doc/Section_commands.html#cmd-3`.

[2]The spectrum is the list of eigenvalues for the particular eigenproblem.

the two switching functions S_s and S_p at endpoints prescribed for the variable in question. A more detailed analysis of the switching functions at these discontinuous regions would have to be employed to guarantee symmetry of the Hessian.

If symmetry is assumed, this property along with the large degree of sparsity within the Hessian, as determined by the interaction radii, result in the Hessian being both sparse and symmetric. Many numerical methods exist for the efficient diagonalization of such systems. Implementation of such algorithms would output the spectrum of the Hessian and allow the desired calculations to be made.

Bibliography

[1] G. C. Abell. Empirical chemical pseudopotential theory of molecular and metallic bonding. *Physical Review B*, 31, 1985.

[2] B. J. Alder and T. E. Wainwright. Phase transition for a hard sphere system. *Journal of Chemical Physics*, 27, 1957.

[3] M. P. Allen. Introduction to molecular dynamics simulation. *NIC Series*, 23, 2004.

[4] N. L. Allinger and J.-H. Lii. Molecular mechanics - the mm3 force-field for hydrocarbons 2. vibrational frequencies and thermodynamics. *Journal of the American Chemical Society*, 111, 1989.

[5] N. L. Allinger and J.-H. Lii. Molecular mechanics - the mm3 force-field for hydrocarbons 3. the van der waals potentials and crystal data for aliphatic and aromatic hydrocarbons. *Journal of the American Chemical Society*, 111, 1989.

[6] N. L. Allinger, Y. H. Yuh, and J.-H. Lii. Molecular mechanics - the mm3 force-field for hydrocarbons 1. *Journal of the American Chemical Society*, 111, 1989.

[7] N. L. Allinger and. S. Chen and J.-H. Lii. An improved force field (mm4) for saturated hydrocarbons. *Journal of Computational Chemistry*, 17, 1996.

[8] H. C. Andersen. Molecular dynamics simulations at constant pressure and/or temperature. *Journal of Chemical Physics*, 72, 1980.

[9] R. H. Baughman, H. Eckhardt, and M. Kertesz. Structureproperty predictions for new planar forms of carbon: Layered phases containing sp2 and sp atoms. *The Journal of Chemical Physics*, 87, 1987.

[10] M. Born. Thermodynamics of crystals and melting. *Journal of Chemical Physics*, 7, 1939.

[11] C. Braga and K. P. Thomas. A configurational temperature nosé-hoover thermostat. *Journal of Chemical Physics*, 123, 2005.

[12] D. W. Brenner. Empirical potential for hydrocarbons for use in simulating the chemical vapor deposition of diamond films. *Physical Review B*, 42, 1990.

[13] D. W. Brenner. Erratum: Empirical potential for hydrocarbons for use in simulating the chemical vapor deposition of diamond films. *Physical Review B*, 46, 1992.

[14] D. W. Brenner, J.A. Harrison, C. T. White, and R. J. Colton. Molecular dynamics simulations of the nanometer-scale mechanical properties of compressed buckminsterfullerene. *Thin Solid Films*, 206, 1991.

[15] . B. R. Brooks, R. E. Bruccoleri, B. D. Olafson, D. J States, S. Swaminathan, and M. Karplus. Charmm - a program for macromolecular energy, minimization, and dynamics calculations. *Journal of Computational Chemistry*, 4, 1983.

[16] R. Car and M. Parrinello. Unified approach for molecular dynamics and density functional theory. *Physical Review Letters*, 55, 1985.

[17] M. S. Daw and M. Baskes. Embedded-atom method: Derivation and application to impurities, surfaces, and other defects in metals. *Physical Review B*, 29, 1984.

[18] P. de Sainte Claire, K. Song, W. L. Hase, and D. W. Brenner. Comparison of ab initio and empirical potentials for h-atom association with diamond surfaces. *Journal of Chemical Physics*, 100, 1996.

[19] A. Eckmann, A. Felten, A. Mishchenko, L. Britness, R. Krupke, K. S. Novoselov, and C. Casiraghi. Probing the nature of defects in graphene by raman spectroscopy. *Nano Letters*, 12, 2012.

[20] A. N. Enyashin and A. L. Ivanovskii. The squarographites: A lesson in the chemical topology of tessellations in 2- and 3-dimensions. *Physics Status Solidi*, 248, 2011.

[21] J. A. Harrison, S. J. Stuart, D. H. Robertson, and C. T. White. Properties of capped nanotubes when used as spm tips. *Journal of Physical Chemistry B*, 101, 1997.

[22] E. R. Hernández. Molecular dynamics: from basic techniques to applications (a molecular dynamics primer). *AIP Conference Proceedings*, 1077, 2008.

[23] O. G. Jepps, G. Ayton, and D. J. Evans. Microscopic expressions for the thermodynamic temperature. *Physical Review E*, 62, 2000.

[24] A. Kanigel, J. Adler, and E. Polturak. Influence of point defects on the shear elastic coefficients and on the melting temperature of copper. *Computational Physics and Physical Computation*, 12, 2001.

[25] E. A. Castro M. J. Bucknum. The squarographites: A lesson in the chemical topology of tessellations in 2- and 3-dimensions. *Solid State Sciences*, 10, 2008.

[26] G. C. Maitland, M. Rigby, E. B. Smith, and W. A. Wakeham. *Intermolecular forces: their origin and determination.* Calrendon Press, Oxford, 1981.

[27] A. Martini. Lecture 2: Potential energy functions.

[28] D. Marx and J. Hutter. Ab initio molecular dynamics: Theory and implementation. *Modern Methods and Algorithms of Quantum Chemistry*, 1, 2000.

[29] P. M. Morse. Diatomic molecules according to the wave mechanics. ii. vibrational levels. *Physical Review*, 34, 1929.

[30] . N. Nevins, K. S. Chen, and N. L. Allinger. Molecular mechanics (mm4) calculations on alkenes. *Journal of Computational Chemistry*, 17, 1996.

[31] N. Nevins, J.-H. Lii, and N. L. Allinger. Molecular mechanics (mm4) calculations on conjugated hydrocarbons. *Journal of Computational Chemistry*, 17, 1996.

[32] S. Nosé. A unified formulation of the constant temperature molecular-dynamics methods. *Journal of Chemical Physics*, 81, 1984.

[33] S. Plimpton. Fast parallel algorithms for short-range molecular dynamics. *Journal of Computational Physics*, 117, 1995.

[34] J. R. Ray and A. Rahman. Statistical ensembles and molecular dynamics studies of anisotropic solids. *The Journal of Chemical Physics*, 80, 1984.

[35] H. H. Rugh. Dynamical approach to temperature. *Physical Review Letters*, 78, 1997.

[36] A.J. Stone. *The Theory of Intermolecular Forces*. Calrendon Press, Oxford, 1996.

[37] S. J. Stuart, A. B. Tutein, and J. A. Harrison. A reactive potential for hydrocarbons with intermolecular interactions. *Journal of Chemical Physics*, 112, 2000.

[38] J. Tersoff. New empirical model of the structural properties of silicon. *Physical Review Letters*, 56, 1986.

[39] J. Tersoff. New empirical approach for the structure and energy of covalent systems. *Physical Review B*, 37, 1987.

[40] J. Tersoff. Modeling solid-state chemistry: Interatomic potentials for multicomponent systems. *Physical Review B*, 39, 1989.

[41] D. H. Trahan. The mixed partial derivatives and the double derivative. *American Mathematical Monthly*, 76, 1969.

[42] A. R. Ubbelohde. *Melting and Crystal Structure*. Calrendon Press, Oxford, 1965.

[43] L. Verlet. Computer experiments on classical fluids. i. theromodynamical properties of the lennard-jones molecules. *Physical Review*, 159, 1967.

[44] S. J. Weiner, P. A. Kollman, D. A. Case, U. C. Singh, C. Ghio, G. Alagona, S. Profeta, and P. Weiner. A new force-field for molecular mechanical simulation of nucleic acids and proteins. *Journal of the American Chemical Society*, 106, 1984.

List of Figures

List of Tables

Appendices

Appendix A

Spline Derivatives

The explicit expression for the first and second derivatives of all involved spline functions will be discussed herein.

The one dimensional splines will not be explicitly presented due to their simple nature. In general, these one dimensional splines can be represented by an Nth degree polynomial, $\mathcal{P}^N$, with argument χ. The first and second derivatives of such splines are presented in equations A.0.1 and A.0.2.

$$\frac{\partial \mathcal{P}^N(\chi)}{\partial u_q} = \frac{\partial \mathcal{P}^N}{\partial \chi} \cdot \frac{\partial \chi}{\partial u_q} \tag{A.0.1}$$

$$\frac{\partial^2 \mathcal{P}^N(\chi)}{\partial u_q \partial u_q} = \frac{\partial^2 \mathcal{P}^N}{\partial \chi^2} \cdot \frac{\partial \chi}{\partial u_q} \cdot \frac{\partial \chi}{\partial u_p} + \frac{\partial \mathcal{P}^N}{\partial \chi} \cdot \frac{\partial^2 \chi}{\partial u_q \partial u_p} \tag{A.0.2}$$

The treatment of the tricubic splines are more difficult and will now be presented. Both $T(N_{ij}, N_{ji}, N_{ij}^{conj})$ and $\pi_{ij}^{rc}(N_{ij}, N_{ji}, N_{ij}^{conj})$ are tricubic splines in the same variables and only differ by their interpolation points. As such, only the definition tables will be presented for $T(N_{ij}, N_{ji}, N_{ij}^{conj})$.

Table A.1: Definition of a general tricubic spline, with further definitions of its individual arguments.

	A	B	C	D	E
1	$T(N_{ij}, N_{ji}, N_{ij}^{conj})$				
2		N_{ij}			
3			$\sum_{k \neq i,j} w_{ik}(r_{ik})$		$k \in \mathcal{S}_i^0 \setminus \{j\}$
4		N_{ji}			
5			$\sum_{k \neq i,j} w_{jk}(r_{jk})$		$k \in \mathcal{S}_j^0 \setminus \{i\}$
6		N_{ij}^{conj}			
7			$1+$		$\mathcal{S}^\infty$
8			$\left[\sum_{k \neq i,j} w_{ik}(r_{ik}) w_{ki}(N_{ki}) \right]^2 +$		$k \in \mathcal{S}_i^0 \setminus \{j\} \cap \mathcal{S}_i^2$

9			$\left[\sum_{l\neq i,j} w_{jl}(r_{jl})w_{lj}(N_{lj})\right]^2$		$l \in \mathcal{S}_j^0 \setminus \{i\} \cap \mathcal{S}_j^2$

Table A.2: First derivative of a general tricubic spline

	A	B	C	D	E
1	$\frac{\partial}{\partial u_q}\left(T(N_{ij}, N_{ji}, N_{ij}^{conj})\right)$				
2		$\frac{\partial}{\partial N_{ij}}T\cdot$			
3		$\frac{\partial}{\partial u_q}N_{ij}+$			
4			$\sum_{k\neq i,j} w'_{ik}(r_{ik})$		$k \in \mathcal{S}_i^1 \setminus \{j\} \wedge q \in \{i,k\}$
5		$\frac{\partial}{\partial N_{ji}}T\cdot$			
6		$\frac{\partial}{\partial u_q}N_{ji}$			
7			$\sum_{k\neq i,j} \frac{\partial}{\partial u_q}w_{jk}(r_{jk})$		$k \in \mathcal{S}_j^1 \setminus \{i\} \wedge q \in \{j,k\}$
8		$\frac{\partial}{\partial N_{ij}^{conj}}T\cdot$			
9		$\frac{\partial}{\partial u_q}N_{ij}^{conj}$			
10			$2\sum_{k\neq i,j}\left[w_{ik}(r_{ik})w_{ki}(N_{ki})\right]\cdot$		tables 4.9 - 4.11
11			$\left[w'_{ik}(r_{ik})w_{ki}(N_{ki}) + w_{ik}(r_{ik})w'_{ki}(N_{ki})\right]+$		tables 4.9 - 4.11
12			$2\sum_{l\neq i,j}\left[w_{jl}(r_{jl})w_{lj}(N_{lj})\right]\cdot$		tables 4.9 - 4.11
13			$\left[w'_{jl}(r_{jl})w_{lj}(N_{lj}) + w_{jl}(r_{jl})w'_{lj}(N_{lj})\right]$		tables 4.9 - 4.11

Table A.3: First derivative of a general tricubic spline

	A	B	C	D	E
1	$\frac{\partial^2}{\partial u_p \partial u_q}\left(T(N_{ij}, N_{ji}, N_{ij}^{conj})\right)$				
2		$\frac{\partial^2}{\partial N_{ij}^2}T\cdot$			
3		$\frac{\partial^2}{\partial u_p \partial u_q}N_{ij}+$			
4			$\sum_{k\neq i,j} w_{ik}^{'\dagger}(r_{ik})$		$k \in \mathcal{S}_i^1 \setminus \{j\} \wedge q,p \in \{i,k\}$
5		$\frac{\partial^2}{\partial N_{ji}^2}T\cdot$			
6		$\frac{\partial^2}{\partial u_p \partial u_q}N_{ji}$			
7			$\sum_{k\neq i,j} w_{jk}^{'\dagger}(r_{jk})$		$k \in \mathcal{S}_j^1 \setminus \{i\} \wedge q,p \in \{j,k\}$
8		$\frac{\partial^2}{\partial N_{ij}^{conj^2}}T\cdot$			
9		$\frac{\partial^2}{\partial u_p \partial u_q}N_{ij}^{conj}$			
10			$2\sum_{k\neq i,j}\left[w_{ik}'(r_{ik})w_{ki}(N_{ki}) + w_{ik}(r_{ik})w_{ki}'(N_{ki})\right]\cdot$		tables 4.9 - 4.11
11			$w_{ik}^{\dagger}(r_{ik})w_{ki}(N_{ki}) + w_{ik}(r_{ik})w_{ki}^{\dagger}(N_{ki})\Big] +$		tables 4.9 - 4.11
12			$\left(w_{ik}(r_{ik})w_{ki}(N_{ki})\right)\cdot$		tables 4.9 - 4.11
13			$w_{ik}^{'\dagger}(r_{ik})w_{ki}(N_{ki}) + w_{ik}'(r_{ik})w_{ki}^{\dagger}(N_{ki})+$		tables 4.9 - 4.11
14			$w_{ik}^{\dagger}(r_{ik})w_{ki}'(N_{ki}) + w_{ik}(r_{ik})w_{ki}^{'\dagger}(N_{ki})\Big] +$		tables 4.9 - 4.11
15			$2\sum_{l\neq i,j}\left[w_{jl}'(r_{jl})w_{lj}(N_{lj}) + w_{jl}(r_{jl})w_{lj}'(N_{lj})\right]\cdot$		tables 4.9 - 4.11
16			$w_{jl}^{\dagger}(r_{jl})w_{lj}(N_{lj}) + w_{jl}(r_{jl})w_{lj}^{\dagger}(N_{lj})\Big]$		tables 4.9 - 4.11
17			$\left(w_{jl}(r_{jl})w_{lj}(N_{lj})\right)\cdot$		tables 4.9 - 4.11
18			$w_{jl}^{'\dagger}(r_{jl})w_{lj}(N_{lj}) + w_{jl}'(r_{jl})w_{lj}^{\dagger}(N_{lj})+$		tables 4.9 - 4.11
19			$w_{jl}^{\dagger}(r_{jl})w_{lj}'(N_{lj}) + w_{jl}(r_{jl})w_{lj}^{'\dagger}(N_{lj})\Big]$		tables 4.9 - 4.11

Appendix B

Bond Angle and Torsion Angle Definitions and Derivatives

The explicit expression for the first and second derivatives of the bond angles and torsional angles will be presented herein. For the sake of clarity, θ_{jik} is referred to as the bond angle and ω_{kijl} as the torsion angle. These angles only appear as arguments to trigonometric functions throughout the derivation of the Hessian. For this reason they will only be considered in that form as it simplifies things. There are many similarities between θ_{jik} and ω_{kijl}. We will start by calculating the first and second derivatives of $\cos(\theta_{jik})$ and then continue with $\cos(\omega_{kijl})$.

B.1. Bond Angle (θ_{jik}) First Derivative

We begin with the definition of $\cos\left(\theta_{jik}\right)$:

$$\cos\left(\theta_{jik}\right) = \frac{\mathbf{r}_{ji} \cdot \mathbf{r}_{ki}}{|\mathbf{r}_{ji}||\mathbf{r}_{ki}|} \tag{B.1.1}$$

which is equivalent to

$$\cos(\theta_{jik}) = \frac{\mathbf{r}_{ji} \cdot \mathbf{r}_{ki}}{\sqrt{\mathbf{r}_{ji}^2 \mathbf{r}_{ki}^2}} \tag{B.1.2}$$

Taking its derivative, one gets

$$\frac{\partial}{\partial u_q}\cos(\theta_{jik}) = \frac{\frac{\partial}{\partial u_q}\mathbf{r}_{ji} \cdot \mathbf{r}_{ki} + \mathbf{r}_{ji} \cdot \frac{\partial}{\partial u_q}\mathbf{r}_{ki}}{\sqrt{\mathbf{r}_{ji}^2 \mathbf{r}_{ki}^2}} - \frac{\mathbf{r}_{ji} \cdot \mathbf{r}_{ki}\left(2\mathbf{r}_{ji} \cdot \frac{\partial}{\partial u_q}\mathbf{r}_{ji}\mathbf{r}_{ki}^2 + 2\mathbf{r}_{ji}^2\mathbf{r}_{ki} \cdot \frac{\partial}{\partial u_q}\mathbf{r}_{ki}\right)}{2(\mathbf{r}_{ji}^2\mathbf{r}_{ki}^2)^{\frac{3}{2}}} \tag{B.1.3}$$

To simplify things, let's now consider breaking the vectors into their components

$$\mathbf{r}_{ji} := [a_1, a_2, a_3]$$
$$\mathbf{r}_{ki} := [b_1, b_2, b_3]$$

(B.1.4)

Let $\mathcal{A}$ be the set of the vector components, η_i (artificial variables). In this case, this is explicitly given by

$$\mathcal{A} = \{a_1, a_2, a_3, b_1, b_2, b_3\}.$$

(B.1.5)

Using this formulation the derivative of the bond angle is then given by

$$\frac{\partial \cos(\theta_{jik})}{\partial u_{q_i}} = \sum_{\eta_i \in \mathcal{A}} \frac{\partial \cos(\theta_{jik})}{\partial \eta_i} \cdot \frac{\partial \eta_i}{\partial u_{q_i}}$$

(B.1.6)

Returning to the explicit calculation, if we take the derivative with respect to a_1, we see things simplify. This will be done in detail and then symmetry relations will be used to obtain explicit expressions for all six possible derivatives.

First recall the dot product operation:

$$\mathbf{r}_{ji} \cdot \mathbf{r}_{ki} = a_1 b_1 + a_2 b_2 + a_3 b_3$$

(B.1.7)

Also recall what occurs when a derivative of a vector is taken with respect to a scalar:

$$\frac{\partial \mathbf{r}_{ji}}{\partial a_1} = \left[\frac{\partial a_1}{\partial a_1}, \frac{\partial a_2}{\partial a_1}, \frac{\partial a_3}{\partial a_1} \right] = [1, 0, 0]$$

(B.1.8)

Using these two ideas, equation B.1.3 will reduce to a simpler form.

$$\frac{\partial \cos(\theta_{jik})}{\partial a_1} = \frac{b_1 + 0}{\sqrt{\mathbf{r}_{ji}^2 \mathbf{r}_{ki}^2}} - \frac{(a_1 b_1 + a_2 b_2 + a_3 b_3)}{(\mathbf{r}_{ji}^2 \mathbf{r}_{ki}^2)^{\frac{3}{2}}} \left(a_1 \mathbf{r}_{ki}^2 \right)$$

(B.1.9)

$$= \frac{(\mathbf{r}_{ji}^2 \mathbf{r}_{ki}^2) b_1}{(\mathbf{r}_{ji}^2 \mathbf{r}_{ki}^2)^{\frac{3}{2}}} - \frac{\mathbf{r}_{ki}^2 (a_1^2 b_1 + a_1 a_2 b_2 + a_1 a_3 b_3)}{(\mathbf{r}_{ji}^2 \mathbf{r}_{ki}^2)^{\frac{3}{2}}}$$

(B.1.10)

$$= \frac{\mathbf{r}_{ki}^2}{(\mathbf{r}_{ji}^2 \mathbf{r}_{ki}^2)^{\frac{3}{2}}} \left[a_1^2 b_1 + a_2^2 b_1 + a_3^2 b_1 - a_1^2 b_1 - a_1 a_2 b_2 - a_1 a_3 b_3 \right] \tag{B.1.11}$$

$$= \frac{\mathbf{r}_{ki}^2}{(\mathbf{r}_{ji}^2 \mathbf{r}_{ki}^2)^{\frac{3}{2}}} \left[b_1 (a_2^2 + a_3^2) - a_1 (a_2 b_2 + a_3 b_3) \right] \tag{B.1.12}$$

And that is the simplest expression we can find. Fortunately, this has great symmetry proper-
ties.

$$\frac{\partial \cos(\theta_{jik})}{\partial a_1} = \frac{\mathbf{r}_{ki}^2 \left[b_1 (a_2^2 + a_3^2) - a_1 (a_2 b_2 + a_3 b_3) \right]}{(\mathbf{r}_{ji}^2 \mathbf{r}_{ki}^2)^{\frac{3}{2}}} \qquad \frac{\partial \cos(\theta_{jik})}{\partial b_1} = \frac{\mathbf{r}_{ji}^2 \left[a_1 (b_2^2 + b_3^2) - b_1 (b_2 a_2 + b_3 a_3) \right]}{(\mathbf{r}_{ji}^2 \mathbf{r}_{ki}^2)^{\frac{3}{2}}}$$

$$\frac{\partial \cos(\theta_{jik})}{\partial a_2} = \frac{\mathbf{r}_{ki}^2 \left[b_2 (a_1^2 + a_3^2) - a_2 (a_1 b_1 + a_3 b_3) \right]}{(\mathbf{r}_{ji}^2 \mathbf{r}_{ki}^2)^{\frac{3}{2}}} \qquad \frac{\partial \cos(\theta_{jik})}{\partial b_2} = \frac{\mathbf{r}_{ji}^2 \left[a_2 (b_1^2 + b_3^2) - b_2 (b_1 a_1 + b_3 a_3) \right]}{(\mathbf{r}_{ji}^2 \mathbf{r}_{ki}^2)^{\frac{3}{2}}}$$

$$\frac{\partial \cos(\theta_{jik})}{\partial a_3} = \frac{\mathbf{r}_{ki}^2 \left[b_3 (a_2^2 + a_1^2) - a_3 (a_2 b_2 + a_1 b_1) \right]}{(\mathbf{r}_{ji}^2 \mathbf{r}_{ki}^2)^{\frac{3}{2}}} \qquad \frac{\partial \cos(\theta_{jik})}{\partial b_3} = \frac{\mathbf{r}_{ji}^2 \left[a_3 (b_2^2 + b_1^2) - b_3 (b_2 a_2 + b_1 a_1) \right]}{(\mathbf{r}_{ji}^2 \mathbf{r}_{ki}^2)^{\frac{3}{2}}}$$

$$\tag{B.1.13}$$

The $\partial \eta_i / \partial u_{q_i}$ terms must now be incorporated. The α_i terms can further be broken down into
individual atom coordinates. We begin by explicitly showing the definitions

$$\mathbf{r}_{ji} = [a_1, a_2, a_3] = [u_{j_1} - u_{i_1}, u_{j_2} - u_{i_2}, u_{j_3} - u_{i_3}]$$
$$\mathbf{r}_{ki} = [b_1, b_2, b_3] = [u_{k_1} - u_{i_1}, u_{k_2} - u_{i_2}, u_{k_3} - u_{i_3}] \tag{B.1.14}$$

where, for example, u_{j_1}, is the x-coordinate for the position of the jth atom.

Clearly

$$\frac{\partial \eta_i}{\partial u_{q_i}} = 0 \tag{B.1.15}$$

for all $q \notin \{i, j, k\}$. Thus we only consider for when $q \in \{i, j, k\}$. The derivatives can then be
computed as

Table B.1: Table form of artificial variable derivatives.

∂ $\backslash$ ∂	a_1	b_1	a_2	b_2	a_3	b_3
u_{i_1}	-1	-1	0	0	0	0
u_{i_2}	0	0	-1	-1	0	0
u_{i_3}	0	0	0	0	-1	-1
u_{j_1}	1	0	0	0	0	0
u_{j_2}	0	0	1	0	0	0
u_{j_3}	0	0	0	0	1	0
u_{k_1}	0	1	0	0	0	0
u_{k_2}	0	0	0	1	0	0
u_{k_3}	0	0	0	0	0	1

$$
\begin{aligned}
\frac{\partial a_\alpha}{\partial u_{i_\beta}} &= -\delta_{\alpha\beta} & \frac{\partial b_\alpha}{\partial u_{i_\beta}} &= -\delta_{\alpha\beta} \\
\frac{\partial a_\alpha}{\partial u_{j_\beta}} &= \delta_{\alpha\beta} & \frac{\partial b_\alpha}{\partial u_{j_\beta}} &= 0 \\
\frac{\partial a_\alpha}{\partial u_{k_\beta}} &= 0 & \frac{\partial b_\alpha}{\partial u_{k_\beta}} &= \delta_{\alpha\beta}
\end{aligned}
\tag{B.1.16}
$$

where $\alpha, \beta \in \{x, y, z\}$ are a Euclidean coordinate. A tabular summary of this can be found in table B.1. Now one is able to fully represent all theta derivatives in terms of the position coordinates of every atom using equations B.2.3, B.1.13 and table B.1.

B.2.   Bond Angle (θ_{jik}) Second Derivative

Now we can focus on taking the second derivative. Using the same outline for the first derivative, the second derivative can be expressed as

$$
\frac{\partial^2 \cos(\theta_{jik})}{\partial u_{q_i} \partial u_{p_i}} = \sum_{\eta_i, \eta_j \in \mathcal{A}} \frac{\partial^2 \cos(\theta_{jik})}{\partial \eta_i \partial \eta_j} \frac{\partial \eta_i}{\partial u_{q_i}} \frac{\partial \eta_j}{\partial u_{p_i}} + \frac{\partial \cos(\theta_{jik})}{\partial \eta_i} \frac{\partial^2 \eta_i}{\partial u_{q_i} \partial u_{p_i}}
\tag{B.2.1}
$$

Clearly

$$
\frac{\partial^2 \eta_i}{\partial u_{q_i} \partial u_{p_i}} \equiv 0
\tag{B.2.2}
$$

and thus equation B.2.1 reduces to

$$
\frac{\partial^2 \cos(\theta_{jik})}{\partial u_{q_i} \partial u_{p_i}} = \sum_{\eta_i, \eta_j \in \mathcal{A}} \frac{\partial^2 \cos(\theta_{jik})}{\partial \eta_i \partial \eta_j} \frac{\partial \eta_i}{\partial u_{q_i}} \frac{\partial \eta_j}{\partial u_{p_i}}
\tag{B.2.3}
$$

In total there will be 36 second derivatives, of which 21 will be unique. Only six will be

presented herein. The other thirty are then simply a matter of swapping coordinates.

$$\frac{\partial^2 \cos(\theta_{jik})}{\partial a_1^2} = \frac{-3a_1(a_2^2 + a_3^2)b_1 + 2a_1^2(a_2b_2 + a_3b_3) - (a_2^2 + a_3^2)(a_2b_2 + a_3b_3)}{\mathbf{r}_{ji}^2\sqrt{\mathbf{r}_{ji}^2\mathbf{r}_{ki}^2}} \tag{B.2.4}$$

$$\frac{\partial^2 \cos(\theta_{jik})}{\partial a_1 \partial a_2} = \frac{(2a_1^2a_2b_1 - a_2(a_2^2 + a_3^2)b_1 - a_1^3b_2 + a_1(2a_2^2b_2 - a_3^2b_2 + 3a_2a_3b_3))}{\mathbf{r}_{ji}^2\sqrt{\mathbf{r}_{ji}^2\mathbf{r}_{ki}^2}} \tag{B.2.5}$$

$$\frac{\partial^2 \cos(\theta_{jik})}{\partial a_1 \partial a_3} = \frac{(2a_1^2a_3b_1 - a_3(a_3^2 + a_2^2)b1 - a_1^3b_3 + a_1(2a_3^2b_3 - a_2^2b_3 + 3a_3a_2b_2))}{\mathbf{r}_{ji}^2\sqrt{\mathbf{r}_{ji}^2\mathbf{r}_{ki}^2}} \tag{B.2.6}$$

$$\frac{\partial^2 \cos(\theta_{jik})}{\partial a_1 \partial b_1} = \frac{a_1b_1(a_2b_2 + a_3b_3) + (a_2^2 + a_3^2)(b_2^2 + b_3^2)}{(\mathbf{r}_{ji}^2\mathbf{r}_{ki}^2)^{\frac{3}{2}}} \tag{B.2.7}$$

$$\frac{\partial^2 \cos(\theta_{jik})}{\partial a_1 \partial b_2} = \frac{-b_1(a_1a_2b_1 + (a_2^2 + a_3^2)b_2) + a_1a_3b_2b_3 - a_1a_2b_3^2}{(\mathbf{r}_{ji}^2\mathbf{r}_{ki}^2)^{\frac{3}{2}}} \tag{B.2.8}$$

$$\frac{\partial^2 \cos(\theta_{jik})}{\partial a_1 \partial b_3} = \frac{-b_1(a_1a_3b_1 + (a_2^2 + a_3^2)b_3) + a_1a_2b_2b_3 - a_1a_3b_2^2}{(\mathbf{r}_{ji}^2\mathbf{r}_{ki}^2)^{\frac{3}{2}}} \tag{B.2.9}$$

Using this information, and the values presented in table B.1, computing the second derivative of the bond angle is a trivial extension of the above derivation.

B.3. Torsion Angle (ω_{kijl}) First Derivative

Torsional angles only appear as arguments to trigonometric functions. The definition is presented in equation B.3.1.

$$\cos(\omega_{kijl}) = \frac{\mathbf{r}_{ji} \times \mathbf{r}_{ik}}{|\mathbf{r}_{ji} \times \mathbf{r}_{ik}|} \cdot \frac{\mathbf{r}_{ij} \times \mathbf{r}_{jl}}{|\mathbf{r}_{ij} \times \mathbf{r}_{jl}|} \tag{B.3.1}$$

Define

$$\mathbf{r}_{ij} := [-a_1, -a_2, -a_3]$$
$$\mathbf{r}_{ji} := [a_1, a_2, a_3]$$
$$\mathbf{r}_{ik} := [-b_1, -b_2, -b_3]$$
$$\mathbf{r}_{jl} := [c_1, c_2, c_3]$$
(B.3.2)

Now the set $\mathcal{A}$ of our artificial variables is $\mathcal{A} = \{a_1, a_2, a_3, b_1, b_2, b_3, c_1, c_2, c_3\}$.

The first derivative can be represented as

$$\frac{\partial \cos(\omega_{kijl})}{\partial u_{q_i}} = \sum_{\eta_i \in \mathcal{A}} \frac{\partial \cos(\omega_{kijl})}{\partial \eta_i} \cdot \frac{\partial \eta_i}{\partial u_{q_i}}$$
(B.3.3)

Calculating the explicit representation is a tedious and laborious task that will not be done here. The interested reader can refer to the C++ code for the explicit representations of the torsional derivative.

B.4. Torsion Angle (ω_{kijl}) Second Derivative

The second derivative can be seen as

$$\frac{\partial^2 \cos(\omega_{kijl})}{\partial u_{q_i} \partial u_{p_i}} = \sum_{\eta_i, \eta_j \in \mathcal{A}} \frac{\partial^2 \cos(\omega_{kijl})}{\partial \eta_i \partial \eta_j} \frac{\partial \eta_i}{\partial u_{q_i}} \frac{\partial \eta_j}{\partial u_{p_i}} + \frac{\partial \cos(\omega_{kijl})}{\partial \eta_i} \frac{\partial^2 \eta_i}{\partial u_{q_i} \partial u_{p_i}}$$
(B.4.1)

Clearly

$$\frac{\partial^2 \eta_i}{\partial u_{q_i} \partial u_{p_i}} \equiv 0$$
(B.4.2)

and thus equation B.2.1 reduces to

$$\frac{\partial^2 \cos(\omega_{kijl})}{\partial u_{q_i} \partial u_{p_i}} = \sum_{\eta_i, \eta_j \in \mathcal{A}} \frac{\partial^2 \cos(\omega_{kijl})}{\partial \eta_i \partial \eta_j} \frac{\partial \eta_i}{\partial u_{q_i}} \frac{\partial \eta_j}{\partial u_{p_i}}$$
(B.4.3)

Again, this is a very tedious task and the explicit representation will not be computed here. The interested reader can refer to the C++ code for the explicit representations of the torsional second derivatives.